

Impetus Planum *presents* **A-X**



In response to the 2020-2021 AIAA Light Attack Aircraft Undergraduate
Design Competition
















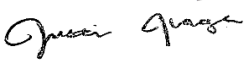



Presented by California State Polytechnic University Pomona

Aerospace Engineering Department

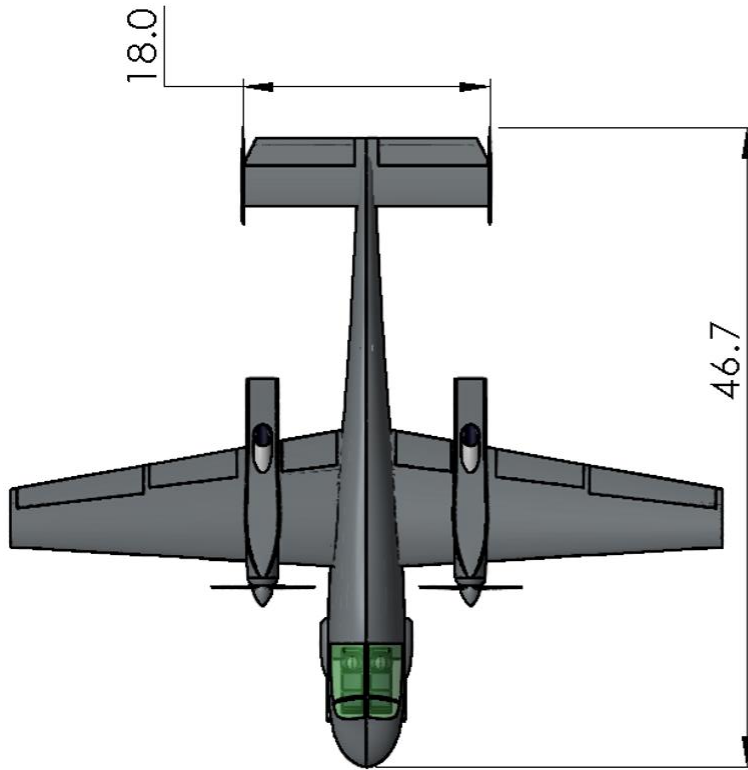
Aircraft Design 2020-2021

Impetus Planum Organizational Chart

 <p>Andrew Kinkele Program Manager Performance</p>	 <p>Erik Olson Program Deputy Weapons Integration</p>	 <p>Eduardo Garcia Rogel Structures CAD Modeling</p>
 <p>Waralee Minanandana Weight & Balance Aerodynamics</p>	 <p>Nicolas Matar Aircraft Sizing Stability & Control</p>	 <p>Justin Ilagan Landing Gear Integration</p>
 <p>Daniel Jadah Adams Aerodynamics</p>	 <p>Seham Hajhussein Cost Scheduling</p>	

Name	Email	AIAA Number	Signature
Andrew Kinkele	ajkinkele@cpp.edu	1070037	
Erik Olson	edolson@cpp.edu	1193226	
Eduardo Garcia Rogel	egarciarogel@cpp.edu	1230213	
Waralee Minanandana	wminanandana@cpp.edu	1194253	
Nicolas Matar	nfmatar@cpp.edu	1230212	
Justin Ilagan	jilagan@cpp.edu	1179348	
Daniel Jadah Adams	dmjadahadams@cpp.edu	1217830	
Seham Hajhussein	sehajhussein@cpp.edu	1218639	
Dr. Donald Edberg (Advisor)	deberg@cpp.edu	22972	

3 View Drawings



MTOW	18,700 lbs
Empty Weight	11,960 lbs
W/S	49 lbf/ft ²
P/W	0.26 HP/lbf
Takeoff/Landing Distance	3,130 ft/ 3,540 ft
Payload	3,000 lbs

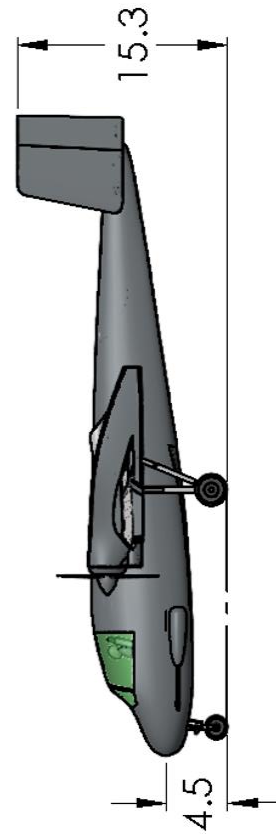
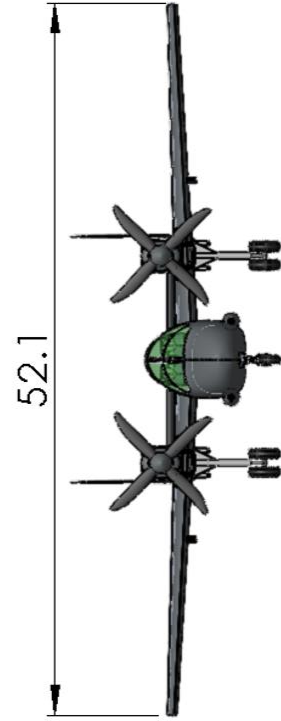


Table of Contents

Impetus Planum Organizational Chart.....	1
3 View Drawings.....	2
Table of Contents.....	3
List of Figures.....	7
List of Tables.....	10
List of Acronyms.....	12
Executive Summary.....	13
1. Requirements.....	14
1.1. Design Mission Profile.....	15
1.2. Ferry Mission Profile.....	15
1.3. Requirement Tracking and Compliance Matrix.....	16
2. Design Evolution.....	17
2.1. Design Down Selection.....	17
3. Weapons Integration & Survivability (Erik).....	20
3.1. Internal Gun Selection.....	21
3.2. Deployable Munitions.....	23
3.3. Counter Measures.....	25
3.4. Armor.....	25
3.5. Ejection Seats.....	25
4. Initial Sizing.....	27
4.1. Baseline Aircraft.....	27
4.2. Constraint Diagram.....	27
4.3. Initial Weight Estimation.....	28
5. Wing Design.....	30
5.1. Wing Position.....	31



5.2. Aspect Ratio	31
5.3. Wing Sweep & Taper Ratio.....	32
5.4. Airfoil Selection	33
5.5. High Lift Device.....	35
6. Stability and Control.....	37
6.1. Vertical Tail.....	37
6.2. Horizontal Tail.....	39
6.3. Control Surface Sizing.....	40
6.4. Static Stability.....	40
6.5. Horizontal and Vertical Tail Airfoil	42
7. Weight and Balance.....	43
7.1. Detailed Weight Breakdown.....	43
7.2. C.G. Travel	45
8. Fuselage Layout.....	47
8.1. Pilot Accommodations and Viewing Angle	47
8.2. Tip Back Angle and Turnover Angle	47
9. Propulsion.....	49
9.1. Initial Engine Trade Studies	49
9.2. Propulsion Integration	50
9.3. Propeller Sizing	51
9.4. Propulsion Mapping and Performance	52
10. Landing Gear Integration.....	54
10.1. Landing Gear Configuration Selection	54
10.2. Static and Dynamic Loads, and CBR Requirement	54
10.3. Tire Selection.....	55
10.4. Landing Gear Retraction.....	56



11. Performance.....	57
11.1. Drag Buildup	57
11.2. Operational Envelope	59
11.3. Normal Operation Takeoff and Landing.....	59
11.4. Balanced Field Length.....	60
11.5. Mission Profile Details	61
11.6. Mission Fuel Burn	62
12. Material Selection.....	65
13. Structural Analysis	66
13.1. V-n Diagram.....	66
13.2. Wing Structure.....	67
13.2.1. Wing Load Paths.....	67
13.2.2. Wing Shear Diagram and Moment Diagram.....	69
13.2.3. Wing Bending Analysis	70
13.3. Fuselage Structure	71
13.3.1. Fuselage Load Paths	71
13.3.2. Fuselage Shear Diagrams and Moment Diagrams	72
13.3.3. Fuselage Bending Analysis	74
14. Flight Systems	76
14.1. Fuel Systems.....	76
14.2. Electrical Systems.....	78
14.3. Pneumatic Systems	79
14.4. Hydraulics.....	79
15. Storage and Transportation.....	81
15.1. Enclosure	81
15.2. Aircraft Transportation	81



16. Cost.....	82
16.1. Design Drivers and Assumptions	82
16.2. Methodology.....	83
16.2.1. LCC Method	83
16.2.2. Modified DAPCA IV Method.....	85
16.3. Unit Flyaway Costs	85
16.3.1. Cost Comparison.....	86
16.4. Breakeven Data.....	87
16.5. Operations & Maintenance Costs	89
16.6. Service Life Requirement	89
16.6.1. LCC Method	89
16.6.2. Modified DAPCA IV Method.....	90
16.6.3. Final Operations Cost	90
16.7. Program Life Cost and Disposal	91
17. Entry into Service Schedule.....	92
18. TRL Tracking	93
References	94

List of Figures

Figure 0-1 Diamondback Overview with Shelter and Weapons.....	13	
Figure 1-1 Design Mission Profile	15	
Figure 1-2 Ferry Mission Profile	15	
Figure 2-1 Turboprop (Left) and Jet (Right) Concepts.....	18	
Figure 3-1 Diamondback with Possible Armament.....	20	
Figure 3-2 Integrated Gun Placement	22	
Figure 3-3 Bomb Bay with GBU-49s	23	
Figure 3-4 Wing Pylons with AGM-114 Hellfires and LAU-61	24	
Figure 3-5 MHU-83 Loading Bomb Bay	24	
Figure 3-6 Cockpit Titanium Bathtub.....	25	
Figure 4-1 Aircraft Constraint Diagram	28	
Figure 5-1 Top-view of wing planform	30	
Figure 5-2 MTOW vs. Wing Loading and Aspect Ratio	32	
Figure 5-3 Effect t/c with Mach Drag Divergence using the Korn equation	33	
Figure 5-4 Airfoil Lift Curve Slopes	34	
Figure 5-5 Airfoil Drag Polars.....	34	
Figure 5-6 NACA 4415 Profile	35	
Figure 5-7 Lift Curves with Effects of High Lift Devices	36	
Figure 6-1 Minimum Control Speed.....	38	
Figure 6-2 Vertical Tail Geometry	38	
Figure 6-3 Notch Chart.....	39	
Figure 7-1 C.G. Balance and Travel Diagram	46	
Figure 8-1 Pilot Layout	Figure 8-2 Pilot Viewing Angle Measurement.....	47
Figure 8-3 Aircraft Ground Clearance Measurements with Tip Back Angle	48	
Figure 8-4 Aircraft CG Distance Measurements and Turnover Angle Measurement	48	
Figure 8-5 Aircraft Front View with Rollover Angle Measurement	48	
Figure 9-1 PW-126A MTOW vs. Wing Loading and Aspect Ratio.....	50	



Figure 9-2 Sea Level Static TSFC vs. Propeller Diameter51

Figure 9-3 Sea Level Static Thrust vs. Propeller Diameter52

Figure 9-4 Generic Engine Map at Sea Level from Raymer Appendix E.352

Figure 9-5 PW-126A Engine Map Cacluated From Raymer’s Generic Engine53

Figure 10-1 Landing Gear Retraction.....56

Figure 11-1 Darg Buildup Landing Case.....57

Figure 11-2 Drag Buildup Loiter Case58

Figure 11-3 L/D vs. CL58

Figure 11-4 Operational Envelope.....59

Figure 11-5 Takeoff Overview60

Figure 11-6 Landing Overview60

Figure 11-7 Balance Field Length60

Figure 11-8 Fuel Flow vs. Speed.....61

Figure 11-9 Fuel per Nautical Mile62

Figure 11-10 Design Mission Altitude Profile.....63

Figure 11-11 Deisgn Mission Weight Profile.....63

Figure 11-12 Ferry Mission Altitude Profile64

Figure 11-13 Ferry Mission Weight Profile.....64

Figure 13-1 Twin Turbo Prop V-n Diagram.....66

Figure 13-2 Aerodynamic Wing Loading Diagram.....67

Figure 13-3 Inertial Wing Loading Diagram68

Figure 13-4 Total Wing Loading Diagram68

Figure 13-5 Wing Shear Diagram.....69

Figure 13-6 Wing Moment Diagram69

Figure 13-8 Wing Hat Stringers and C-channel Spars.....70

Figure 13-9 Wing Structure71

Figure 13-10 Fuselage Loading Diagram72

Figure 13-11 Fuselage Shear Diagram Forward of Wing Leading Edge.....72

Figure 13-12 Fuselage Moment Diagram Forward of Wing Leading Edge	73
Figure 13-13 Fuselage Shear Diagram Aft of Wing Traile Edge	73
Figure 13-14 Fuselage Moment Diagram Aft of Wing Trailing Edge (TE)	74
Figure 13-15 Fuselage Critical Cross Section at 14.5ft from Nose	75
Figure 13-16 Aircraft Structure	75
Figure 14-1 Diamondback with External Fuel Tanks	76
Figure 14-2 Fuel System Block Diagram	77
Figure 14-3 Electrical System Diagram.....	78
Figure 14-4 Pneumatic System Block Diagram.....	79
Figure 14-5 Hydraulic System Block Diagram	80
Figure 15-1 Diamondback in 20m EFASS Hangar	81
Figure 15-2 Diamonback and EFASS in the C-17 Aircraft	81
Figure 16-1 Hourly Rate Historical Data Chapter 24 Nicolai and Carichner	84
Figure 16-2 LCC Breakeven Point (1 Lot)	87
Figure 16-3 DAPCA IV Breakeven Point (1 Lot)	88
Figure 16-4 LCC Breakeven Point (10 Lots).....	88
Figure 16-5 DAPCA IV Breakeven Point (10 Lots).....	89
Figure 17-1 Entry Into Service Schedule.....	92

List of Tables

Table 1-1 Compliance Matrix System Level Requirements	16
Table 2-1 Design Review Schedule.....	17
Table 2-2 Aircraft Concepts Summary at the Time of Downselection.....	18
Table 2-3 Aircraft Concept Costs	18
Table 2-4 Aircraft Concepts Compliance Matrix	19
Table 3-1 Comparison Gun System Figures of Merit.....	21
Table 3-2 Integrated Gun Trade Study	22
Table 3-3 Ejection Seat Trade Study	26
Table 4-1 Metrics of Comparison Aircraft	27
Table 4-2 Design and Ferry Mission Weight Fractions	29
Table 4-3 Estimated and Final MTOW and Fuel Weights	29
Table 5-1 Wing Planform Parameters	30
Table 5-2 Wing Design Trade Study	31
Table 5-3 NACA 4415 Airfoil Parameters	35
Table 5-4 Flap Sizing Parameters.....	36
Table 6-1 Tail Configuration Comparisons	37
Table 6-2 Control Surface Parameters	40
Table 6-3 Static Stability of the Aircraft	41
Table 7-1 N&C Refined Weight Component Estimations.....	43
Table 7-2 Aircraft Detailed Weight Breakdown.....	44
Table 9-1 Engine Candidate Specifications.....	49
Table 9-2 Engine Configuration Trade Study.....	51
Table 9-3 Raymer Generic Turboprop Engine and PW-126A Specifications	53
Table 10-1 Landing Gear Selection Trade Matrix Results	54
Table 10-2 Static Loading and Maximum Dynamic Loads on Landing Gear	55
Table 10-3 Selected Tires	55
Table 11-1 Drag Buildup Configurations	57



Table 11-2 Takeoff and Landing Summary	59
Table 11-3 Mission Profiles Fuel Burn and Duration.....	62
Table 14-1 Fuel Tanks Quantity and Volume.....	76
Table 16-1 Important Variables for Cost Analyses	82
Table 16-2 Hourly Rates Assumed for Analyses.....	83
Table 16-3 LCC Acquisition Costs Summary	84
Table 16-4 Material Based Weight Factors	85
Table 16-5 DAPCA IV Acquisition Costs Summary	85
Table 16-6 Unit Flyaway Costs	86
Table 16-7 RDT&E Costs	86
Table 16-8 Unit Flyaway Cost Comparison	86
Table 16-9 Operations and Maintenance Costs for 25 Years of Service	90
Table 16-10 Operations and Maintenance Costs for 25 Years of Service	90
Table 16-11 Final Operations Costs for 25 Years	90
Table 16-12 Diamondback Program Life Cost Breakdown.....	91
Table 18-1 Component TRL Tracking.....	93

List of Acronyms

AIAA	- American Institute Aeronautics and Astronautics
APU	- Auxiliary Power Unit
AR	- Aspect Ratio
b	- Wingspan
BFL	- Balanced Field Length
C_D	- Coefficient of Drag
C_{HT}	- Horizontal Tail Coefficient
C_L	- Coefficient of Lift
C_{VT}	- Vertical Tail Coefficient
ESHP	- Equivalent Shaft Horsepower
ff	- Fuel flow
ft	- Feet
ISA	- International Standard Atmosphere
JSSG	- Joint Service Specification Guides
KEAS	- Knots Equivalent Airspeed
kts	- Knots
L/D	- Lift to Drag Ratio
LE	- Leading Edge
MAC	- Mean Aerodynamic Chord
M_{cruise}	- Mach Cruise
M_{DD}	- Mach Drag Divergence
M_{dmin}	- Minimum Coefficient of Drag
MIL SPEC	- Military Specification
MTOW	- Max Takeoff Weight
NACA	- National Advisory Committee for Aeronautics
NM	- Nautical Mile
OEI	- One Engine Inoperative
OPR	- Oral Progress Report
P/W	- Power to Weight Ratio
RAT	- Ram Air Turbine
RFP	- Request for Proposal
SFC	- Specific Fuel Consumption
S_{HT}	- Horizontal Tail Reference Area
SRR	- System Requirements Review
S_{VT}	- Vertical Tail Reference Area
T/W	- Thrust to weight ratio
TE	- Trailing edge
TRL	- Technology Readiness Level
TSFC	- Thrust Specific Fuel Consumption
W/S	- Wing loading
Λ	- Sweep angle
λ	- Taper ratio

Executive Summary

Impetus Planum is offering our A-X Diamondback, a fixed-wing light-attack aircraft that can outperform an attack helicopter in weapons delivery at a considerable cost savings. The aircraft carries two M-230 chain guns, twice that of the AH-64 Apache, and 3,000 pounds of bombs, missiles, and rockets. It can take off and land from austere fields in less than 4,000 feet and deliver munitions to a target 100 nautical miles away in less than 20 minutes. Its ability to takeoff from a forward operating base and quickly arrive to battle, then loiter on station for 4 hours, makes it an outstanding resource to support ground forces. Our proposal delivers not only a competitive aircraft, but a complete system covering aircraft transportation, shelter, armament, and operation. The Diamondback's superior armament, austere field capability, and survivability make it the best value for this mission.



Figure 0-1 Diamondback Overview with Shelter and Weapons

1. Requirements

The Diamondback will be capable of operating from austere field conditions to provide close air support to ground forces at short notice. The aircraft will enter service in 2025 to be certified for military standard airworthiness (MIL-STD-516C) and maintain guidance provided in the Joint Service Specification Guides (JSSGs). Critical technologies procured on the aircraft are at a technology readiness level (TRL) of 8 or above. The AIAA Request for Proposal (RFP) requires the Diamondback to take off and land over a 50 feet obstacle in less than or equal to 4,000 feet at a density altitude up to 6,000 feet with semi-prepared runways, such as, grass or dirt surfaces with a California Bearing Ratio of 5 [1]. The aircraft will accommodate a crew of two with zero-zero ejection seats, 3,000 pounds of armament via wing pylons and a bomb bay, and an integrated gun for ground targets. The Diamondback will maintain a service ceiling greater than or equal to 30,000 feet and serve 15,000 hours over a 25-year period.

The Diamondback is designed to meet the requirements stated in the AIAA RFP. The objective is to deliver an affordable austere field light attack aircraft that has more mission and survivable capabilities than an attack helicopter.

1.1. Design Mission Profile

The design mission profile visualizes the general mission the aircraft will perform at full payload requirement. The design mission consists of a total cruise distance of 200 nautical miles at an altitude of 10,000 feet. The cruise speed is calculated to be 355 knots from the 20 minutes of descent time to the loiter location at 3,000 feet altitude. A four hour loiter phase at 3,000 feet is considered with no stores dropped. The design mission profile is portrayed in figure 1-1 below with each stage called out and numbered in sequential order.

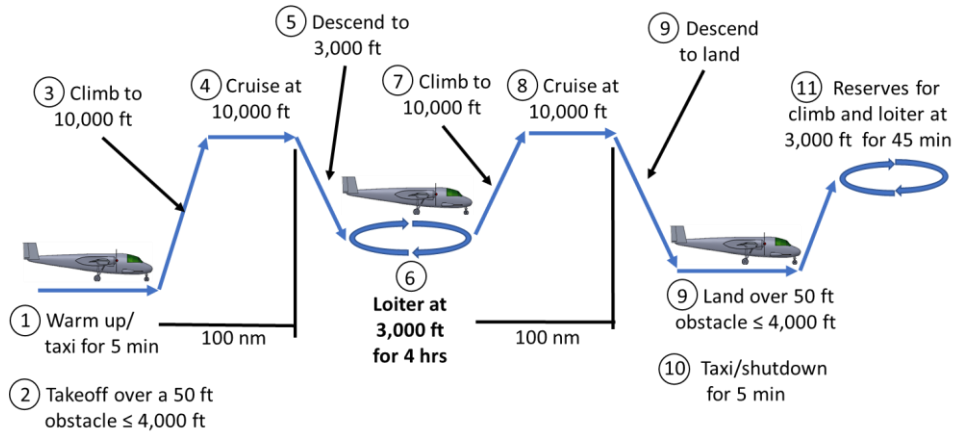


Figure 1-1 Design Mission Profile

1.2. Ferry Mission Profile

The ferry mission profile visualizes the long-range mission the aircraft will perform at 60% of payload required. The ferry mission consists of a total cruise distance of 900 nautical miles at an altitude of 18,000 feet. There is no loiter phase due to the long-range of 900 nautical miles required by the RFP. The ferry mission profile is shown in figure 1-2 below with each stage called out and numbered in sequential order.

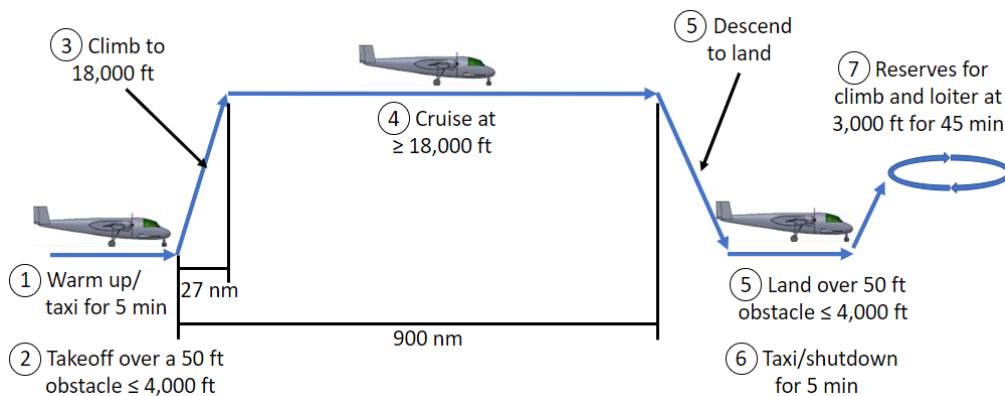


Figure 1-2 Ferry Mission Profile

1.3. Requirement Tracking and Compliance Matrix

Table 1-1 below displays the system level requirements as stated in the RFP. Additional requirements like design and ferry mission capabilities, TRL 8 or above, and aircraft span ≤ 56 ft were developed to further comply with the RFP and military standards. The requirements are ranked in order of mission criticality with their corresponding requirement type and reference number. Requirement types that begin with a “T” are technical and “M” are managerial. The reference numbering system correlates to the order of the requirements stated in the RFP and is utilized for quick referencing throughout the design process.

Table 1-1 Compliance Matrix System Level Requirements

Req. Rank	Req. Type and Ref. #	Requirement	Status	Verification Method	Actual Value
1	T1.0	Capable of taking off and landing from austere fields	Meets	Takeoff/landing analysis	Takeoff distance: 3,243 ft
					Landing distance: 3,711 ft
2	T9.0	Design mission capability	Meets	Breguet range analysis + time iterative analysis	Mission capable
3	T2.0	Survivability considerations	Meets	Chaff/flare system, cockpit armor	RR170 Mk3 Chaff, MJU-50/B Flares, titanium armor
4	T8.0	Crew: Two, both with zero-zero ejection seats	Meets	Similar aircraft comparison	MK-16 ejection seat
5	T3.0	Payload: 3000 lbs of armament	Meets	Weapons configuration, weight and balance	Payload capable
6	T5.0	Integrated gun for ground targets	Meets	Internal gun trade study	M230 (x2)
7	T4.0	Capable of carrying/deploying 500 lbs bombs, missiles, and rockets	Meets	Weapons configuration	Weapon capable
8	T6.0	Service life: 15,000 hours over 25 years	Meets	Fatigue analysis	Based on number of cycles airframe can endure during missions
9	T10.0	Ferry mission capability	Meets	Breguet range analysis + time iterative analysis	Mission capable
10	M1.0	Entry into service in 2025	Meets	Production timeline	Product lifetime schedule
11	T12.0	TRL 8 or above for all technologies	Meets	TRL tracking	TRL 8 and above
12	T7.0	Service ceiling $\geq 30,000$ ft	Meets	Constraint diagram	31,000 ft
13	13.0	Aircraft span ≤ 56 ft	Meets	Army maintenance standards	52 ft

2. Design Evolution

The design process began in November of 2020. Every few weeks our team presented an oral progress review consisting of our aircraft current capabilities, trade studies, analysis, and current issues to our faculty advisor at Cal Poly Pomona, Dr. Edberg. Our team also had the opportunity to present to two different panels of engineers, one from Northrop Grumman and another from Lockheed Martin Skunk Works, and receive the judges' feedback.

Two design concepts were carried from the System Requirements Review (SRR) through Oral Progress Review #4 (OPR4). After OPR4, a down selection analysis was conducted and the design process continued with one concept.

Table 2-1 Design Review Schedule

Name	Date
System Requirements Review	11/4/2020
Oral Progress Review #1 – Advisor	11/30/2020
Oral Progress Review #2 – Advisor	2/3/2021
Oral Progress Review #3 – Advisor	2/24/2021
Oral Progress Review #4 – Northrop Grumman	3/19/2021
Design Down Selection	4/2/2021
Oral Progress Review #5 – Lockheed Martin	4/16/2021
Proposal Submittal	5/14/2021

2.1. Design Down Selection

Two aircraft concepts were developed after SRR and carried through OPR4, after which, using the feedback from Northrop Grumman, a down selection was conducted. The two aircraft concepts are summarized by the three view drawings shown on table 2-1.

Since we are fledgling engineers, the impacts of configuration decisions that we made early in the design process were not always known. Our team created two distinct concepts to fully explore the design space, one propeller driven, one jet driven. However, the aircraft did have some similarities because the analysis in later phases of the design showed that certain design choices could not be made for the sake of variation. The results were two competitive designs that explored different propulsion, weapons integration, and crew integrations concepts.

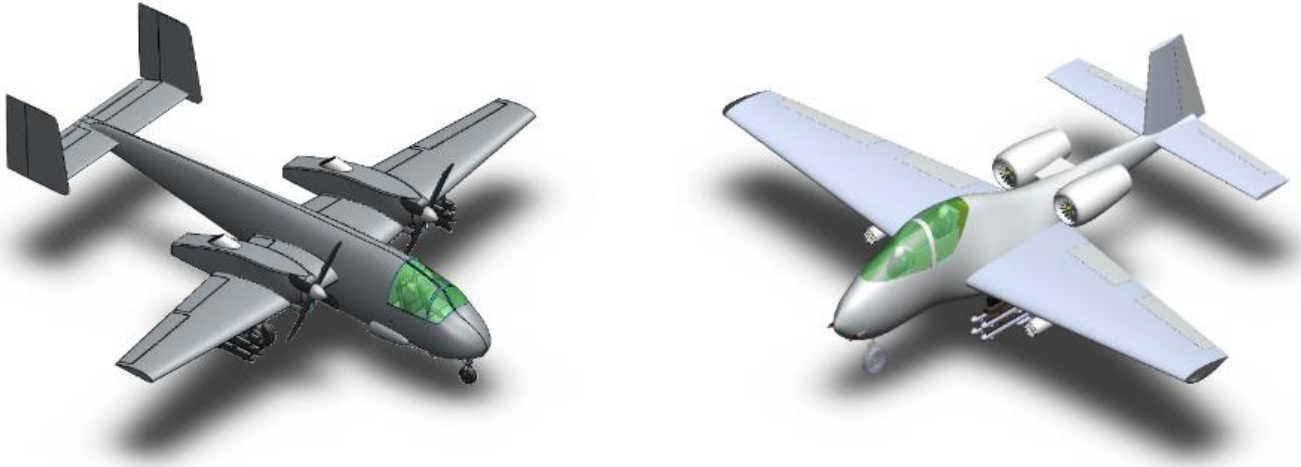


Figure 2-1 Turboprop (Left) and Jet (Right) Concepts

Table 2-2 Aircraft Concepts Summary at the Time of Downselection

Concept	MTOW (lbs)	Empty Weight (lbs)	S(ft ²)	W/S (lbs/ ft ²)	T/W or P/W	Payload (lbs)
Jet Concept	18,100	9,300	440	41	0.44	3,000
Turboprop Concept	17,800	10,600	340	51	0.31	3,000

Table 2-2 shows the aircraft specifications at the time of down selection. Since both aircraft meet all the RFP requirements, as shown in table 2-4, and the RFP requests the “best value” aircraft, down selection was based on total program cost. A total production quantity was not stated in the RFP, so cost analysis was conducted assuming 500 units, or 10 lots of 50 units. Table 2-3 shows that the Turboprop concept has a higher acquisition cost, but lower program cost because its operating costs are lower. Additionally, if the service life of the aircraft were to be extended, this lower operating cost would lead to additional savings over the Jet Concept. For this reason, the turboprop design was selected and will from this point forward will be referred to as the A-X Diamondback.

Table 2-3 Aircraft Concept Costs

Design	25 Year Program Cost (500 units)	Fly Away Cost per Aircraft
Jet Aircraft	\$285.8B	\$15.0M
Turboprop Aircraft	\$248.6B	\$16.5M

Table 2-4 Aircraft Concepts Compliance Matrix

Req. Type and Ref. #	Requirement	Jet Concept	Turboprop Concept
T1.0	Capable of taking off /landing from austere fields	Takeoff: 3,040 ft	Takeoff: 3,243 ft
		Landing: 3,717 ft	Landing: 3,711 ft
T9.0	Design mission capability	Meets	Meets
T2.0	Survivability considerations	Meets	Meets
T8.0	Crew: Two, both with zero-zero ejection seats	MK-16	MK-16
T3.0	Payload: 3000 lbs of armament	3,000 lbs	3,000 lbs
T5.0	Integrated gun for ground targets	M230	M230
T4.0	Capable of deploying bombs, missiles, etc.	Meets	Meets
T6.0	Service life: 15,000 hours over 25 years	Meets	Meets
T10.0	Ferry mission capability	Meets	Meets
M1.0	Entry into service in 2025	Meets	Meets
T12.0	TRL 8 or above for all technologies	Meets	Meets
T7.0	Service ceiling \geq 30,000 ft	Meets	Meets
T13.0	Aircraft span \leq 56 ft	53 ft	49 ft

3. Weapons Integration & Survivability

AIAA’s RFP requires this design to be capable of carrying 3,000 pounds of armament, possess an integrated gun for ground targets, and be capable of carrying and deploying a variety of weapons, including missiles, rockets and 500-pound bombs, figure 3-1. It also states requirements for survivability such as armor, countermeasures, and zero-zero ejection seats. Each piece of equipment must be of TRL 8 or higher, meaning the weapons and survivability equipment must have already been fielded and proven capable.

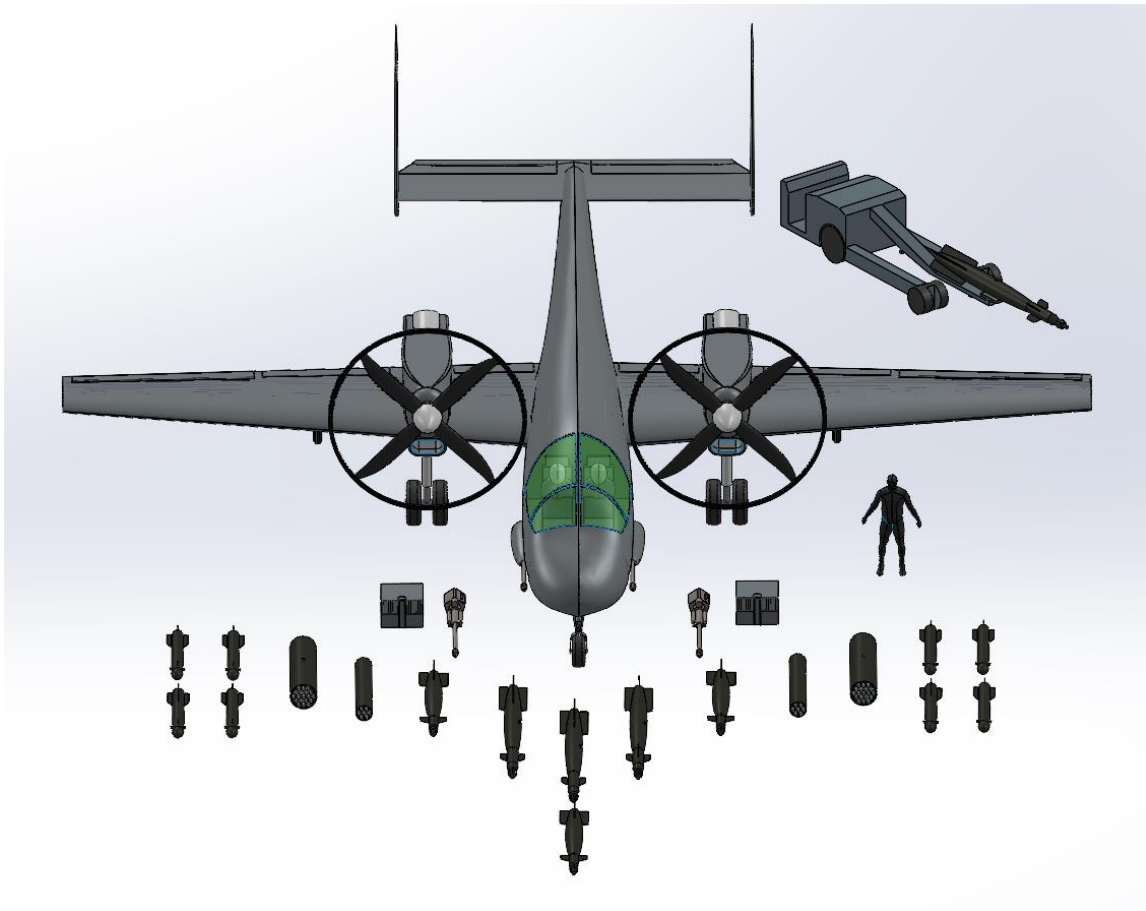


Figure 3-1 Diamondback with Possible Armament

We approached integration of weapons and survivability equipment with a ground up mindset. We initially decided on selecting the integrated gun, munitions, and deployable weapons such as bombs, rockets, and missiles to meet the mission requirements and keep the aircraft competitive with other light attack aircraft and helicopters. We designed the cockpit to accommodate sufficient armor because returning the pilots home safely is as important as

completing the mission. We then designed the Diamondback around the selected weapons systems and survivability equipment to provide a mission-capable platform that could outperform existing helicopters and aircraft.

3.1. Internal Gun Selection

One of the main purposes of the Diamondback is to complete missions currently only feasible with attack helicopters. We considered gun systems from other aircraft when selecting the integrated gun. The well-known Boeing AH-64 Apache uses a single M-230 chain gun as its primary weapon system. The Diamondback needed to be able to outperform the Apache but keep its weapon system light weight to stay within in the light attack aircraft category. For this reason, a larger weapon, the GAU-8A used on Fairchild Republic’s A-10 Thunderbolt was set as the upper limit for weapon selection.

Four initial integrated gun weapon systems were selected for comparison. The GAU-22, a single M-242 Bushmaster, a set of four M3-P .50 caliber machine guns, and twin M-230s. Each were ranked against the high and low comparison limits. The figures of merit for this comparison were gun weight, effective range, gun time on target with allowable ammunition weight, cost, anti-armor capabilities, and effectiveness. Effectiveness was measured by multiplying the firing rate with the projectile weight and dividing by the accuracy, in units of pounds/second/milliradian. This provided a numerical value for munitions the Diamondback could accurately get on target during an attack run. Table 3-1 below shows the comparison systems figures of merit and the corresponding trade study weight assigned to each. The trade study in table 3-2 provides the final scores rewarded to each gun system.

Table 3-1 Comparison Gun System Figures of Merit

Measurement	Units	Weight	Comparison Gun Systems	
			GAU-8 (A-10)	M-230 (Apache)
Gun Weight	lbs	10%	620	130
Range	ft	10%	4000	2460
Effectiveness	lbs/s/milliradian	25%	10.4	5.6
Gun Time	seconds	15%	17	107
Cost	\$	20%	160,000	110,000
Anti-Armor	Yes/No	20%	Yes	Yes

High Comparison Low Comparison

Sources: [15] [16] [17] [20]

Table 3-2 Integrated Gun Trade Study

Measurement	Weighted Scores			
	GAU-22 (x1)	M230 (x2)	M242 (x1)	M3P (x4)
Mass	0.2	0.2	0.2	0.2
Range	0.2	0.2	0.25	0.25
Effectiveness	0.25	0.5	0.25	0.25
Gun time	0.3	0.3	0.375	0.3
Cost	0.2	0.2	0.2	0.5
Anti-armor	0.5	0.5	0.5	0.2
Total	1.65	1.9	1.775	1.7

Winning out over the other three-gun systems with a weighted score of 1.9 was the twin M-230 chain guns. This system has a total weight of 260 pounds, a combined fire rate of 1,250 rounds per minute [18] at an effective range of 4,920 feet. With the 3,000-pound weight restriction, the Diamondback can carry up to 1,200 rounds of M-789 high explosive dual purpose 30mm ammunition [19]. This provides a firing time of 58 seconds at full load with each round having anti-personnel and anti-armor capabilities. At a range of 3,280 feet, the M-230 can place 80% of its rounds within eight feet.

To feed the twin cheek-mounted M-230s, a link-less feed chute system will be used. This reduces weight by removing the need for individual links between each round. The ammunition will be stored in two 600 round magazines, independently feeding each gun. The magazines will be loaded while on the ground by a hand-fed onboard loading system, figure 3-2. To stay within the 3,000-pound payload restriction, the number of M-789 rounds loaded can be adjusted as the munition’s loadout changes.

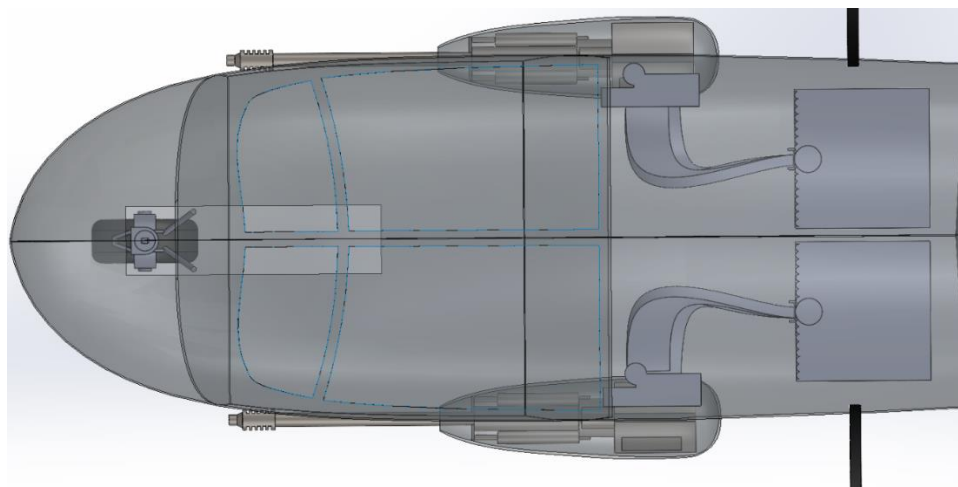


Figure 3-2 Integrated Gun Placement

3.2. Deployable Munitions

The Diamondback was designed knowing that not all attack missions will be gun runs. A substantial loadout of bomb, rockets, and missiles was then considered when designing the number of hard points and their locations. As a twin wing-mounted turboprop aircraft, wing space for pylons was reduced. This design includes one wing pylon per wing, mounted on the outboard side of the propeller. To complement the two wing pylons, the space and structure for a 67 ft³ internal bomb bay was implemented.

With two wing pylons and three internal bomb bay hard points shown in figure 3-3, the Diamondback can accommodate up to five smart bombs, for example either the 250-pound GBU-59 or 500-pound GBU-49. Instead of bombs, each pylon can support a rack of two or four AGM-114 air-to-ground Hellfire guided missiles, or an LAU-61 or LAU-131 rocket pod, shown in figure 3-4, each containing 19 or 7 Hydra-70 smart rockets, respectively. Looking towards the future, each hardpoint can structurally support up to 1,500 pounds and keep a factor of safety of 1.5. This flexibility permits dozens of different weapon types to be loaded. With a diverse combination of deployable ordinance, the Diamondback can engage both infantry and armored targets during a single mission.

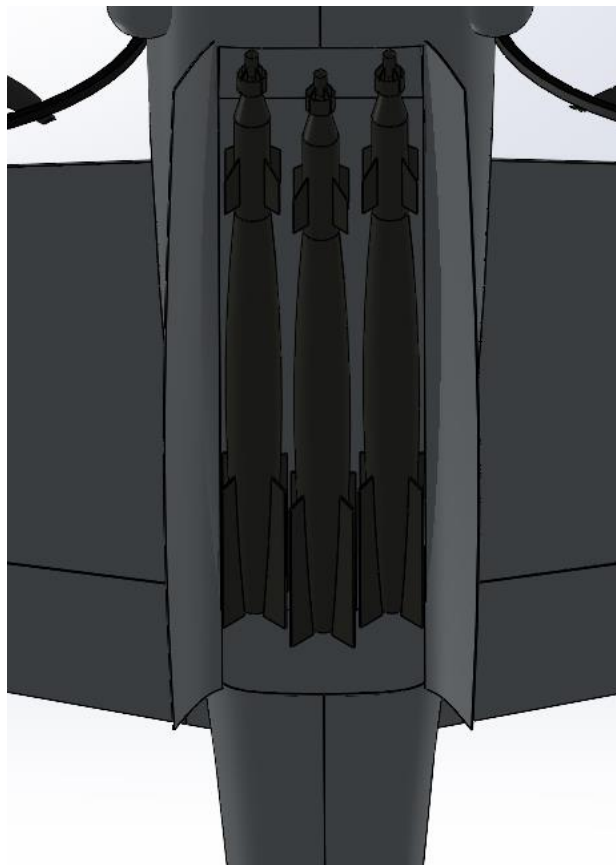


Figure 3-3 Bomb Bay with GBU-49s

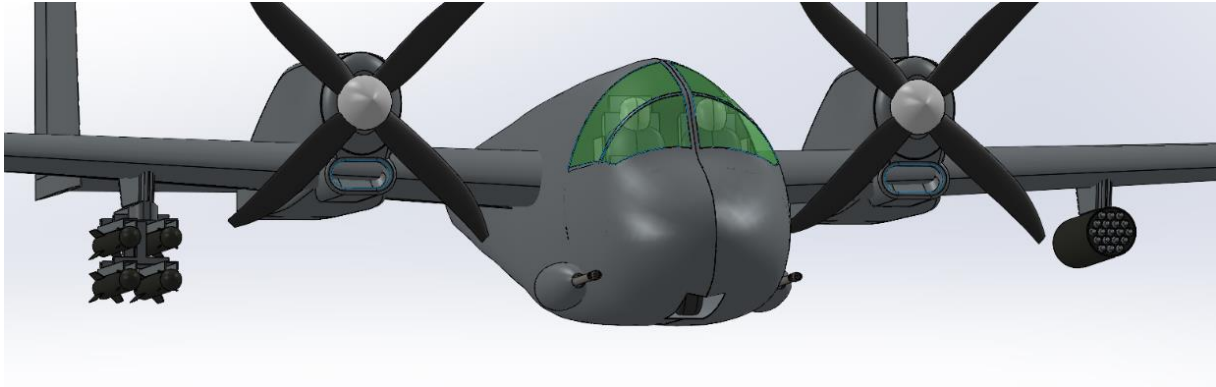


Figure 3-4 Wing Pylons with AGM-114 Hellfires and LAU-61

To load the heavier deployable munitions on the Diamondback, an MHU-83 munitions lift by Hydraulics International, Inc. will be used. The large tires of the MHU-83 allow it to be used on austere fields without sinking into the soft soil. The high landing gear and empennage clearance of the Diamondback allows the MHU-83 to load the Diamondback from the rear as shown in figure 3-5. This approach allows the most room to the munitions lift and any personnel required. Additionally, rear loading allows the bomb bay to be loaded while the engines are running for a quick airfield turnaround time. For bombs that are too heavy to load by hand, the MHU-83 will also be used to load deployable munitions on the wing pylons.

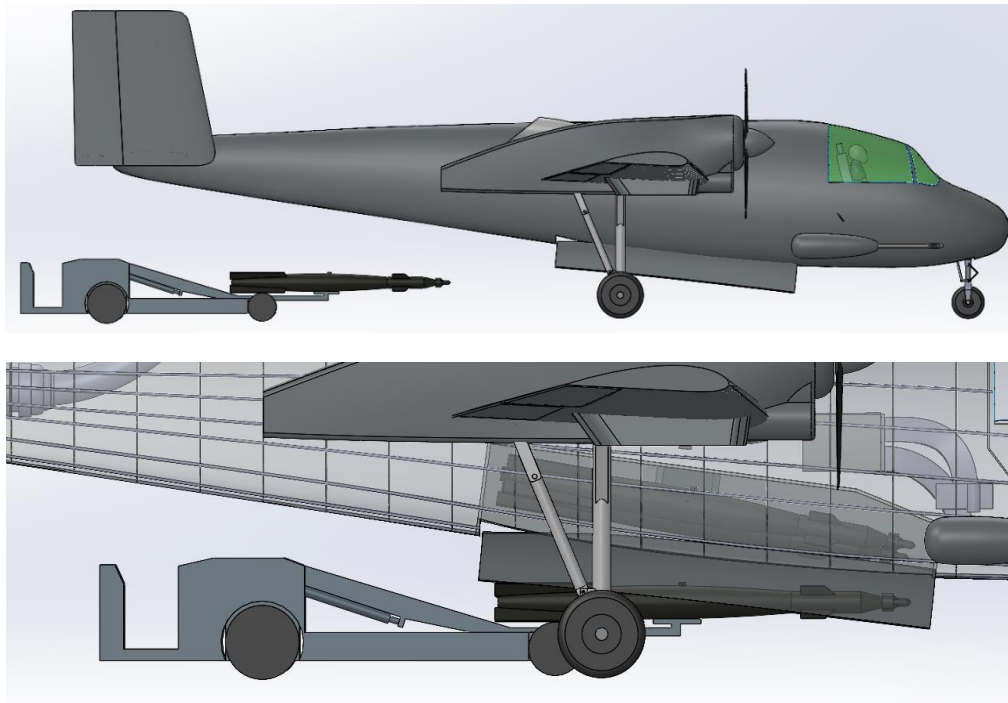


Figure 3-5 MHU-83 Loading Bomb Bay

3.3. Counter Measures

As with all attack aircraft, there is a chance that it could be locked and fired upon with surface-to-air or air-to-air guided weapons. To mitigate this, the AN/ALE-47 countermeasure dispenser system was designed into the Diamondback. Storing up to 120 shots, the four dispenser units deploy either the RR-170 Mk3 or MJU-50/B. These advanced chaff and flares are commonly used as anti-missile lock and IR decoy countermeasures by the U.S. military.

3.4. Armor

To keep the pilots safe from unguided munitions such as shrapnel and small arms fire, we integrated 739 pounds of armor plating. Titanium plates will surround the pilots with up to one inch of armor. This titanium “bathtub” will protect the pilots from below, behind, the front and the sides up to the shoulder, without restricting the pilot’s visibility, shown in figure 3-6. The front wind screen also incorporates bullet-resistant glass as an extra level of protection.

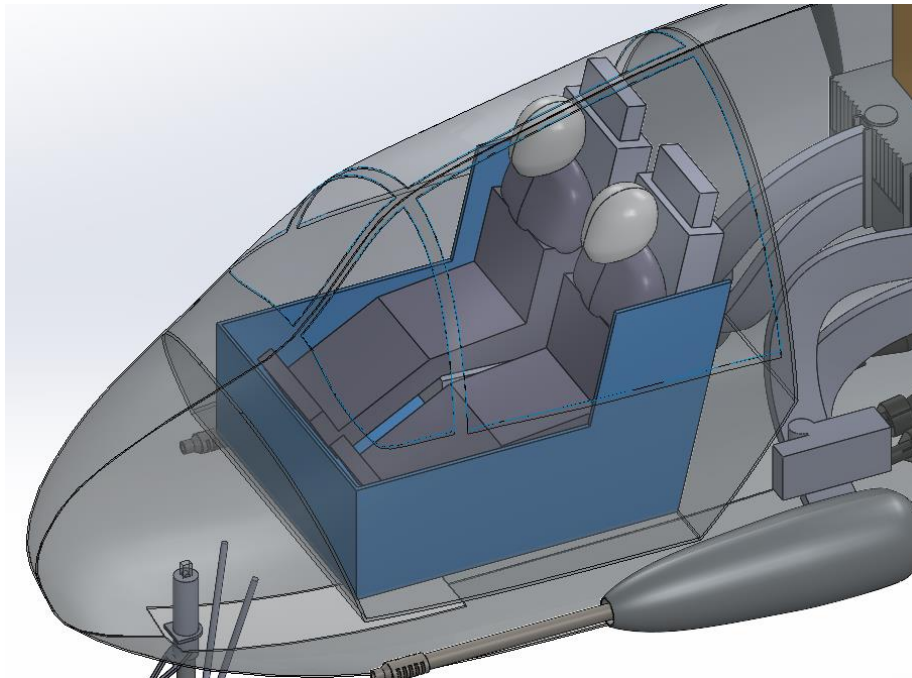


Figure 3-6 Cockpit Titanium Bathtub

3.5. Ejection Seats

In the event the Diamondback has suffered enough damage to render it unflyable, the pilots will have the option to safely eject from the aircraft. To satisfy the zero-zero ejection seat requirement, a trade study was performed

to select the best fit. Several ejection seats from existing aircraft within the design’s weight category were studied. Seat and crew weight, minimum and maximum ejection altitudes and airspeeds were compared in table 3-3. We found that the Mk-16 by Martin-Baker best fit the Diamondback’s needs. At 231 pounds each, this lightweight ejection seat has the required zero-zero capability and a maximum ejection speed necessary for the design mission profile. During the ejection sequence, the two high visibility top windscreens are jettisoned, opening a path for the ejection seats to clear the aircraft.

Table 3-3 Ejection Seat Trade Study

Name	Seat Weight (lbs)	Crew Weight (lbs)	Min. Speed (kts)	Min. Altitude (ft)x10 ³	Max. Altitude (ft)x10 ³	Max Airspeed (kts)	Available Ejection Sequence	TRL
Mk11	--	132-279	Zero	60	40	400	Yes	9
Mk16-US16LA	231	137-270	Zero	Zero	50	370	Yes	9
ACES 5	245	140-211	Zero	Zero	50	600	Yes	9
ACES 2	245	103-245	Zero	Zero	60	600	Yes	9

Sources [23] [24]

- Mk11 weight was unavailable
- Seat candidates are from similar aircraft:
 - Mk11: Pilatus PC-9
 - Mk16: Beechcraft T-6 Texan II
 - ACES 5: F-15, F-16, F-22
 - ACES 2: A-10



Mk-16
Courtesy of Martin-Baker

4. Initial Sizing

4.1. Baseline Aircraft

Impetus Planum started by analyzing aircraft with similar roles. The first notable aircraft is the A-10 Warthog. Although it is substantially larger than a light attack aircraft, it is famous for its durability and success in the ground support role. The OV-10 Bronco was also researched because of its use in the Vietnam conflict as a light attack aircraft. Finally, the T-6 Texan, and A-29 Super Tucano were also identified as modern-day light attack aircraft. The values shown in table 4-1 summarize the basic characteristics of the predecessors.

Table 4-1 Metrics of Comparison Aircraft

Variable	A-10	OV-10	A-29
MTOW (lbs)	50,000	14,450	11,900
Aspect Ratio	6.5	5.5	6.4
Wing Loading (lbs/ft ²)	99	50	56
Power/Thrust to Weight Ratio	0.36 HP/lbs	0.14 lbs/lbs	0.13 lbs/lbs

Sources: [12] [13] [14]

4.2. Constraint Diagram

Constraint diagrams were constructed to identify the valid design space of power to weight and wing loading. Figure 4-1 below shows the valid design space for the turboprop design concept as well as the initially selected design point and the design point of the current Diamondback. The initial design point allowed ample room from the two critical constraints which prevents weight growth and other deficiencies from reducing the aircraft’s capabilities below the required specifications. The comparison aircraft are plotted on the constraint diagram as well.

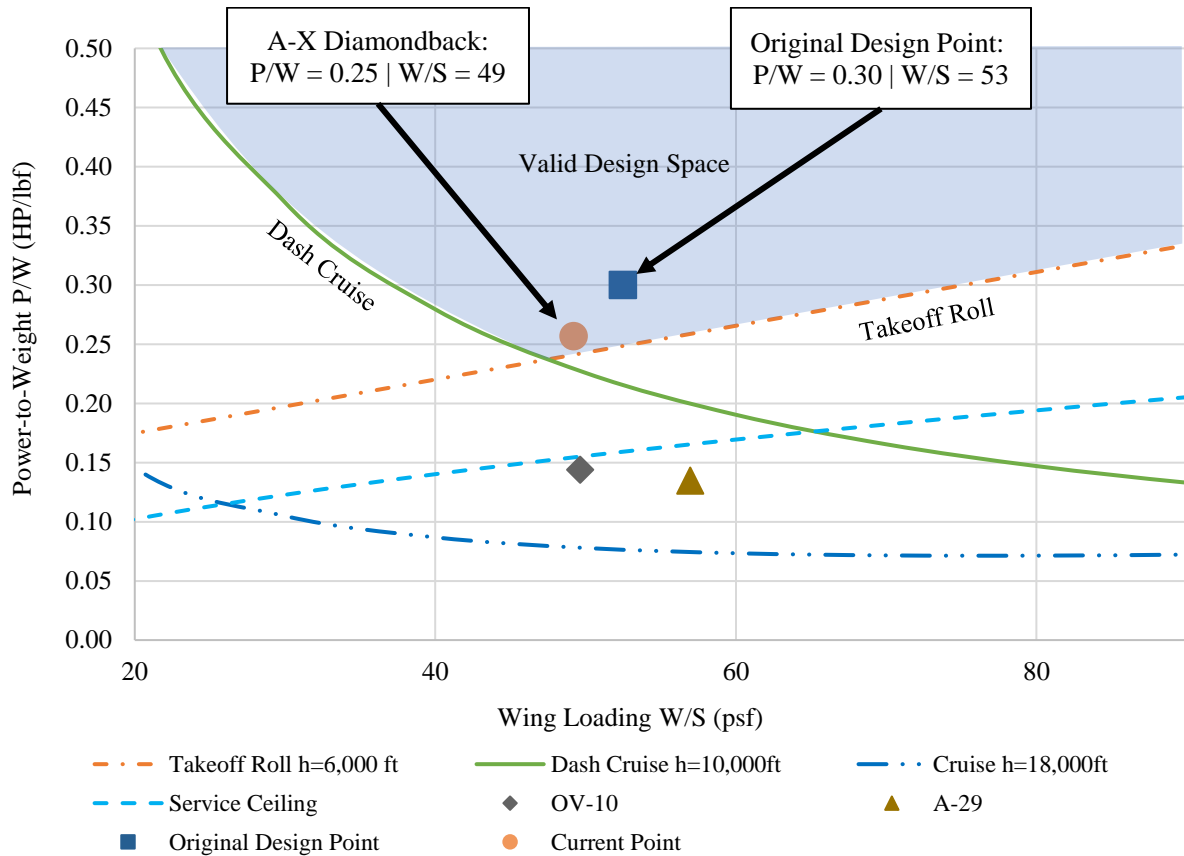


Figure 4-1 Aircraft Constraint Diagram

4.3. Initial Weight Estimation

After constructing constraint diagrams, the initial MTOW was estimated by finding weight fractions for each mission segment. Cruise and loiter weight fractions were calculated using the Breguet range equation; all others were recommendations from Nicolai and Carichner Section 5.4 [2]. SFC estimates were found in Raymer's table 3.4 [3]. The product of all the weight fraction for a mission yields the overall mission weight fraction and by conjunction, the mission fuel fraction. Aircraft sizing and fuel requirements were dictated by the design mission because, as shown in table 4-2, the fuel fraction for the design mission was found to be larger than that of the ferry mission.

Table 4-2 Design and Ferry Mission Weight Fractions

Design Mission		Ferry Mission	
Phase	Fraction	Phase	Fraction
Takeoff	0.970	Takeoff	0.970
Climb	0.985	Climb	0.985
Cruise	0.983	Cruise	0.888
Descent	1.000	Descent	1.000
Loiter	0.916	Taxi/Shutdown	0.995
Climb	0.985	Climb	0.985
Cruise	0.983	Reserve Loiter	0.984
Descent	1.000	W_{final}/W_0	0.818
Taxi/Shutdown	0.995	W_f/W_0	0.182
Climb	0.985		
Reserve Loiter	0.984		
W_{final}/W_0	0.803		
W_f/W_0	0.197		

Initial MTOW and empty weight estimates were calculated using a historical trend for twin turboprop aircraft. The findings from the preliminary weight estimation are shown in table 4-3. Ultimately, these weight estimates were 15% less than our final weight of the Diamondback due to optimistic loiter SFC and L/D values used during the initial sizing phase.

Table 4-3 Estimated and Final MTOW and Fuel Weights

Weights	Initial Estimate	Diamondback
MTOW (lbs)	17,400	18,700
Fuel Weight (lbs)	3,170	3,500

5. Wing Design

The austere field performance requirement indicates designing an aircraft capable of low-speed aerodynamics which are crucial for short takeoff and landing conditions. The main factors that contribute to aerodynamics are wing design, aspect ratio, sweep, taper ratio, and airfoil selection. Furthermore, increasing the aerodynamic lift capabilities of the Diamondback will be incorporated high lift devices.

Wing area was obtained from the constraint diagram and weight estimation analysis in section 4.3. The aspect ratio, sweep, and taper ratio were selected based on sizing calculations and recommendations from Raymer [3], N&C [2], and Schaufele [7]. Since M_{dd} is greater than M_{cruise} , wing sweep is not needed; therefore, the wing has a sweep of 0° . Aspect and taper ratio were determined to minimize wing loading. Considering the austere field performance, the wing geometry was carefully developed to maximize aerodynamic efficiency and decrease wing weight which is ideal for low-speed flight characteristics. Wing parameters are shown in table 5-1, and a top view of the wing planform is portrayed in figure 5-1.

Table 5-1 Wing Planform Parameters

Parameter	Symbol	Value
Span	b	52.1 ft
Wing Loading	W/S	49 lbs/ft ²
Wing Area	S	380 ft ²
Aspect Ratio	AR	7
Taper Ratio	l	0.4
Quarter Chord Sweep	$\Lambda_{1/4}$	0°
Leading Edge Sweep	Λ_{LE}	3.5°
Mean Aerodynamic Chord	MAC	7.9 ft
Root Chord	c_r	10.4 ft
Tip Chord	c_t	4.2 ft

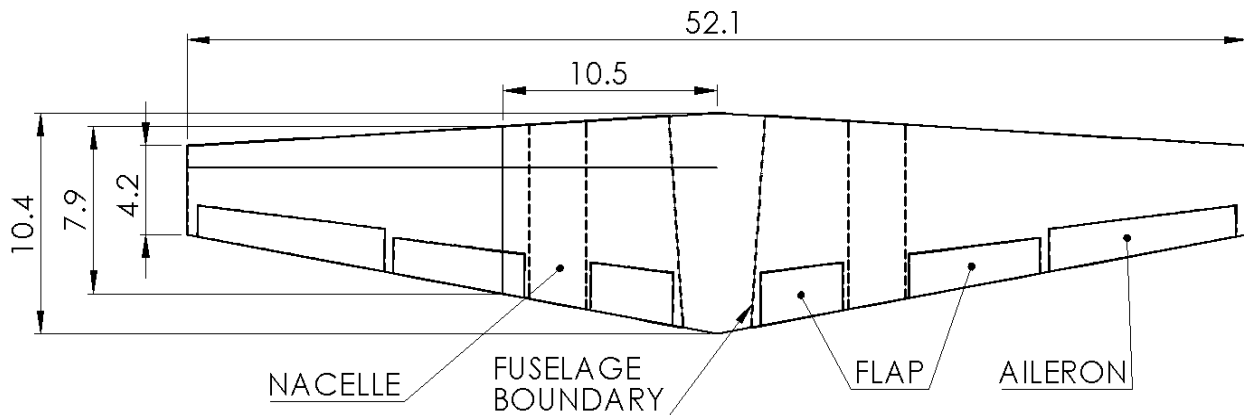


Figure 5-1 Top-view of wing planform

5.1. Wing Position

Initially, a low-wing design was ruled out due to the lack of ground clearance needed while operating from austere fields. Even though a low wing configuration provides an excellent location for retractable landing gear, the ability to operate from austere field conditions is the Diamondback’s number one priority. A high-wing was considered due to the advantages of ground visibility; however, it was soon eliminated because a high-wing design would result in a more challenging landing gear configuration located on the wing. A retractable tricycle landing gear configuration was most desirable for the Diamondback due to austere field conditions. Therefore, a mid-wing design was selected for ground visibility, compatibility with retractable tricycle landing gear, easy access to load/unload wing pylons, clearance for the propellers, and slightly increased ground effect during takeoff. Considering the Diamondback is tailored to operate from austere fields, a mid-wing provides enough ground clearance to complete its mission. Using the considerations for the three wing designs, a trade study was conducted, shown below in table 5-2. Weights for each criterion were carefully selected based on austere field characteristics.

Table 5-2 Wing Design Trade Study

Criteria	Weight	Scale	Low	Mid	High
Ground clearance	0.40	5 = Most Clearance 1 = Least Clearance	1	4.5	5
Ground effect during takeoff	0.25	5 = Greatest 1 = Least	5	3.5	2
Weapon pylon loading & unloading	0.35	5 = Least Difficult 1 = Most Difficult	5	3.5	2
Total Weights	1		11	11.5	9

5.2. Aspect Ratio

Aspect ratio was selected to balance the aerodynamic efficiency and structural weight. Using the Breguet range equation and the weight estimation technique from Nicolai and Carichner Chapter 20 [2], the relationship between aspect ratio, wing loading, and MTOW is shown by figure 5-2. The dash cruise and takeoff curves from the constraint diagram were added to constrain the design space. The design point, shown by the green dot, was selected to minimize MTOW while maintaining ample margin from all constraints to allow room for the aircraft to evolve during the design process. Early in the design process a span limit constraint of 56 ft was added so our aircraft could fit inside the mobile hanger.

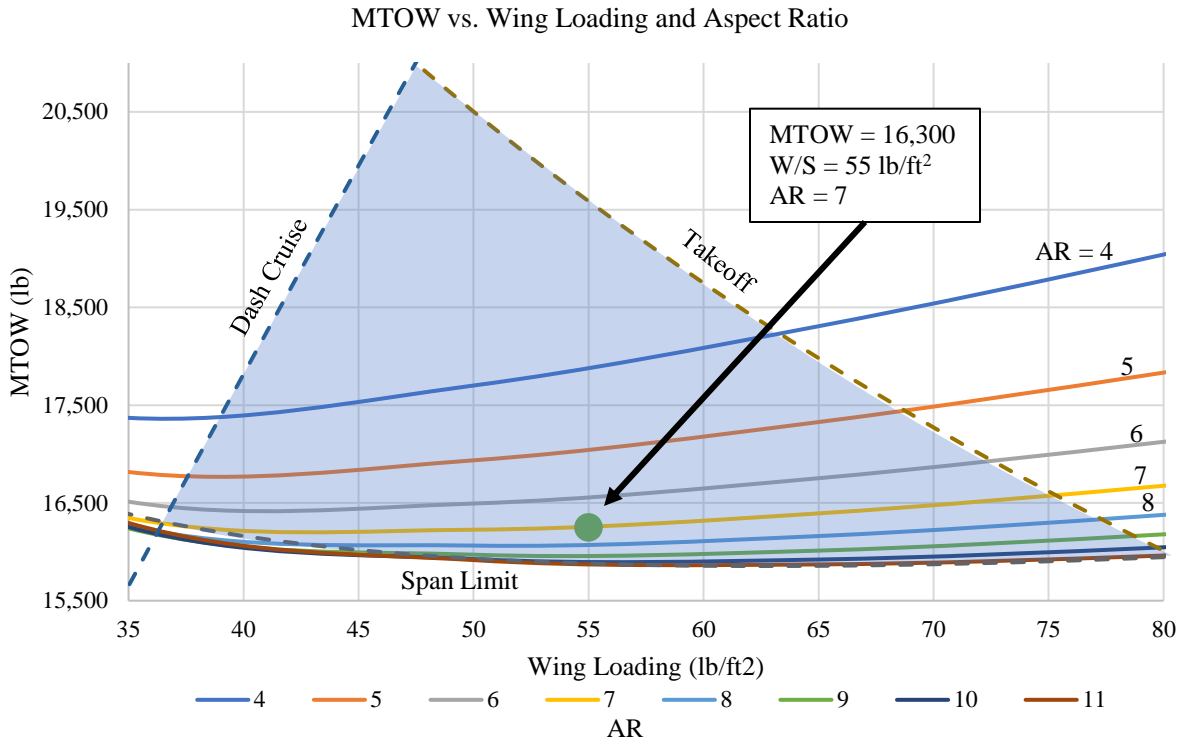


Figure 5-2 MTOW vs. Wing Loading and Aspect Ratio

5.3. Wing Sweep & Taper Ratio

The Korn equation below was used to further assess the need for wing sweep and determine an acceptable t/c for the wing airfoil. The airfoil technology factor, k_A , is 0.87 for conventional airfoils and the lift coefficient, c_l , was calculated to be 0.17 at M_{cruise} of 0.53.

Equation 5-1 Korn Equation

$$Korn\ equation: M_{DD} = \frac{k_A}{\cos\Lambda} - \frac{\left(\frac{t}{c}\right)}{\cos^2\Lambda} - \frac{c_l}{10\cos^3\Lambda}, k_A = 0.87, c_l = 0.17$$

Figure 5-3 was developed using the Korn equation to calculate M_{dd} varied with t/c at a wing sweep of 0° . Cruise Mach is also plotted to determine the difference between M_{dd} and M_{cruise} . Figure 5-3 shows that airfoil candidates with t/c ratios of up to 0.36 could be selected without the consequence of compressibility drag.

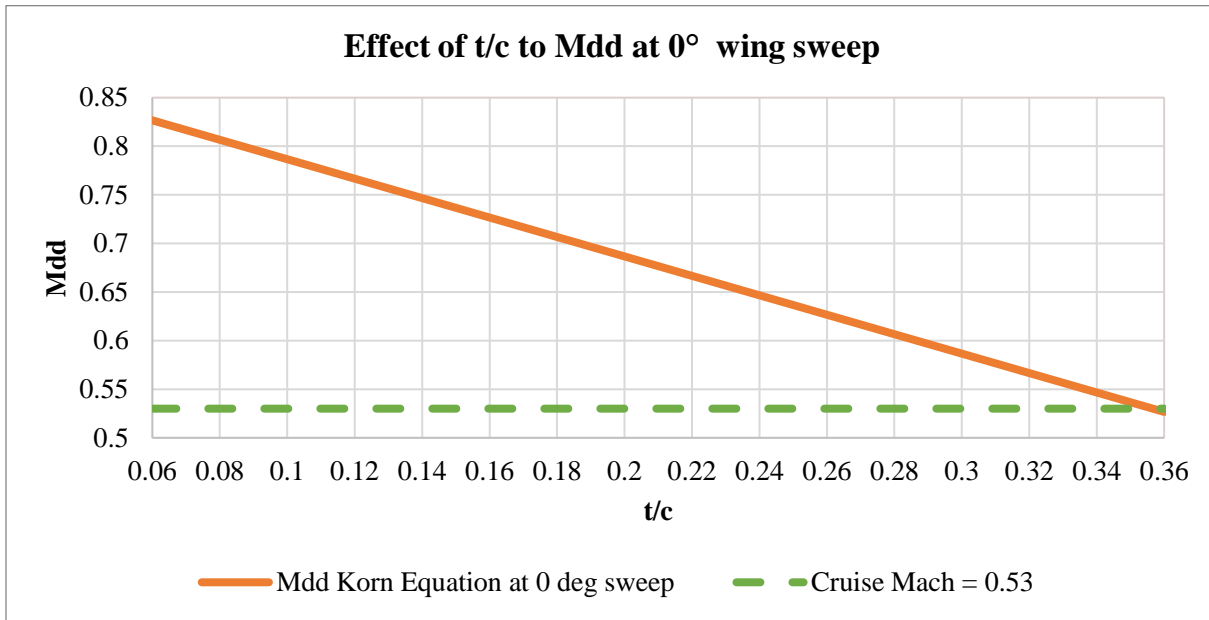


Figure 5-3 Effect t/c with Mach Drag Divergence using the Korn equation

A wing taper ratio of 0.4 was selected based on the recommendation from Nicolai and Carichner [2] as it provides a minimum finite span downwash effects and minimum induced drag on the wing. A taper ratio of 0.4 provides the ideal balance between wing weight and elliptical wing loading.

5.4. Airfoil Selection

NACA airfoils were researched to deliver desirable cruise characteristics and a moderate to high C_{lmax} for short takeoff and landing performance. Furthermore, a relatively high thickness ratio was considered for increased fuel capacity in the wing and decreased wing weight. Investigating the appropriate airfoil for the wing began with weighing the advantages and disadvantages of the four-digit, five-digit, and six-series NACA airfoil families. Five- and six-series airfoils deliver poor stall characteristics compared to four-digit airfoils. Six-series airfoils are primarily optimized for laminar flow at high speeds, while four-series airfoils deliver high angle of attack performance. Considering the advantages of 4-series airfoils and the low-speed lift characteristics they deliver, the 4-series family was selected to help narrow down the wing airfoil selection.

Four-digit NACA airfoil data was retrieved from Abbot and Von Doenhoff’s Theory of Wing Sections [6] at a Reynolds number of 9×10^6 with no flap deflection. Even though this Reynolds number is higher than our cruise Reynolds number, the airfoil data is more conservative than simulated data. Five airfoil candidates are plotted in figure 5-4 and figure 5-5 below for a clearer visualization of the lift and drag polar characteristics.

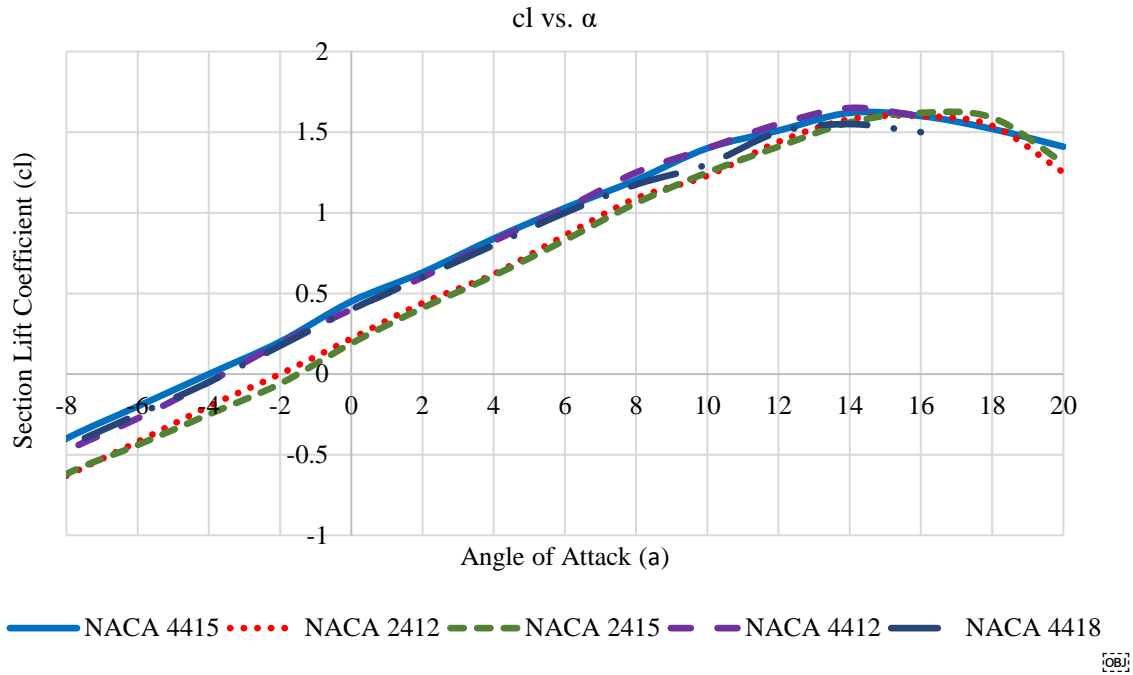


Figure 5-4 Airfoil Lift Curve Slopes

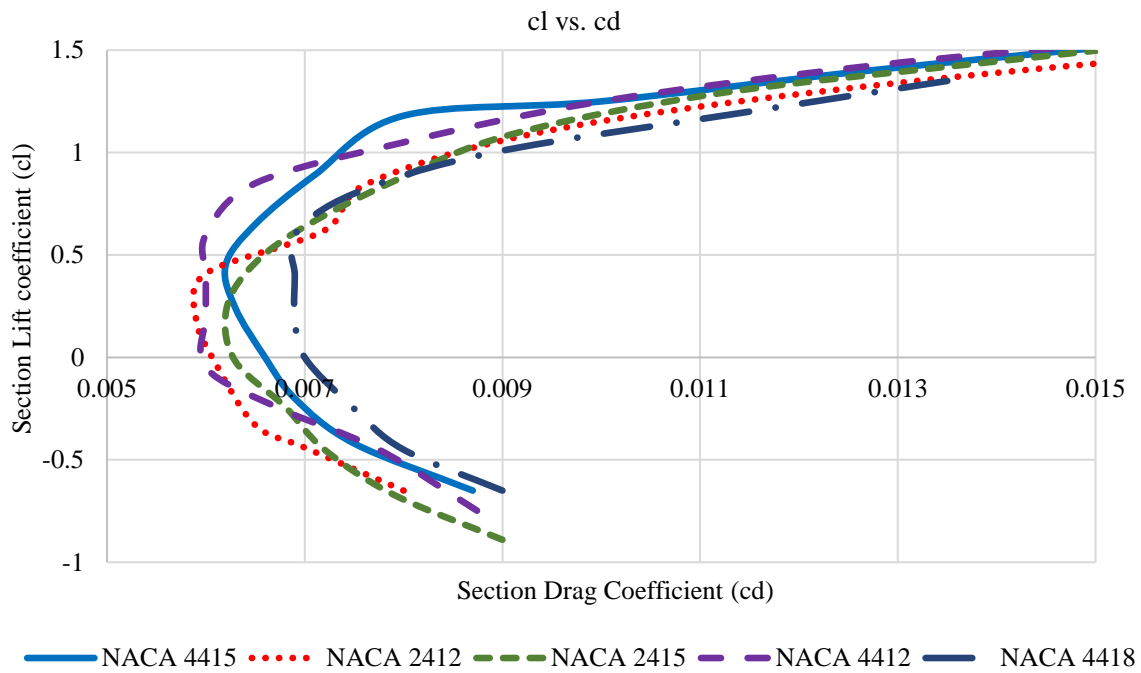


Figure 5-5 Airfoil Drag Polars

The lift-curves slopes in figure 5-4 are similar; however, the NACA 2412 and 2415 have the highest stall angle at approximately 16 degrees. Comparing the drag polar curves, the NACA 4418 was an outlier primarily due to

its higher C_{dmin} . The NACA 2412 and 4412 achieved the lowest C_{dmin} in this analysis. The NACA 4415 was selected due to its acceptable lift curve slope and stall angle. Its drag polar performance lands between the other airfoils which is acceptable for the low-speed cruise conditions the Diamondback will encounter. The NACA 4415 is displayed in figure 5-6 with its parameters in table 5-3.

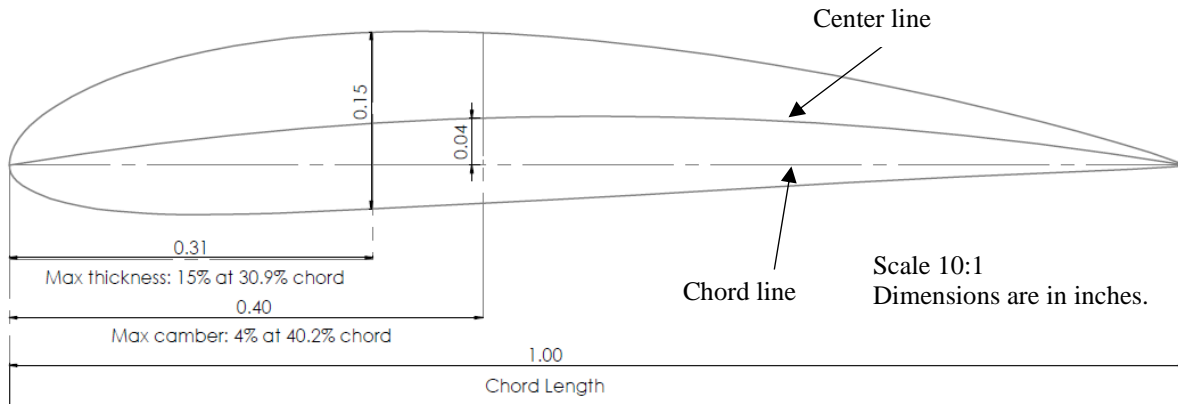


Figure 5-6 NACA 4415 Profile

Table 5-3 NACA 4415 Airfoil Parameters

Stall Angle	Max C_l	Max C_l/C_d	t/c max
14°	1.62	147.5	0.15

5.5. High Lift Device

Once the airfoil was selected, the maximum section lift coefficient of the NACA 4415 was used to calculate the C_{Lmax} the aircraft can achieve with a clean configuration and determine the need for high lift devices. Figure 5-6 shows that the selected airfoil gives the aircraft a C_{Lmax} that is much lower than the C_{Lmax} value of 1.7 required for landing obtained from the constraint diagram, figure 5-8. To reach the required lift coefficient value, flaps were implemented as the high lift device at the same lift-curve slope to improve the Diamondback’s lift performances during both takeoff and landing configurations.

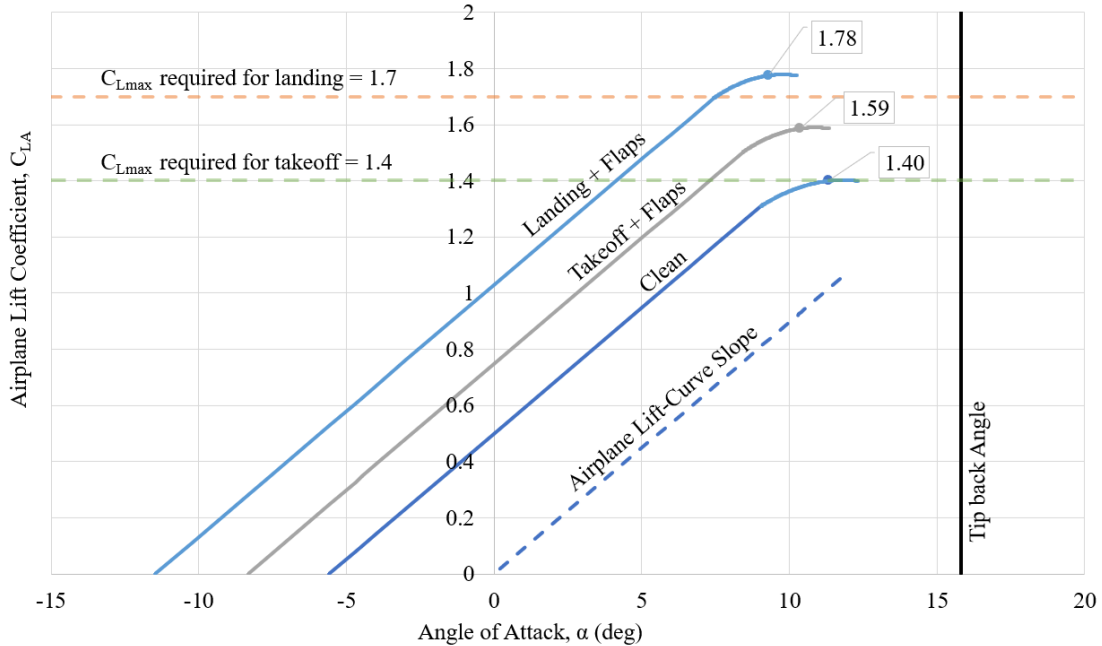


Figure 5-7 Lift Curves with Effects of High Lift Devices

Leading edge slats were unnecessary because the desired C_{Lmax} was achieved with plain flaps. Flaps were sized, shown in table 5-5, to give both configurations higher than required C_{Lmax} values. This provides margin for actual lift generation might be experienced when compared to ideal calculated values. With the effects of flaps included, the Diamondback can perform the takeoff and landing in less than the distance required at angles of attack that are well below the maximum tip back angle.

Table 5-4 Flap Sizing Parameters

Parameters	Value
Flapped-to-wing area ratio (S_{wf}/S_w)	0.4
Flap extension ratio (c_f/c)	0.25
Landing deflection angle	15
Takeoff deflection angle	40

6. Stability and Control

When initially looking at the tail, we considered 4 different options for our configuration, shown in table 6-1. We compared both the weight and parasitic drag of each configuration. Ultimately, we decided to go with an H-tail configuration despite its increased weight and drag from the additional vertical stabilizer and required structures. We assumed the same horizontal tail for each configuration to simplify the weight and drag calculations. We felt that the added redundancy of the two vertical stabilizers for survivability outweighed the increase in weight and drag.

Table 6-1 Tail Configuration Comparisons

Parameters	H-tail	Cruciform	T-Tail	Conventional
S_{HT} (ft ²)	63.52	63.52	63.52	63.52
AR_{HT}	4.25	4.25	4.25	4.25
W_{HT} (lbs.)	173.7	158	158	158
S_{VT} (ft ²)	30.41 (total)	27.65	27.65	27.65
AR_{VT}	1.2	1.7	1.7	1.7
W_{VT} (lbs)	48.81	65.34	75.6	53.2
W_{tail} (lbs)	222.5	223.3	233.5	211.2
f_{tot}	0.473	0.42	0.438	0.42
C_{Dp}	0.0015	0.0013	0.0014	0.0013

6.1. Vertical Tail

To initially size the vertical tail for an H-tail, we used historical data from similar aircraft to get a vertical tail volume coefficient, and then the area was divided among both vertical stabilizers with a 5% margin to each, to provide the desired redundancy. To verify that tail sizing, we utilized one engine inoperative (OEI) analysis to both check the minimum control speed of the aircraft and size the vertical stabilizers. To size the stabilizers using OEI analysis, the calculations assumed that the minimum control speed $V_{MC} = 1.13V_{S,TO}$, where $V_{S,TO}$ is the stall speed at takeoff. However, further analysis showed that bigger stabilizers were required to have the minimum control speed be lower than the takeoff speed V_{TO} and touchdown speed V_{TD} . We obtained the minimum control speed, shown in figure 6-1, using the following assumptions:

- Aftmost CG location
- Turboprop performance at various altitudes and Mach numbers is like the data found in Raymer Appendix E.3 [3]
- C_n from aileron deflections is neglected.

The resulting vertical tail geometry for each of the stabilizers is shown in Figure 6-2.

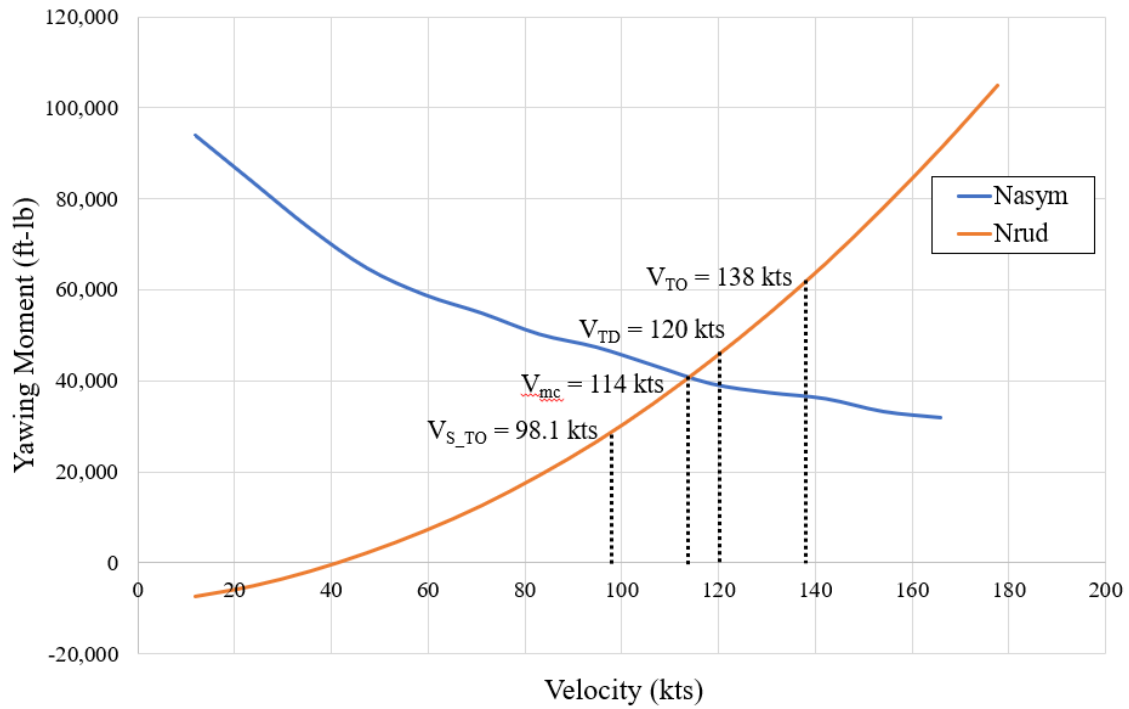
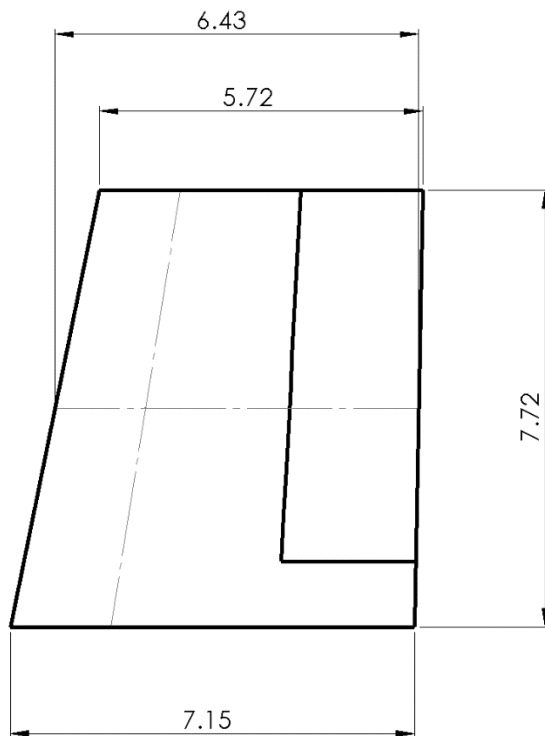


Figure 6-1 Minimum Control Speed



For each vertical tail	
S_{VT}	49.6 ft ²
AR	1.2
MAC	6.2 ft
$\Lambda_{1/4}$	9°
λ	0.8

Figure 6-2 Vertical Tail Geometry

6.2. Horizontal Tail

Like the vertical tail, we initially sized the horizontal tail using historical data from similar aircraft to get a horizontal tail volume coefficient. To better refine the sizing, the team used a Notch chart to get a horizontal tail volume coefficient using the existing aircraft geometry. The equations used can be found in Raymer [3]. The resulting Notch chart is shown in figure 6-3. We constructed the plot based on the control authority required in the following scenarios:

- Static margin with C.G. at the aftmost position (Rear stability limit)
- Landing with flaps extended and C.G. at the foremost position (Landing flare)
- Takeoff with C.G. at the foremost position (Nosewheel liftoff)

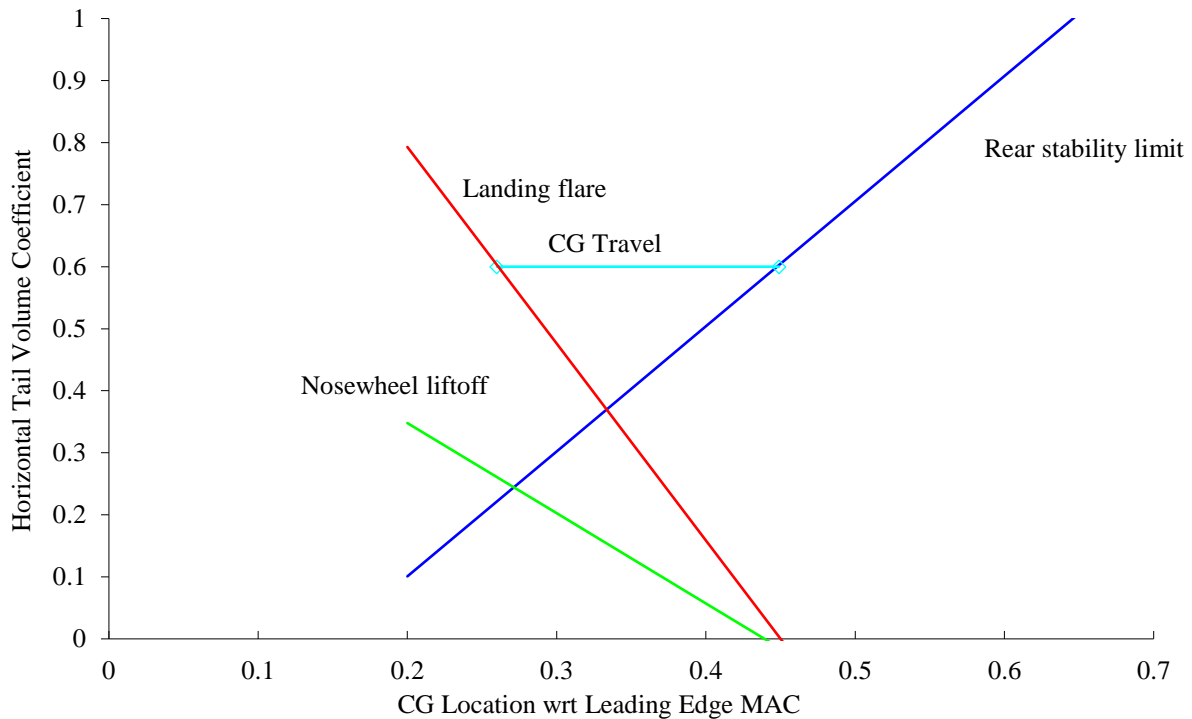


Figure 6-3 Notch Chart

The limits are then plotted in terms of horizontal tail volume coefficient versus C.G. location as a percent of MAC. A horizontal line equal in length to the maximum allowable C.G. travel of the aircraft is fitted between the limits to give the horizontal tail volume coefficient to size the horizontal tail. The resulting horizontal tail geometry is shown in figure 6-4.

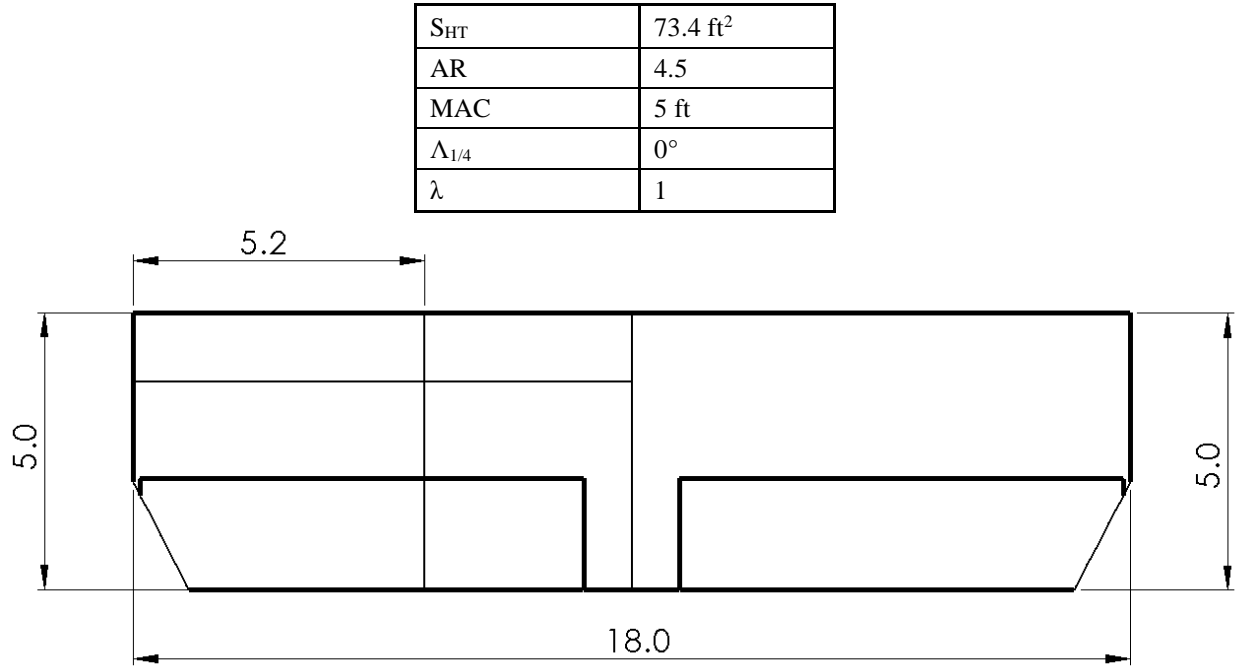


Figure 6-4 Horizontal Tail Geometry

6.3. Control Surface Sizing

The aileron, rudder and elevator were initially sized based on historical data and assumed values of similar sized aircraft from Raymer [3]. We then sized the rudder using OEI analysis. To size the elevator, the Notch charts from Raymer [3] were also used. To size the ailerons, charts and equations found in Raymer [3] were used. The control surface parameters are displayed in table 6-2. These parameters correspond to a single control surface, such as a single aileron or a single rudder.

Table 6-2 Control Surface Parameters

Control Surface	Deflection Range	Span (ft)	Chord Ratio	Area Ratio	Quantity
Aileron	± 25 degrees	9.16	0.34	0.12	2
Elevator	± 30 degrees	7.95	0.33	0.35	2
Rudder	± 26 degrees	7.72	0.33	0.3	2

6.4. Static Stability

We also examined the static stability of the aircraft by checking the following stability coefficients:

- $C_{m,\alpha}$ for longitudinal stability

- $C_{n,\beta}$ for directional stability
- $C_{l,\beta}$ for roll stability

We calculated the neutral point as well to compare against the rear stability limit of the Notch chart. Additionally, we conducted a simulation in AVL to compare the stability coefficients and neutral point found by hand calculations. However, we found a discrepancy between the AVL results and hand calculations due to the AVL model not including fuselage contribution to the coefficients. For the hand calculations, we used equations from Raymer [3] and Nelson [11]. The results of both simulation and hand calculations are detailed in table 6-3. Because the hand calculations include fuselage contribution, we trust the hand calculations more for the static stability of the aircraft. The neutral point of the aircraft also lands in a similar location to the rear stability limit of the Notch chart, which further validates hand calculations over AVL.

Table 6-3 Static Stability of the Aircraft

	Static Stability Coefficients (AVL)			Static Stability Coefficients (Hand Calcs)		
	Coefficient	Value	Stable/Unstable	Coefficient	Value	Stable/Unstable
Longitudinal Stability	$C_{m\alpha}$	-2.663 /rad	Stable	$C_{m\alpha}$	-0.8589 /rad	Stable
Directional Stability	$C_{n\beta}$	0.1079 /rad	Stable	$C_{n\beta}$	0.1699 /rad	Stable
Roll Stability	$C_{l\beta}$	0.0382 /rad	Unstable	$C_{l\beta}$	-0.2271 /rad	Stable
			$X_{NP} = 78\% \text{ MAC}$			$X_{NP} = 50\% \text{ MAC}$

6.5. Horizontal and Vertical Tail Airfoil

Selecting an airfoil for the horizontal and vertical stabilizers began with investigating symmetrical airfoils. The NACA 0009 airfoil was chosen for both stabilizers because of its symmetrical properties and moderate amount of thickness which makes it ideal for tail assemblies. The NACA 0009 airfoil is shown in figure 6-5.

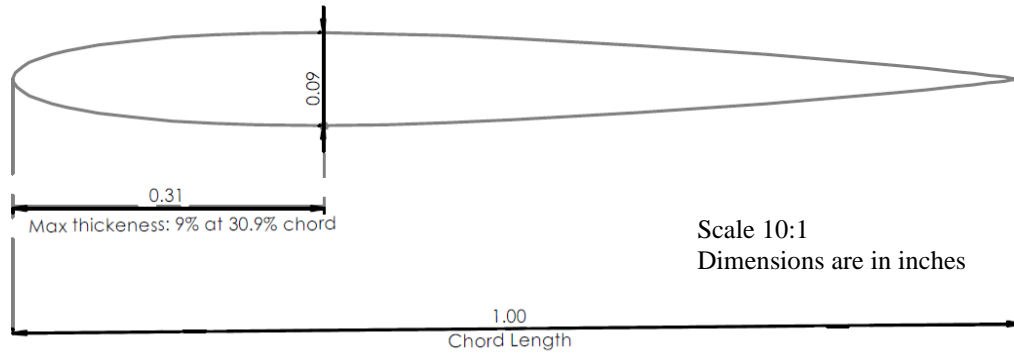


Figure 6-5 NACA 0009 Profile

7. Weight and Balance

7.1. Detailed Weight Breakdown

The maximum takeoff weight of the aircraft was initially sized at 17,400 pounds, as shown in table 4-3, using weight fractions for each mission segment and the weight estimation equations from Nicolai and Carichner section 20 [2]. As the design progressed, the weight estimation was refined using more accurate information and substituting selected components where applicable. Table 7-1 shows each components weight used in the final weight estimation.

Table 7-1 N&C Refined Weight Component Estimations

Component Groups	Equations Used [2]	Weight (lbs)
Wing	20.2	900
Horizontal Tail	20.3a	250
Vertical Tail	20.3b	167
Fuselage	20.4	892
Landing Gear	20.6	700
Engines	Manufacturer data	2,124
Engine Controls	20.24	80
Starting Systems	20.29	36
Propellers	20.31	991
Prop Controls	20.32	14
Surface Controls	20.35	565
Flight Instruments	20.39	16
Engine Instruments	20.40	10
Fuel System	20.16, 20.19, 20.20, 20.21	306
Ejection Seats	20.47	150
Avionics	Table 8.7	300
Electrical System	20.44	3,463
Emergency Equipment	20.48	39
Air Conditioning/ Anti-icing	20.66	146

The empirical formulations used in Nicolai and Carichner section 20 [2] came from many sources such as the U.S. Air Force, U.S. Navy, and commercial aircraft. The estimations were calibrated on a case-by-case basis. Structural analysis and material selection conducted for the wing and fuselage components were implemented into SolidWorks software to obtain the exact mass properties of those components. Other component groups including the landing gear, ejection seats, and electrical system, were calculated with values obtained from actual trade studies selection weights on table 3-3 and table 10-1. Refined weight estimations of the Raymer [3] method was used to derive a more precise weight when compared to similar aircraft.

Table 7-2 Aircraft Detailed Weight Breakdown

Component	Weight (lbs)	Distance from Nose (ft)	Weight Fraction
Wing	2,050	17	0.12
Tail	440	42	0.03
Fuselage	1,750	22	0.16
Landing Gear	640	13	0.05
Nacelle	150	20	0.01
Propellers	990	14	0.09
Flight Controls	600	34	0.05
Instruments	160	7	0.01
Fuel System	310	16	0.03
Electrical	510	15	0.05
Avionics	300	13	0.03
Furnishings	460	8	0.04
AC/ Anti-icing	150	12	0.01
Armor	740	6	0.07
Engines	2,120	17	0.19
Gun	260	8	0.02
Loader	80	10	0.007
Magazine	200	16	0.02
Flare Dispenser	30	40	0.002
Empty Weight	11,960	C.G.	34.8 % MAC
Fuselage Fuel	1,850	19	Fuel, Payload, and Crew
Wing Fuel	1,420	19	
Gun Ammunition	1,530	16	
Armament	1,450	19	
Counter Measures	20	40	
Pilot	400	7	
MTOW	18,700	C.G.	32.8 % MAC

The component weight analysis was further expanded by applying armor, gun, loader, magazine, and flare dispenser components to the calibrated empty weight. Shown in table 7-2, ammunition, armament, and counter measure components were also applied to the maximum takeoff weight. The component weights are derived from manufacturer weight data of the weapon integration selections in table 3-1 and considered in the aircraft's refined weight estimation to account for its unique mission that requires additional components to meet the light attack aircraft performance requirements.

Using the C.G. location of each component, a C.G. can be estimated for the entire aircraft structure. The calculation is performed by determining the added component C.G. locations using the tip of aircraft nose as the x-

direction datum, the aircraft centerline as the y-direction datum, and the bottom of the aircraft as the z-direction datum, along with wing location and mean aerodynamic chord.

Provided the component weights and C.G. location found in table 7-2, combined with the fuel weight found in the initial sizing analysis, the aircraft will have an empty weight of 11,960 pounds with C.G. located at 34.8% MAC and a maximum takeoff weight of 18,700 pounds with C.G. location shifted forward to 32.8% MAC.

7.2. C.G. Travel

The C.G. limits of this aircraft were obtained from the Notch chart in figure 6-3 with the forward C.G. limit located at the landing flare limit, the aft C.G. limit located at the rear stability limit, and a C.G. range of 10% MAC. Using the C.G. limits of 28.5-38.5% MAC from the Notch chart ensures that the Diamondback remains fully stable during flight.

With the weight and balance restrictions in place, four cases were considered: fully loaded maximum takeoff weight for both fuel-loaded first, empty, only payload and only fuel. The C.G. travel for the cases is shown in figure 7-1. All loading cases except for empty includes crew.

To gain more insight of the C.G. behavior of the aircraft during flight, an analysis of the C.G. travel during design mission was added to the weight and balance analysis. The weight fraction ratio at each mission segment from the initial aircraft sizing in table 4-2 was used to determine the fuel reduction at each phase. The fuel reduction coupled with the assumption of all the payload loaded being dropped by the end of the loiter phase results is shown by the dotted line in figure 7-1.

The C.G. travel of the aircraft under different loading configurations and throughout the design mission profile is well within the C.G. limitations, with 2% forward and 4% aft additional margin from the restriction set by the notch chart.

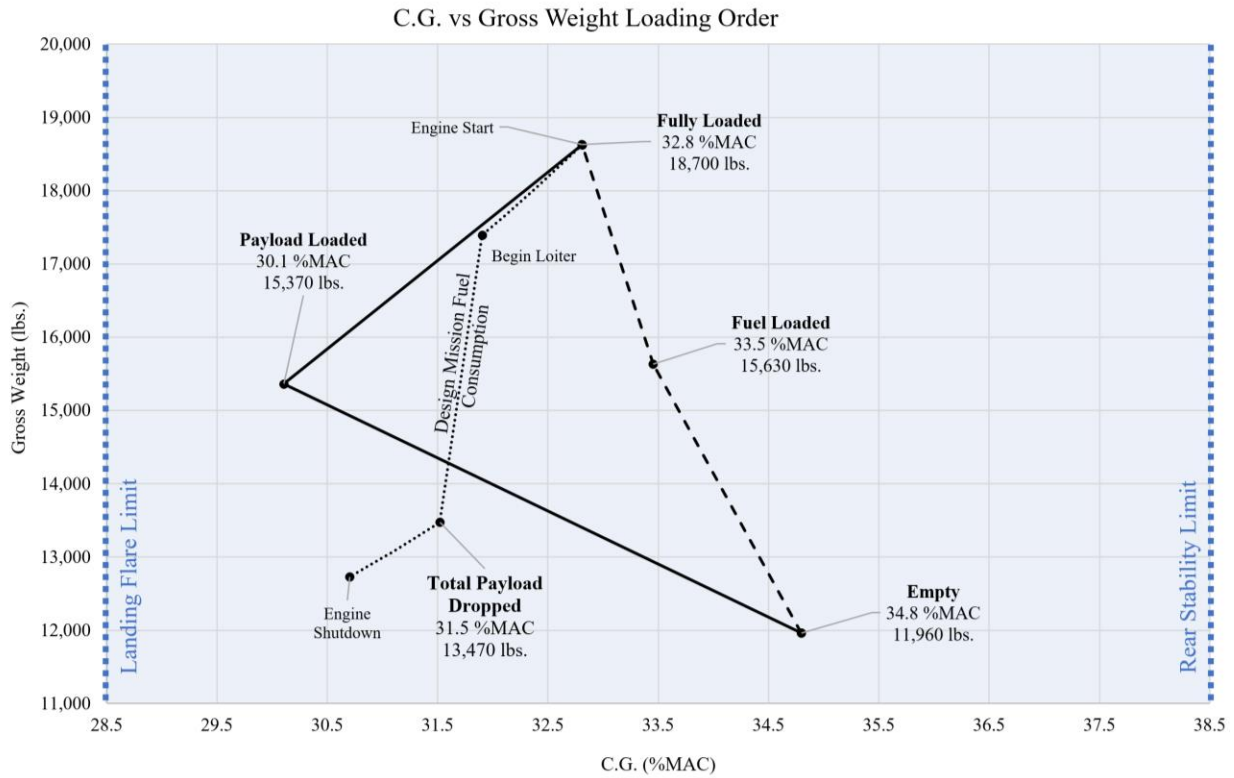


Figure 7-1 C.G. Balance and Travel Diagram

8. Fuselage Layout

8.1. Pilot Accommodations and Viewing Angle

The cockpit configuration shown in figure 8-1 was selected primarily to provide both pilots with the same visibility within the aircraft. This is important as it ensures that both pilots can maximize their viewing angles to be able to operate the aircraft and perform the mission. It is important to note that the model uses a human with a height of 5'8". The configuration resulted in a fuselage design with minimal drag, as previous attempts to explore a tandem pilot configuration resulted in a fuselage design with significantly higher drag and a more limited space for integration of various aircraft components and payload. This is due to the need to place the co-pilot higher to achieve similar viewing angles for tandem configuration.

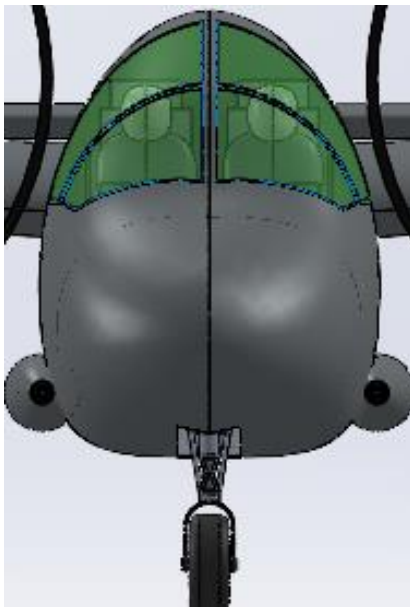


Figure 8-1 Pilot Layout

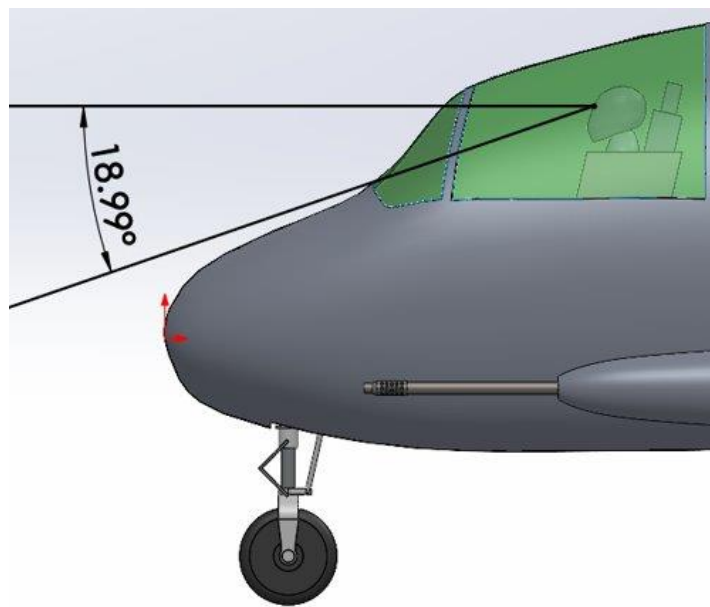


Figure 8-2 Pilot Viewing Angle Measurement

8.2. Tip Back Angle and Turnover Angle

Figure 5-4 show angles of attack of 11 and 10 degrees are needed for takeoff and landing. The landing gear position and empennage design provides a tip back angle of 15.55 degrees, shown in figure 8-3, which exceeds the maximum AOA needed for takeoff and landing. Figure 8-4 shows our aircraft to have a turnover angle of 37.9°, which is less than the maximum recommended turnover angle provided by Raymer’s text of 63° for land-based aircraft.

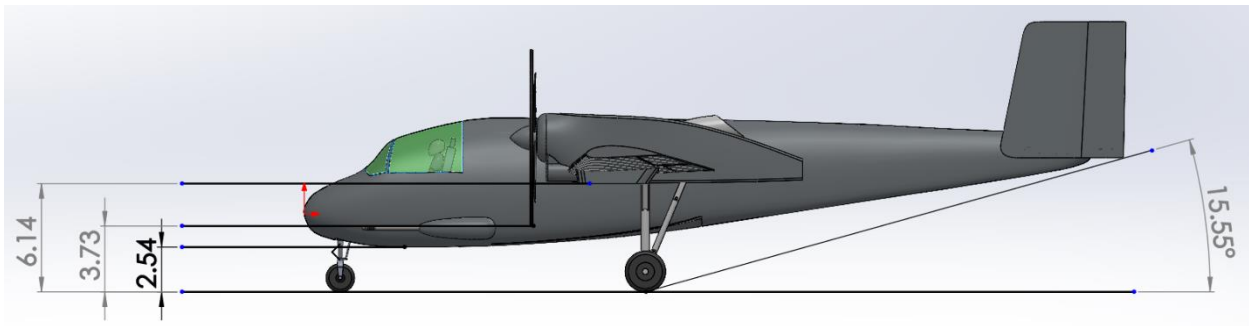


Figure 8-3 Aircraft Ground Clearance Measurements with Tip Back Angle

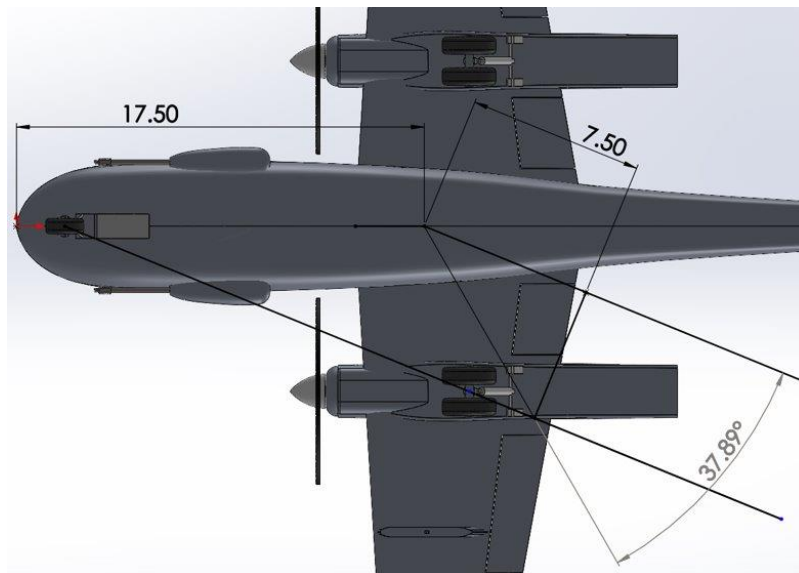


Figure 8-4 Aircraft CG Distance Measurements and Turnover Angle Measurement

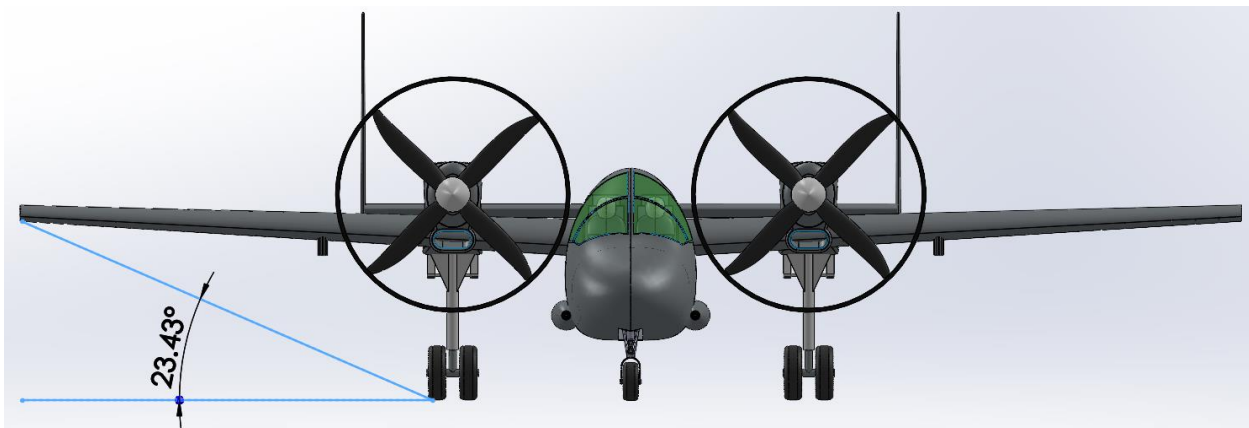


Figure 8-5 Aircraft Front View with Rollover Angle Measurement

9. Propulsion

At the initial phases of the design process little analysis was conducted to discern the pros and cons of each engine type because we believed the differences in the technologies and the engines currently available would not become fully apparent until integrated into an aircraft. Each configuration was equipped with a different engine type so both could be explored. Ultimately, the turboprop configuration was more advantageous due to its higher static thrust which decreased takeoff distance and the lower loiter SFC which decreased the total fuel required. Additionally, a twin-engine configuration was selected for increase survivability and battle damage tolerance.

9.1. Initial Engine Trade Studies

Using the power to weight ratio (P/W) and MTOW at the time of selection, 0.33 and 17,000 lbs respectively, the engines candidates in table 9-1 were selected.

Table 9-1 Engine Candidate Specifications

Engine	Power (eshp)	SFC (lbs/HP/hr)	Weight (lbs)
Pratt Whitney PT6	1,691	0.659	400 lbs
Pratt Whitney PW126A	2,490	0.468	900 lbs
Pratt Whitney PW 127D	2,880	0.468	925 lbs
Pratt Whitney PW 127G	3,058	0.468	1,000 lbs
Rolls Royce AE 2100	4,637	0.46	1,700 lbs

Sources [20] [21] [22]

A similar plot to figure 9-1 was constructed for each engine candidate during the initial sizing phase. Using the Breguet range equation and the weight estimation techniques for Nicolai and Carichner Chapter 20 [2], the relationship between engine weight and SFC can be correlated to aircraft aspect ratio (AR) and MTOW. The design space is then restricted using the wing loading (W/S) vs. power to weight (P/W) lines from the constraint diagram. The PT6 was under powered so its design space was too restrictive, whereas the AE 2100 was overpowered so its design space was excessive and required a high MTOW due to engine weight and fuel burn. The PW126A shown in figure 9-1 was a good balance between ample margin from our constraints and low MTOW. Additionally, the PW-150 family provides numerous engines with varying HP ratings so a more powerful engine could easily be swapped in.

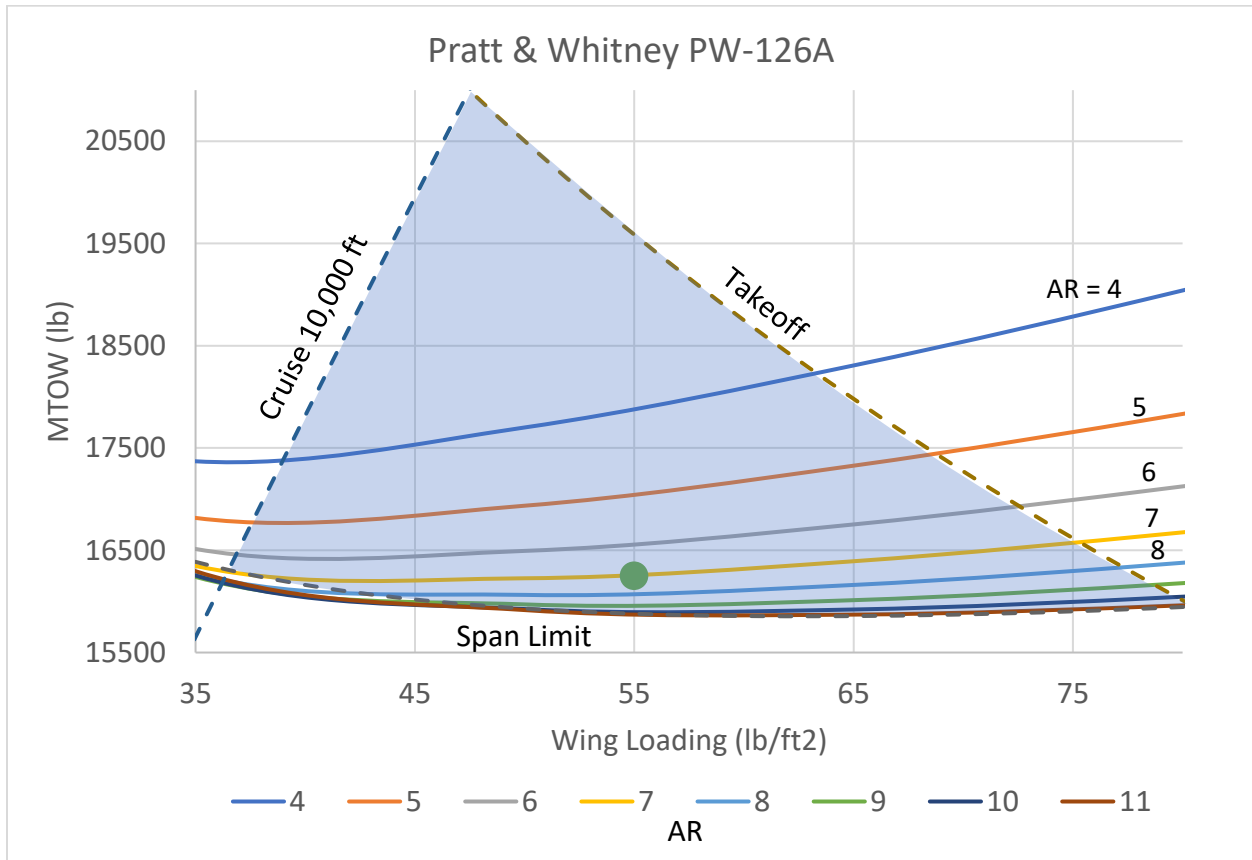


Figure 9-1 PW-126A MTOW vs. Wing Loading and Aspect Ratio

9.2. Propulsion Integration

Two engine configurations were considered: traditional, with one engine on each wing, and push-pull like the Cessna Skymaster. Each were ranked qualitatively in three categories: OEI performance, ground clearance, and installation thrust losses as shown in table 9-2. The traditional configuration scored lower in OEI performance because both engines are away from the centerline whereas the push-pull configuration has both engines on the centerline. The push-pull scored lower for ground clearance because it would have to be provided mostly by landing gear height whereas wing location and landing gear height contribute to the traditional configuration’s propeller clearance. Again, the push-pull configuration scored lower in installed thrust losses because the pusher propeller must be located behind the fuselage which requires additional consideration for airflow. The traditional configuration was selected with the higher weighted score of 3.4.

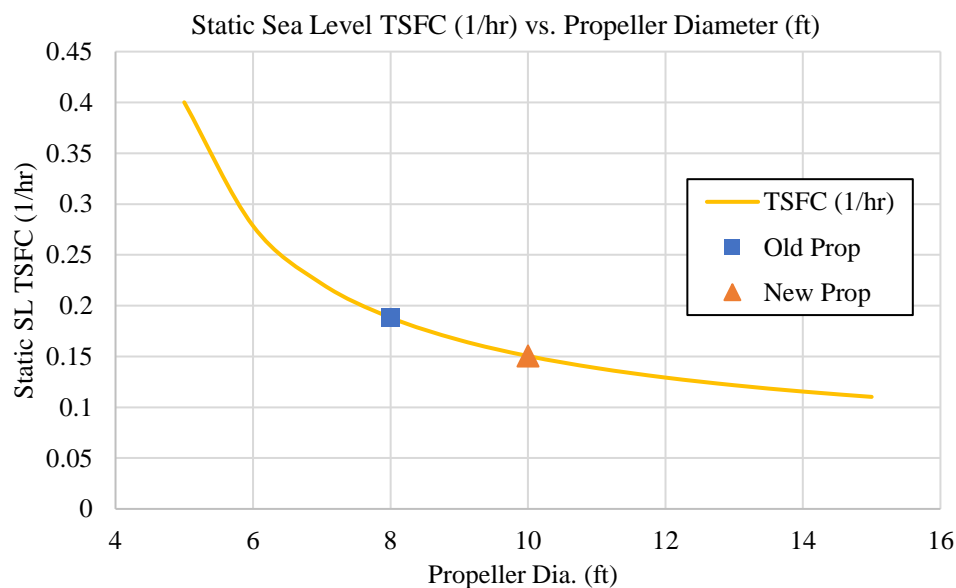
Table 9-2 Engine Configuration Trade Study

Engine Placement			Each Wing	Push-Pull
Criteria	Weight	Scale	Scores	
OEI	0.3	5 = Best	2	5
		1 = Poor		
Ground Clearance	0.4	5 = Most Clearance	4	2
		1 = Least Clearance		
Installed Thrust Loses	0.3	5 = Least Loses	4	2
		1 = Most Loses		
Weighted Totals			3.4	2.9

9.3. Propeller Sizing

The plots provided by Raymer use TSFC whereas most turboprop engines use SFC. For this analysis we converted SFC by multiply by sea-level horsepower and dividing by sea-level static thrust to get the sea-level static TSFC for our engine. This allows both engine and prop characteristics to be considered.

Propeller sizing was governed by ground clearance, wing pylon clearance, propeller disk loading, engine pylon location, and static thrust. Based off other aircraft, the initial design accommodated an 8 ft diameter propeller. However, after further analysis, a larger 10 ft diameter propeller would reduce propeller disk loading thus reducing TSFC by 20%, figure 9-2, and increasing static thrust by 25%, figure 9-3. This reduces fuel requirements and decreases takeoff distance. Static thrust was calculated using figure 17.20 from Nicolai and Carichner [2] which relates propeller disk loading to static thrust.


Figure 9-2 Sea Level Static TSFC vs. Propeller Diameter

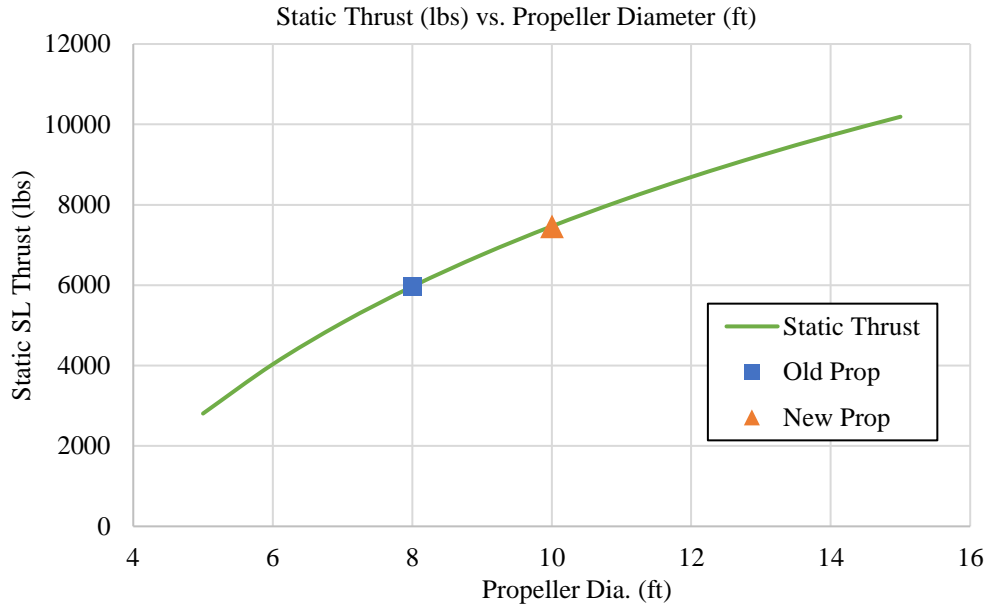


Figure 9-3 Sea Level Static Thrust vs. Propeller Diameter

9.4. Propulsion Mapping and Performance

An engine map is a convenient way to track engine performance throughout its operational envelope. However, a map specific to our selected engine was not readily available so an estimated map was created using data from Raymer Appendix E.3 [2]. Raymer provides plots of uninstalled thrust vs. TSFC for different altitudes as show in figure 9-4. These generic engine plots were normalized using static sea-level thrust and static sea-level TSFC values shown in table 9-3.

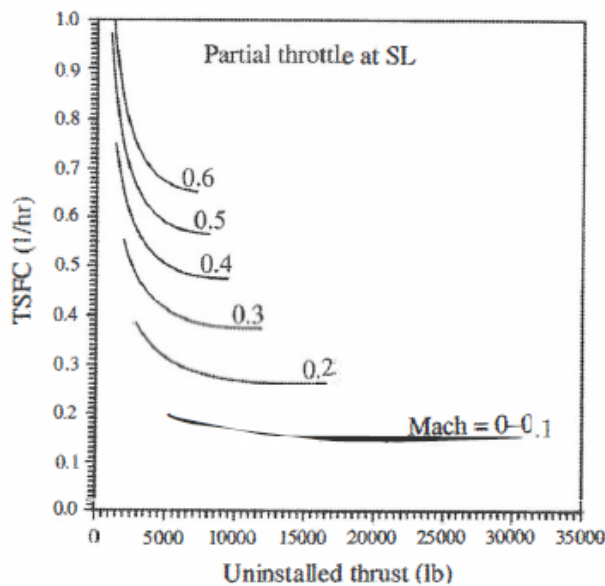
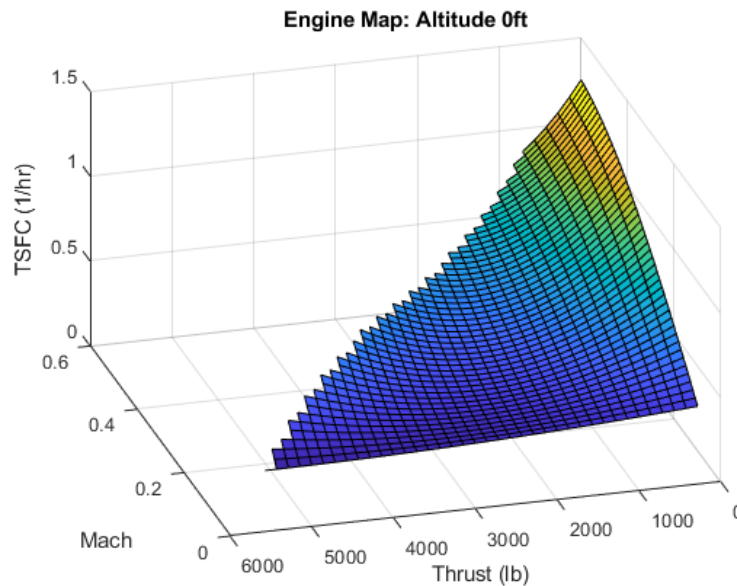


Figure 9-4 Generic Engine Map at Sea Level from Raymer Appendix E.3

Table 9-3 Raymer Generic Turboprop Engine and PW-126A Specifications

Parameters	Raymer Generic Turboprop	PW-126A
Propeller Diameter (ft)	20.5	10
No. of blades	4	4
Sea-level static thrust (lbs)	32,000	7,200
Sea-level static power (HP)	6,500	2,490
Sea-level static TSFC (1/hr)	0.14	0.156

Figure 9-5 shows the new engine mapping for the PW-126A at sea level. Plots were created for altitudes of zero, ten, twenty, and thirty thousand feet. If thrust, Mach number, and altitude are provided then TSFC can be determined. TSFCs at altitudes that do not align with a specific map can be determined by calculating TSFCs on the two adjacent surfaces and then linearly interpolating between them. The diagonal cut on the surface represents the maximum thrust at the corresponding Mach number.


Figure 9-5 PW-126A Engine Map Cacluated From Raymer’s Generic Engine

A time iterative simulation was developed in MATLAB to calculate drag, TSFC, thrust, and weight throughout the mission. Each mission phase is assumed to be steady state, non-accelerating flight, with all forces and moments balanced. This analysis, continued in section 11.5, is extremely valuable because it allows for more accurate fuel burn and operational envelope calculations.

10. Landing Gear Integration

10.1. Landing Gear Configuration Selection

The landing gear was designed to handle maximum loads during takeoff and landing with maximum takeoff weight in austere fields. A retractable tricycle gear design was selected via a trade study that compared 4 different landing gear configurations: fixed tricycle, retractable tricycle, fixed conventional, and retractable conventional. Table 10-1 shows the retractable tricycle gear design was selected as when comparing each configurations weight, wing clearance, pilot visibility, drag, and configuration management. There is one landing gear strut for the nose gear and two for the main gears. The main gear is mounted within the engine nacelles mounted on the aircraft wings. This allows for more space in the fuselage for internally mounted payload, while minimizing the risk of rollover.

Table 10-1 Landing Gear Selection Trade Matrix Results

Unweighted	Retractable Tricycle	Fixed Tricycle	Retractable Conventional	Fixed Conventional
Weight	1	2	2	2.5
Wing/Propeller Clearance	2	2	2	2
Pilot Visibility	2	2	1	1
Drag	2	1	2	1
Configuration Management	2	1	2	1
Weighted Total	1.70	1.65	1.45	1.55

Scale System	
2.5	Extremely well-suited to system objectives
2	Meets/exceeds basic system needs
1	Potential value, but likely unacceptable
-1	Clearly unacceptable to meet system objectives

10.2. Static and Dynamic Loads, and CBR Requirement

Static loading on the main landing gear was designed to be between 82-86% for different loading scenarios. A vertical velocity of 13 ft/s was used for landing calculations based on USAF requirements for trainer aircraft per Raymer [2]. Static and dynamic loads were found and used to size the oleo struts stroke and diameter. A factor of safety of 1.5 was used to account for growth during sizing.

Table 10-2 Static Loading and Maximum Dynamic Loads on Landing Gear

Component	X Distance (ft)	% Load	Loading
CG	17.56	100.00	Full Payload Full Fuel
Nose Gear	15.56	13.56	
Main Gear	2.44	86.44	
CG	17.26	80.98	Full Payload No Fuel
Nose Gear	15.26	15.22	
Main Gear	2.74	84.78	
CG	17.64	82.28	No Payload Full Fuel
Nose Gear	15.64	13.11	
Main Gear	2.36	86.89	
CG	17.61	61.04	No Payload No Fuel
Nose Gear	15.61	13.28	
Main Gear	2.39	86.72	

Dynamic Braking Load on Nose Gear (lbs)	Max Dynamic Load on Main Gear (lbs)
3,960	15,840

10.3. Tire Selection

To ensure optimal performance on austere fields, the California Bearing Ratio requirement was used to select the proper tires. With a California Bearing Ratio of 5, an assumption was made that the tires would have a soil penetration of 0.1 in to minimize sinking during taxiing, takeoff, and landing. Results of the analysis showed that a tire pressure rating no greater than 50 psi would minimize the landing gears ground penetration. Table 10-3 shows the selected tires for the landing gear designs and compares their rated loads to the actual maximum static and dynamic loads on the landing gear. Type III tires were found to be best suited due to their low-pressure ratings. The landing gear brakes and retraction mechanism will be hydraulically operated. A segmented multiple-disc brake design will be integrated within the landing gears. These were selected due to their reliability in the aviation industry. Moreover, the carbon-disk brake variation will be used. This configuration has good braking characteristics for high performance uses while also being lighter than conventional brakes.

Table 10-3 Selected Tires

Landing Gear (# of tires/strut)	Wheel Size/ Tire Size (in)	Pressure (psi)	Manufacturer & Part Number	Rated Static/ Max Load per tire (lbs)	Actual Static/ Actual Max Load per tire (lbs)
Nose (1)	6.0/19.0	48	Goodyear806C81-2	2,800/7,600	2,358/3,960
Main (2)	12.5/27.2	50	Goodyear892C66B1	4,200/11,300	3,760/8,996

10.4. Landing Gear Retraction

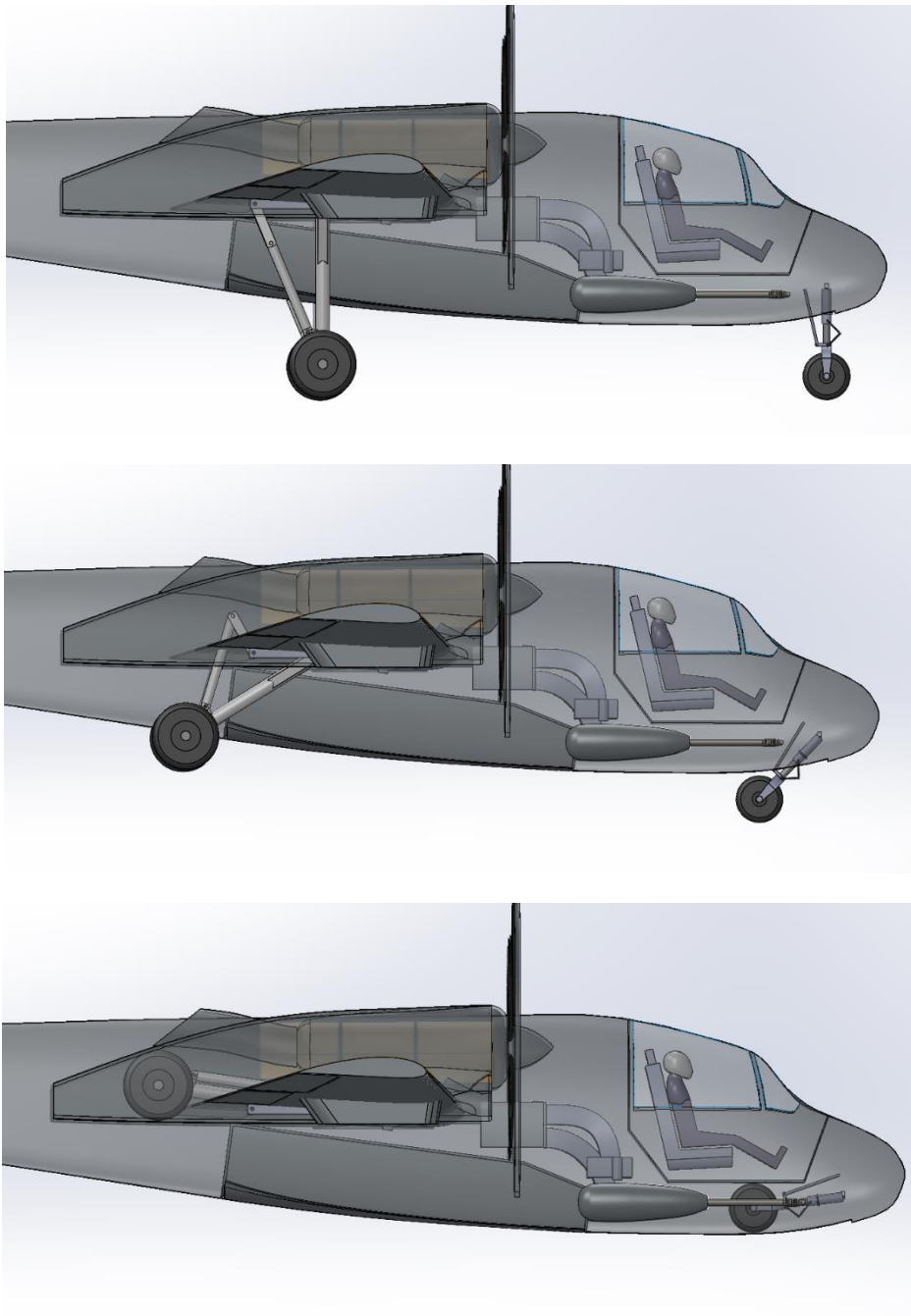


Figure 10-1 Landing Gear Retraction

11. Performance

11.1. Drag Buildup

Drag buildup was calculated for four cases: cruise, loiter, takeoff, and landing as shown in table 11-1. Each case was calculated with the worst-case external payload of eight AGM-114 missiles, four on each wing. Parasite drag was considered for the external payload, fuselage, wing, horizontal tail, vertical tail, landing gear, and engine nacelles. Induced drag was calculated for the wing and flaps.

Table 11-1 Drag Buildup Configurations

Case	Altitude (ft)	Flaps (degree)	Landing Gear
Cruise	10,000	0	Up
Loiter	3,000	0	Up
Takeoff	0	25	Down
Landing	0	40	Down

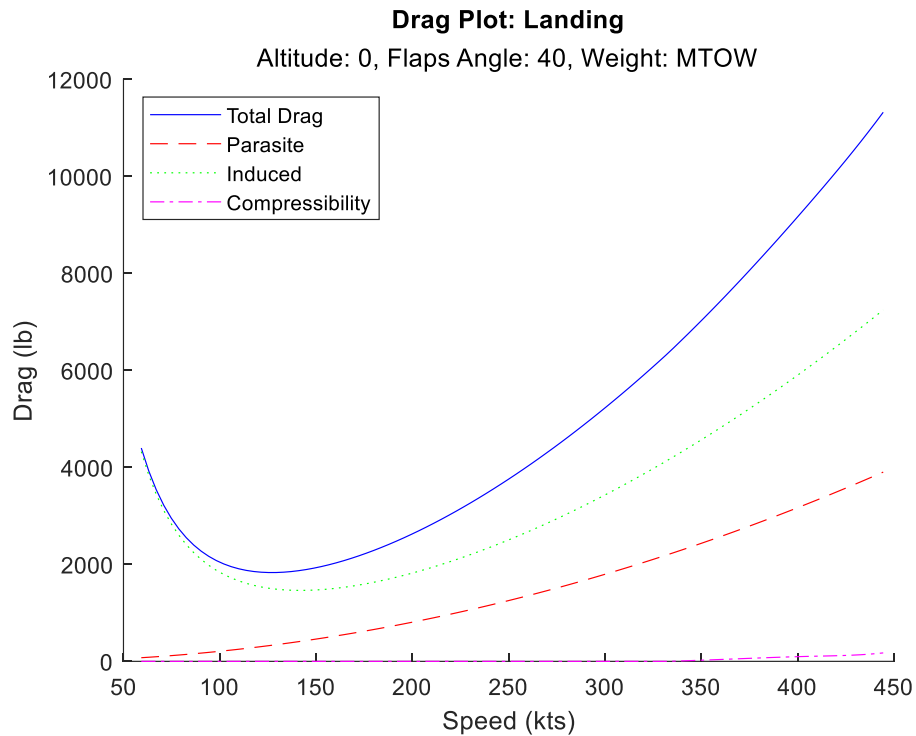


Figure 11-1 Darg Buildup Landing Case

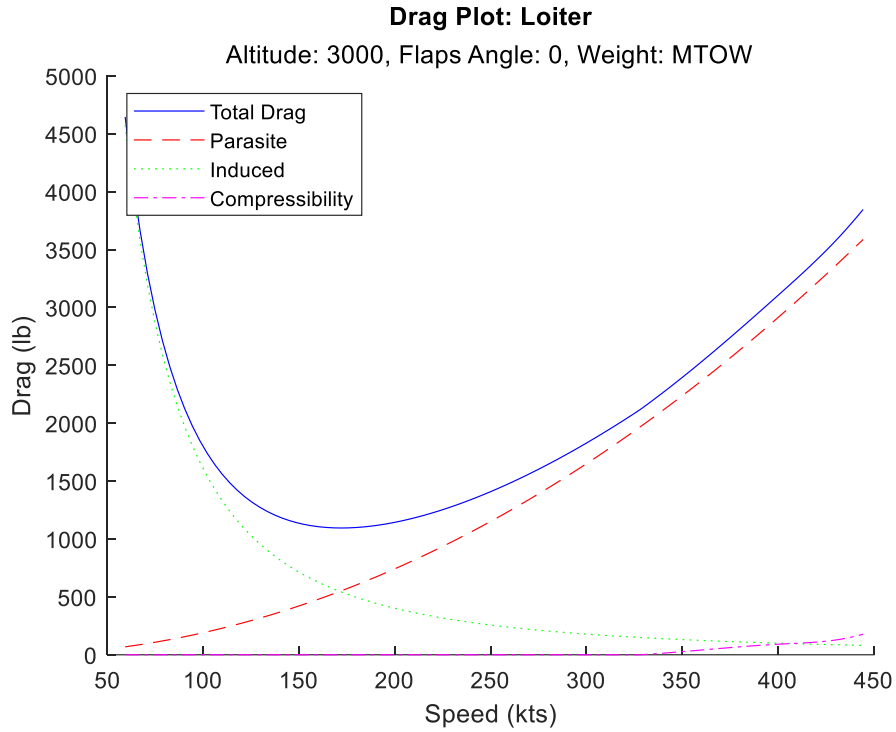


Figure 11-2 Drag Buildup Loiter Case

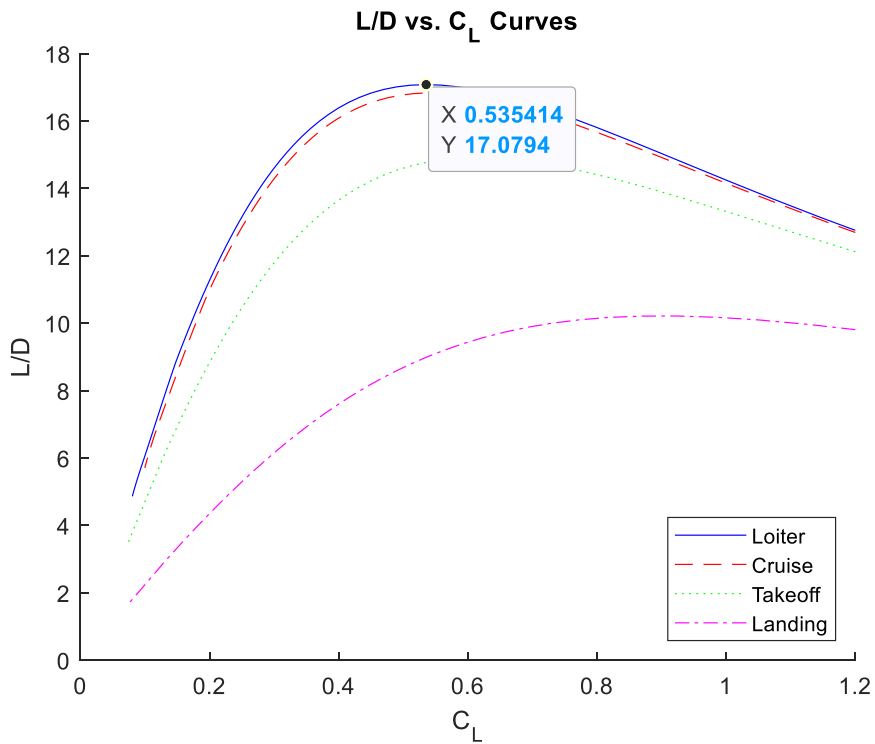


Figure 11-3 L/D vs. C_L

11.2. Operational Envelope

The operating envelope is constrained by three lines: the stall line, service ceiling line, and top speed line. As stated in requirement T7.0, the aircraft has a service ceiling of greater than 30,000 feet, as shown by the blue dotted line on figure 11-4. The yellow triangle shows the dash cruise condition which allows our aircraft to arrive at the loiter station within 20 min of the initial climb, as specified in the RFP design mission profile. Additionally, the green dashed and dotted line shows the large range of speeds the aircraft is capable of during the loiter phase of the mission.

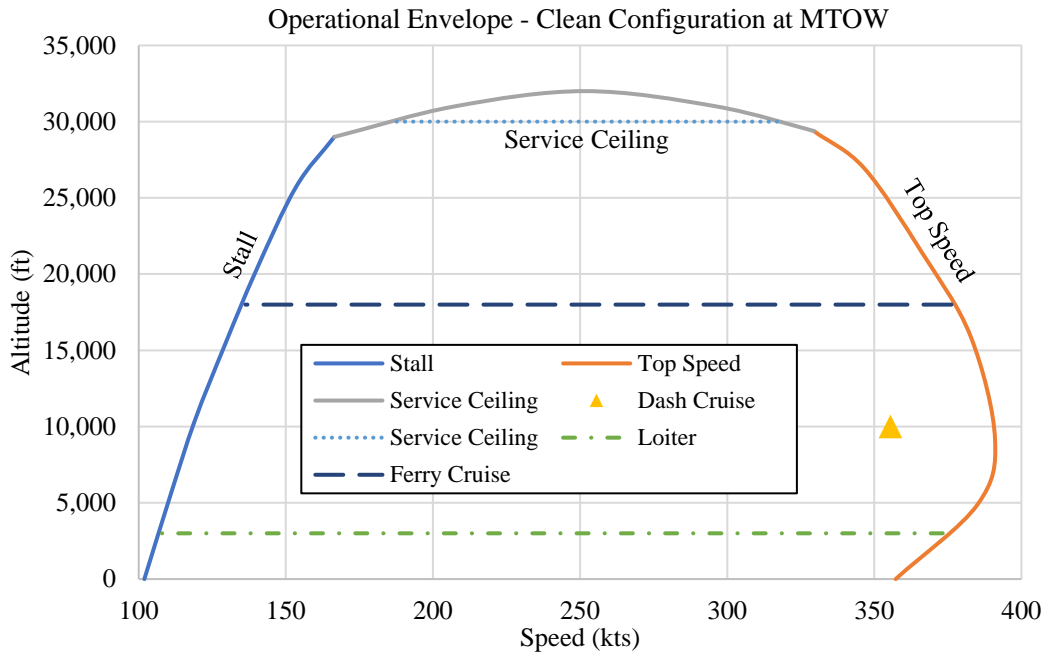


Figure 11-4 Operational Envelope

11.3. Normal Operation Takeoff and Landing

As per the RFP, takeoff and landing were considered at a density altitude of 6,000 ft and the aircraft must clear a 50 ft obstacle in less than 4,000 ft. Takeoff and landing performance was calculated using the technique from Nicolai and Carichner section 10. Both were considered at MTOW to allow for an immediate return to the field after takeoff. Table 11-2, figure 11-5, and figure 11-6 summarizes the results.

Table 11-2 Takeoff and Landing Summary

Parameters	Takeoff	Landing
Weight (lbs)	18,700	18,700
Flap Deflection (degree)	25°	40°
Total Distance (ft)	3,130	3,540

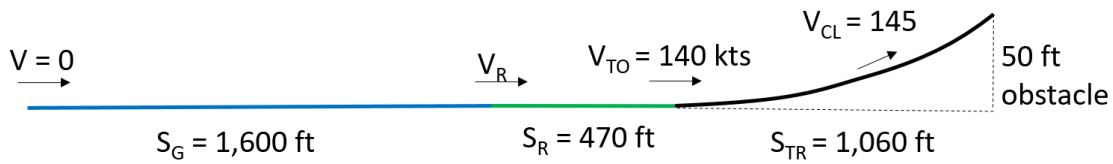


Figure 11-5 Takeoff Overview

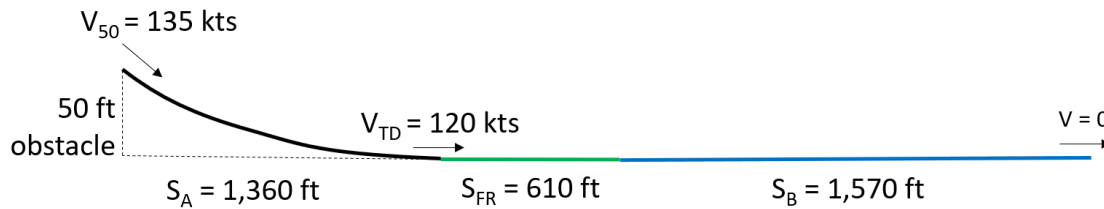


Figure 11-6 Landing Overview

11.4. Balanced Field Length

Figure 11-7 shows the balanced field length analysis. Our aircraft at MTOW will rotate and climb at 140 kts. If an engine fails on takeoff roll before 130 knots is reached, the takeoff should be aborted. Otherwise, the aircraft will not be able to clear the 50 ft obstacle at the end of the runway. If an engine fails after 130 knots, the takeoff can safely continue takeoff and return to the field for a landing.

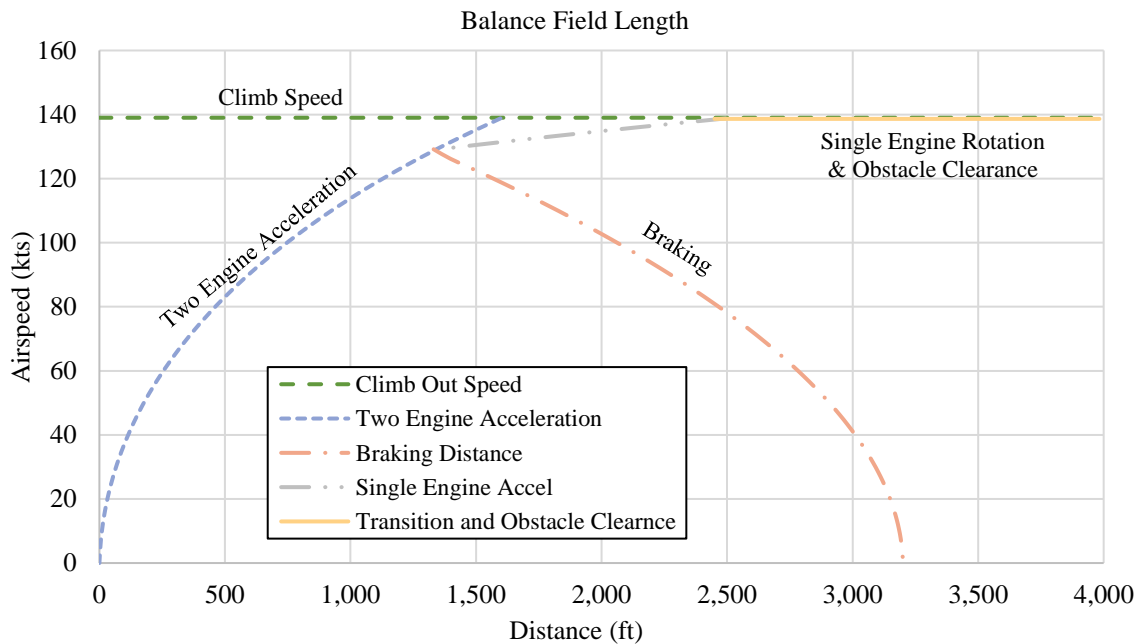


Figure 11-7 Balance Field Length

11.5. Mission Profile Details

Using the engine map from section 9 and the drag calculations from section 11.1, minimum fuel flow speed can be calculated. This is the ideal speed to loiter at because it represents the lowest fuel burn per hour as shown in figure 11-8. This method is more accurate than cruising at the lowest power required speed because it considers the aerodynamic and engine performance. The lowest fuel burn was to close the aircrafts stall speed so a loiter speed of 1.3 x stall was selected because it provides ample margin from stall with minimum increase in fuel flow.

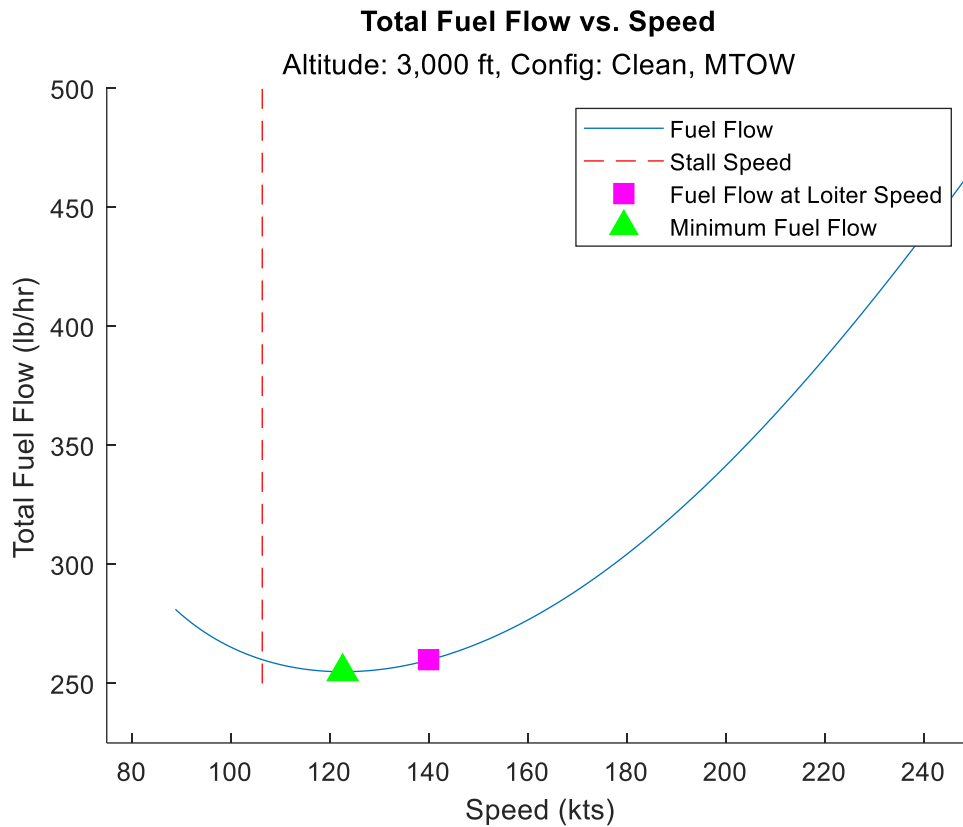


Figure 11-8 Fuel Flow vs. Speed

A similar analysis was done for the cruise mission segment. This only applies to the return cruise portion of the design mission and ferry mission because these segments are not time restricted. Figure 11-9 shows the minimum fuel burn per nautical mile. The minimum fuel per nautical mile speed is sufficiently faster than stall speed so no additional margin is required.

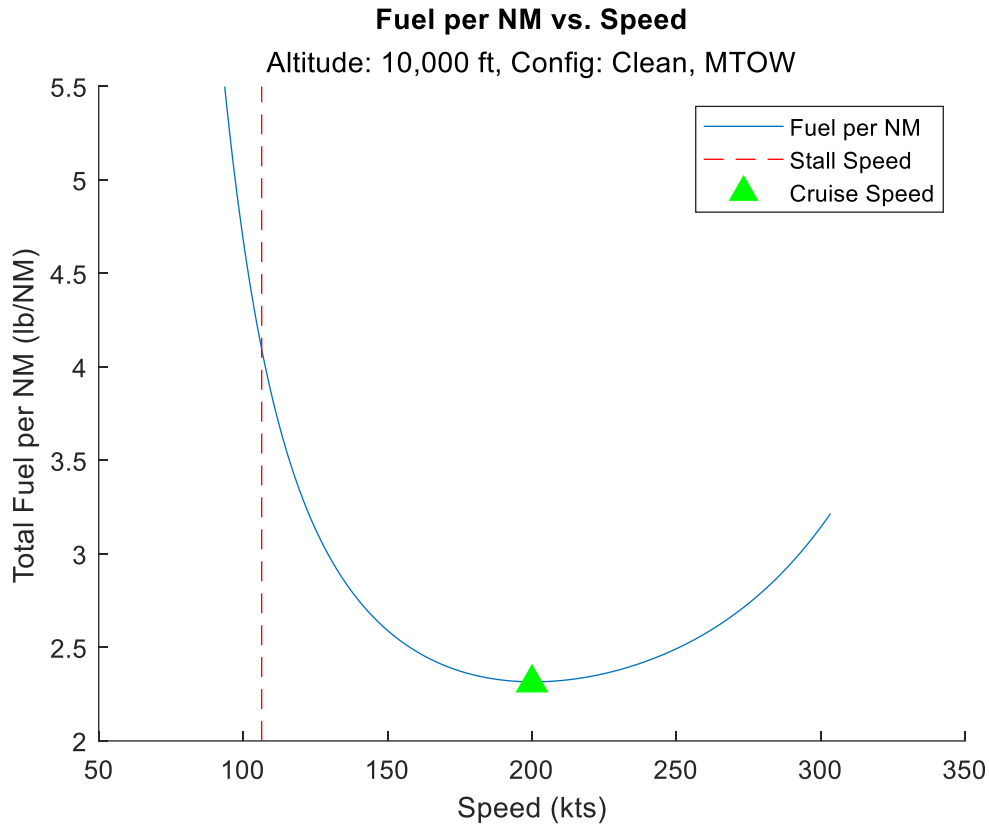


Figure 11-9 Fuel per Nautical Mile

11.6. Mission Fuel Burn

Using the engine map discussed in section 9 and the loiter and cruise speed analysis mentioned previously in this section, a time iterative analysis was conducted to calculate the required fuel. As predicted by the initial fuel estimates, the design mission will require more fuel. Fuel is calculated by comparing the aircraft's initial weight to the final weight. No payload is dropped during either mission, so the difference is the fuel burned. These weight values along with the mission duration are summarized in table 11-3.

Table 11-3 Mission Profiles Fuel Burn and Duration

Parameters	Design Mission	Ferry Mission
Fuel Burn (lbs)	3,100	2,500
Duration	5:50	7:15

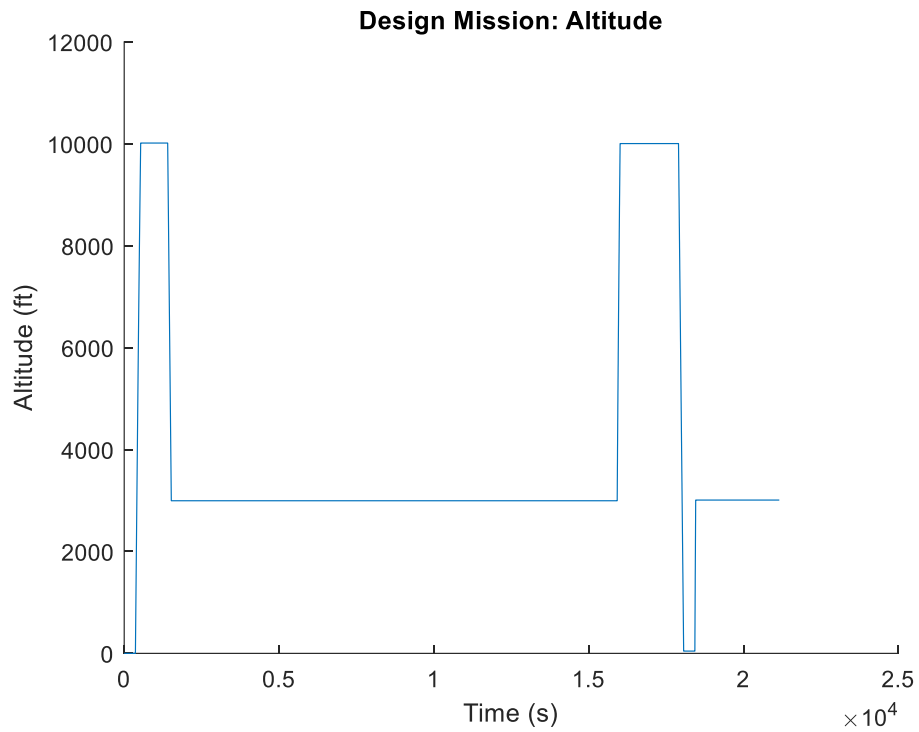


Figure 11-10 Design Mission Altitude Profile

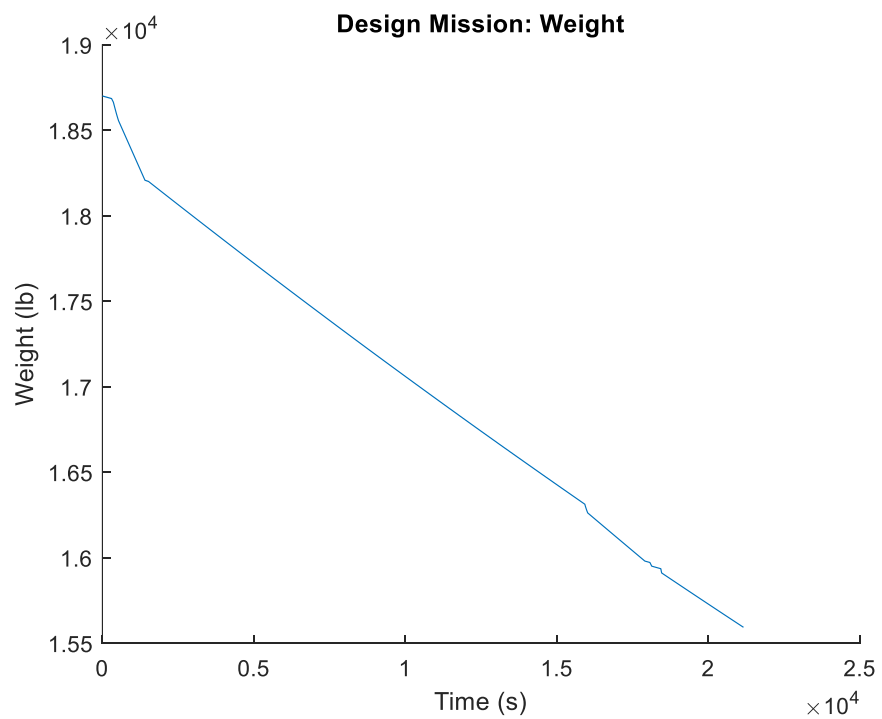


Figure 11-11 Design Mission Weight Profile

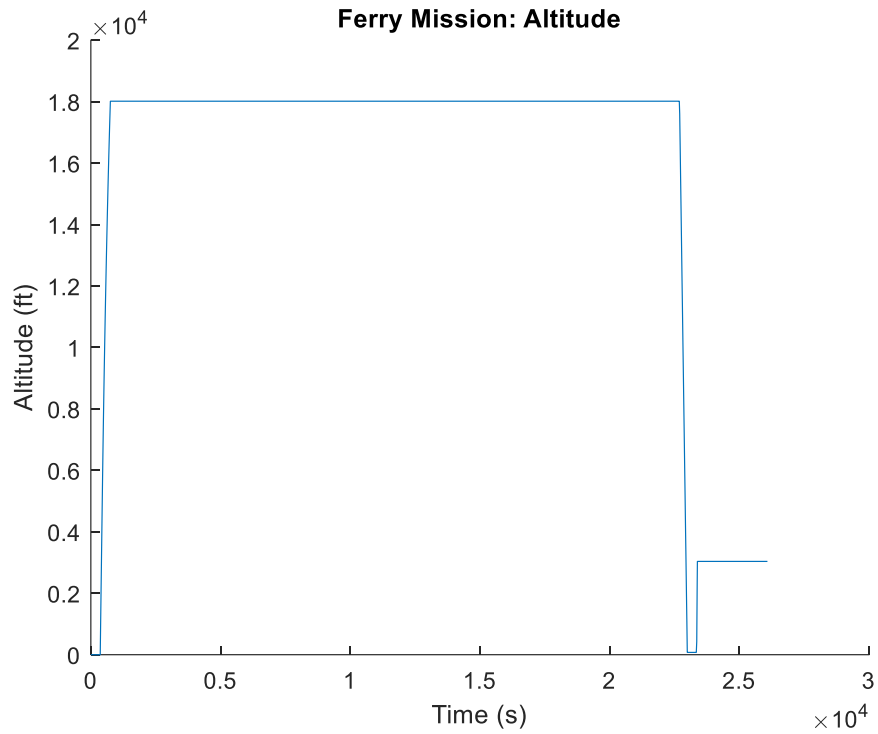


Figure 11-12 Ferry Mission Altitude Profile

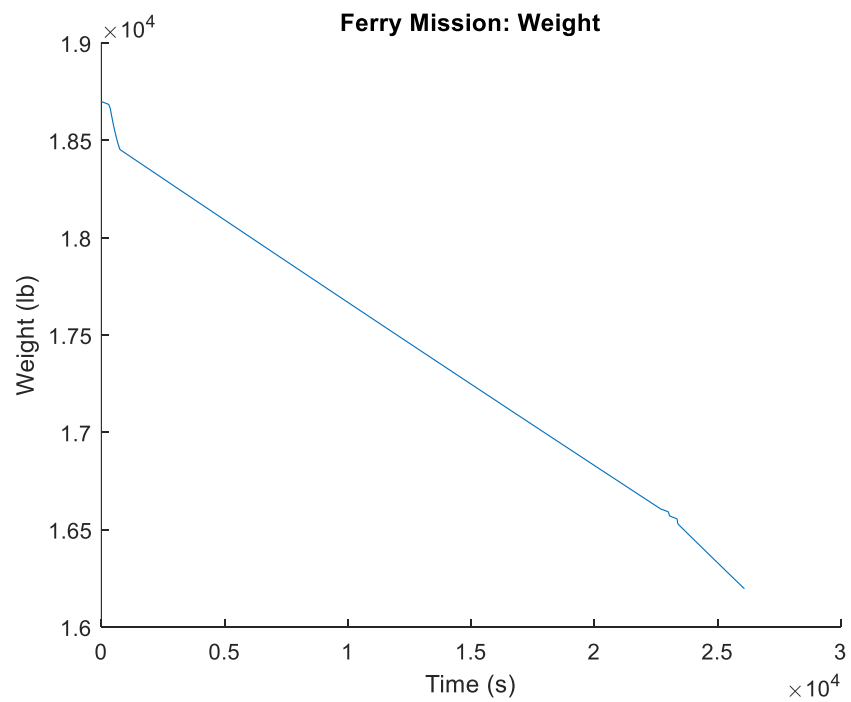


Figure 11-13 Ferry Mission Weight Profile

12. Material Selection

Trends for modern attack aircraft will be followed which include various materials such as composites and alloys. Any part that is to withstand impact forces like the landing gear will use steel alloys. Steel alloys have predictable and high fatigue life as well as a larger elastic modulus when compared to aluminum.

Any external materials such as skins and stringers will be made of aluminum alloys. This will enable ease of maintenance on the battle grounds. Aluminum alloys are easily mended with traditional fasteners and rivets as shown on the figure to the right [9]. Such repairs can be made as needed at base camps after missions. Wing spars and other internal structural components will be composed of carbon epoxy composites as they offer on average 20% weight saving based on Nicolai and Carichner [2]. Carbon epoxy will be used due to its high strength to weight ratio and its wide use in the aerospace industry. Wing spars will be protected by surrounding alloys but if damaged will require mending and/or replacement. The use of a combination between internal composites and external alloys will provide ease of maintenance from outside damage and weight saving which benefits cost, endurance, and range.

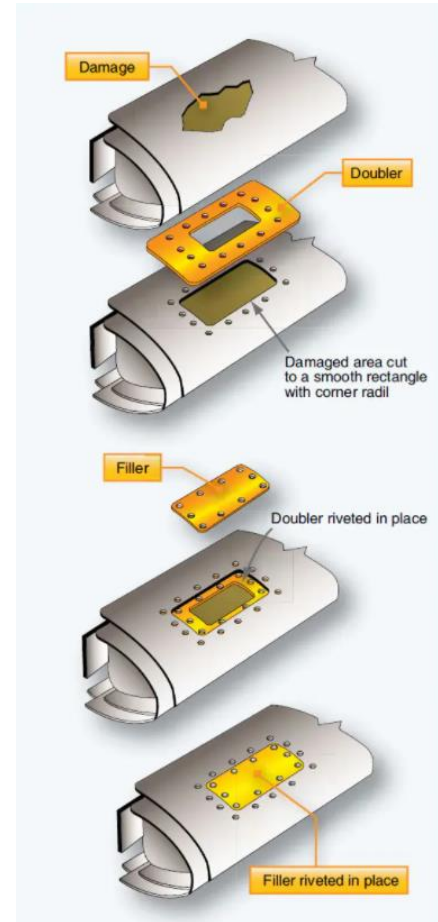


Figure 12-1 Flush Patch Repair

13. Structural Analysis

13.1. V-n Diagram

A V-n diagram is first constructed to outline the flight envelope of the aircraft. The positive and negative load factors of 7.5 and -3.0 as well as information for stall lines and the limit velocity are acquired from military specifications MIL-A-8861B for attack/fighter aircraft at max takeoff weight. Figure 13-1 below represents the flight envelope at sea level for a max takeoff weight of 18,700 pounds and a clean configuration (no flaps or slats deployed). The equivalent airspeeds for stall, corner, cruise, and limit velocities are defined in the figure below with vertical lines, respectively.

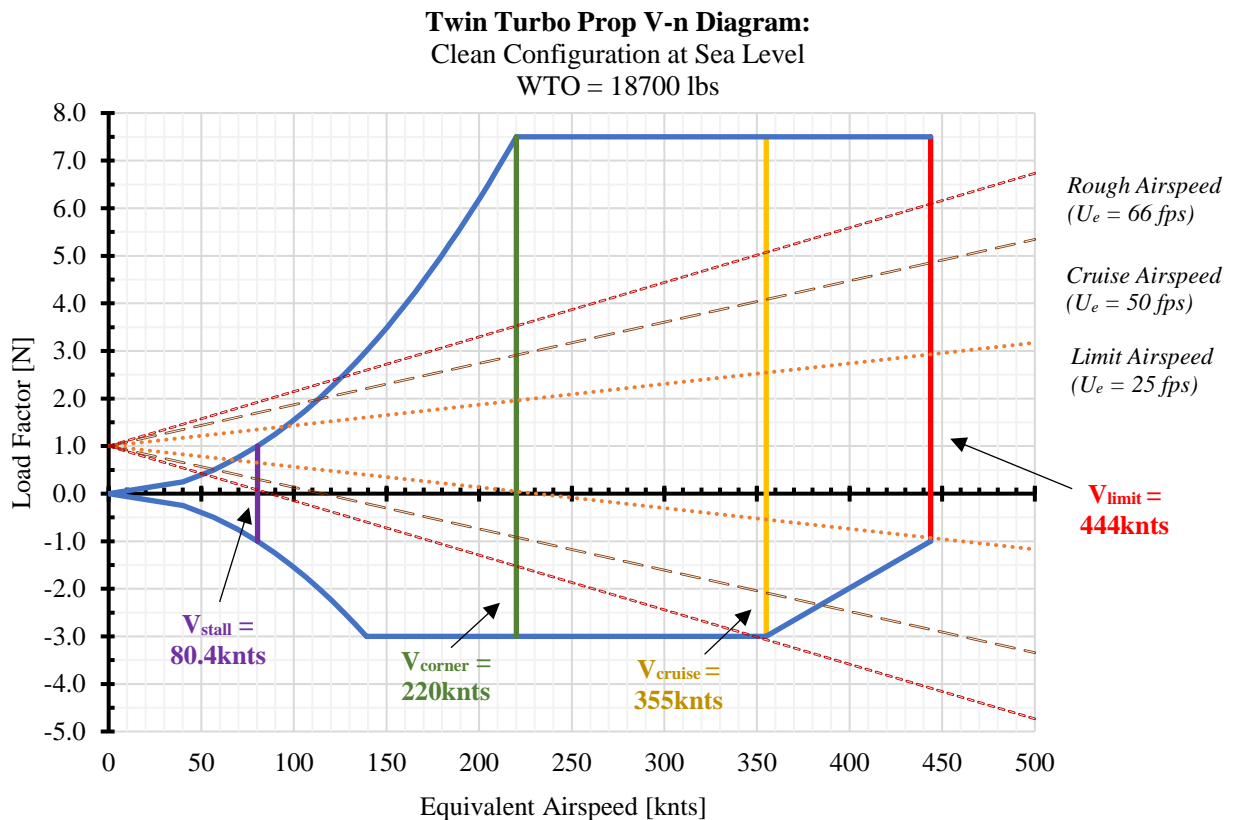


Figure 13-1 Twin Turbo Prop V-n Diagram

A discrete gust analysis is also conducted at the limit, cruise, and rough airspeeds which apply to altitudes in the range of 0 to 20,000 feet. The aircrafts cruise altitude of 10,000 feet falls within this range. The equivalent gust velocities, U_e , are acquired from Nicolai and Carichner [2] figure 19.5 where 25 feet per second (fps), 50 fps, and 66 fps are used for the limit (dive), cruise, and rough airspeeds, respectively. Note that all these gust loads fall within the flight envelope and therefore are not critical to the structural integrity.

13.2. Wing Structure

13.2.1. Wing Load Paths

We analyzed the wing's load paths under the 7.5 load factor. Two different configurations are analyzed, one with the max takeoff weight of 18,700 pounds and another with the empty weight of 11,700 pounds. This is done to compare and acquire the maximum moment at the root of wing. The load paths that pertain to the max takeoff weight had the maximum moment at the root. They are shown below in figures 13-2 through 13-4. The first figure summarizes the elliptical aerodynamic load and the second summarizes structural loads on the wing, such as spars, ribs, fuel, payload pylon, and the engine mount. Figure 13-4 shows the total load path on the wing. The total load path on the wing is then integrated to acquire the shear and moment diagrams.

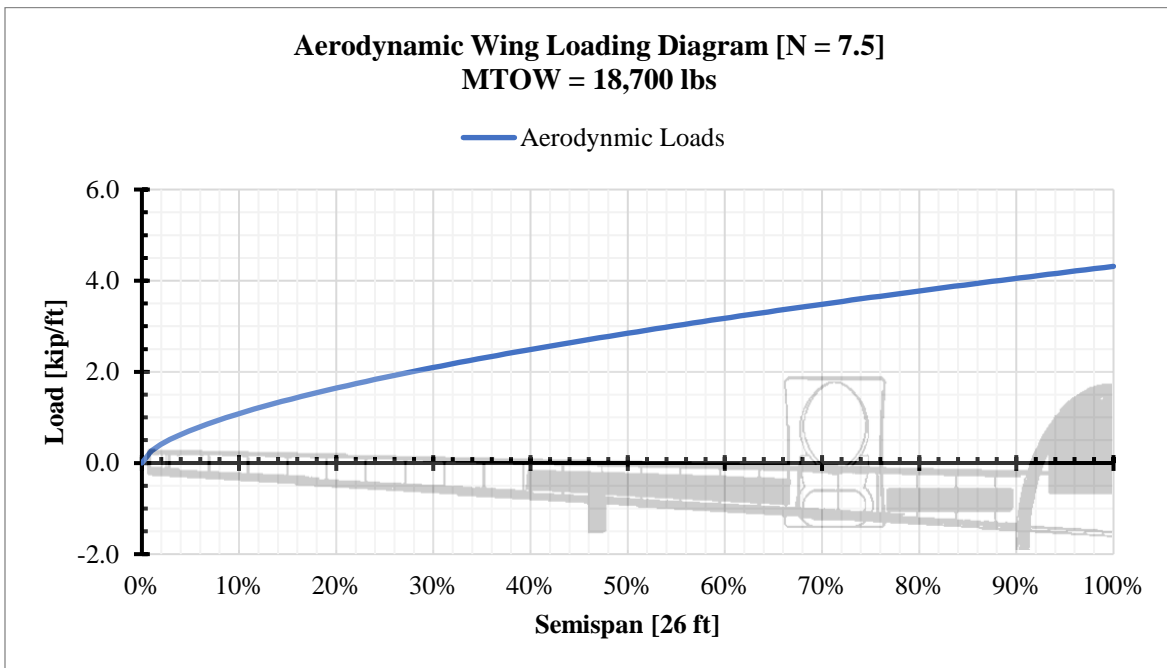


Figure 13-2 Aerodynamic Wing Loading Diagram

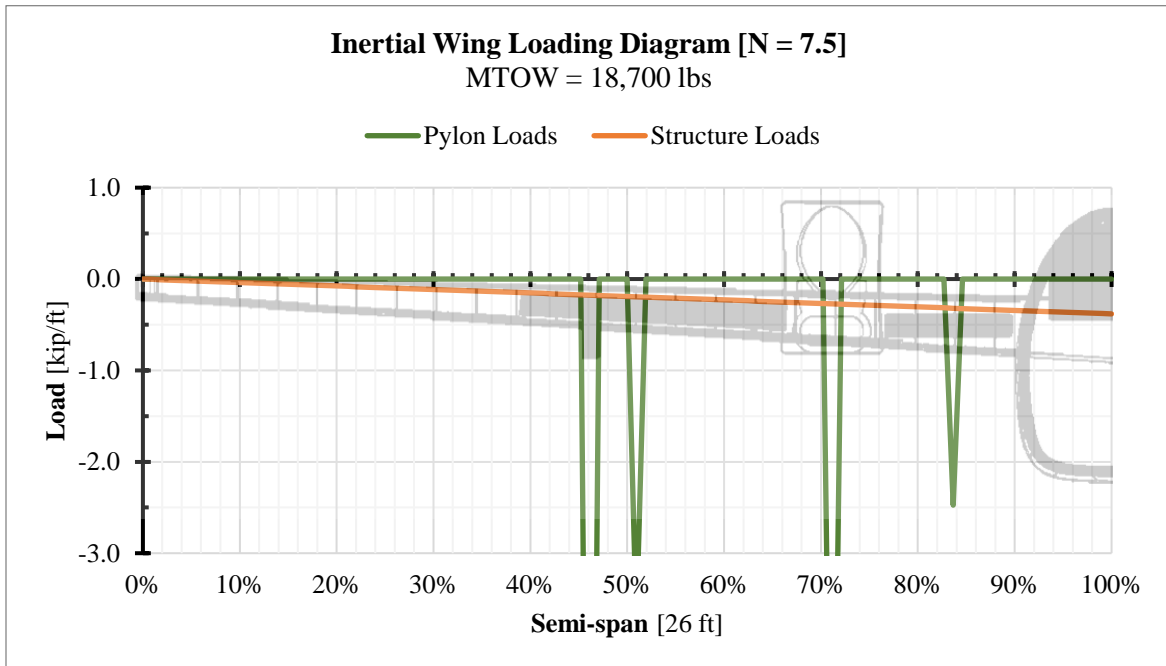


Figure 13-3 Inertial Wing Loading Diagram

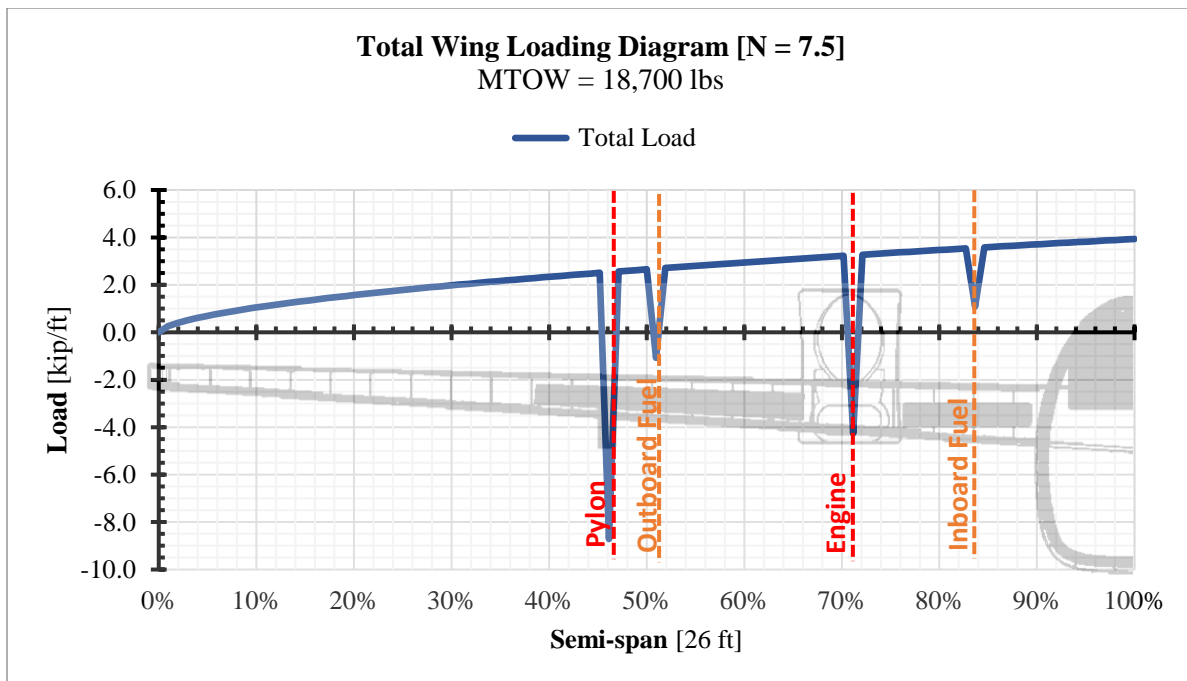


Figure 13-4 Total Wing Loading Diagram

13.2.2. Wing Shear Diagram and Moment Diagram

Integration of the total load on the wing results in the shear diagram shown below in figure 13-5. The maximum shear for max takeoff weight is 40.2 kips. Further integration of the shear diagram results in the moment diagram shown in figure 13-6. The max moment is 386 ft-kips at the root of the wing. This information is carried over to conduct wing bending analysis.

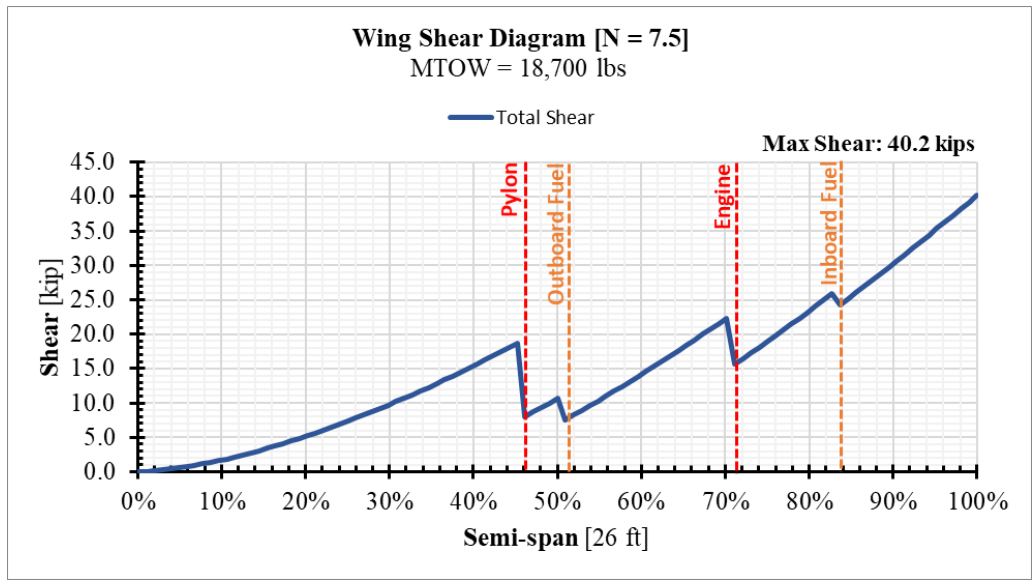


Figure 13-5 Wing Shear Diagram

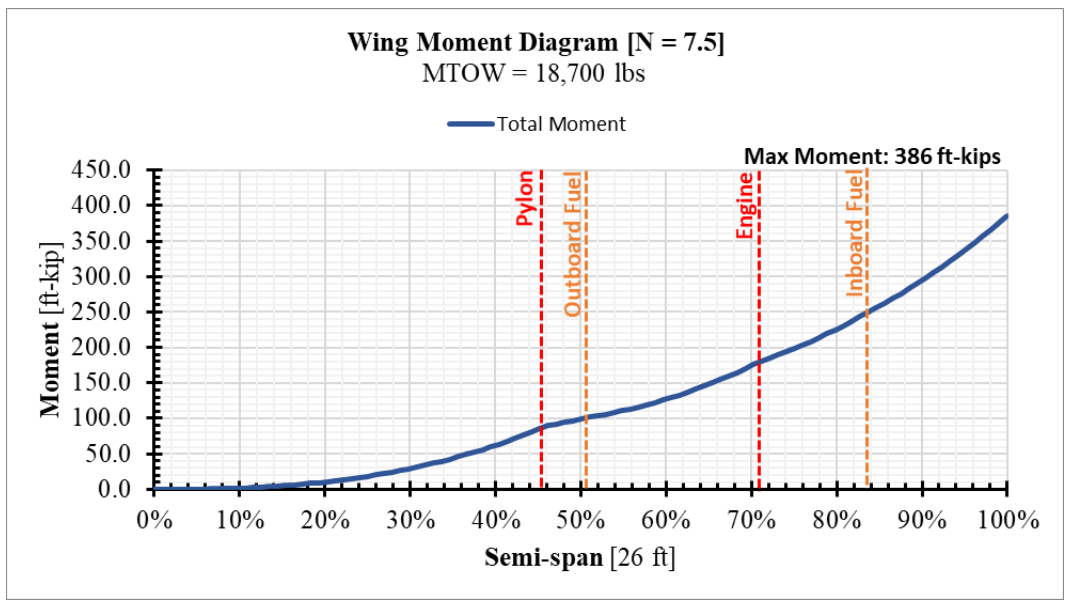


Figure 13-6 Wing Moment Diagram

13.2.3. Wing Bending Analysis

Preliminary wing bending analysis consisted of a hand lumped area analysis with a front spar at 25% of the chord and a rear spar at 75% of the chord. Stringers with an area of 0.5 square inches are placed 8 inches apart from one another as shown in figure 13-7 with the red dots. This information is based on historical data [3]. The spar caps are defined by the black dots. The stringers and spars caps are assumed to take only axial loads (compression and tension). Conducting a bending analysis using the method of lumped areas from Bruhn’s aircraft structure textbook [8] with the 386 ft-kip moment resulted in a max compression stress of 43.8 kips per square inch (ksi) on stringer 7 and a max tension stress of 39.9 ksi on stringer 12 during a 7.5g load.

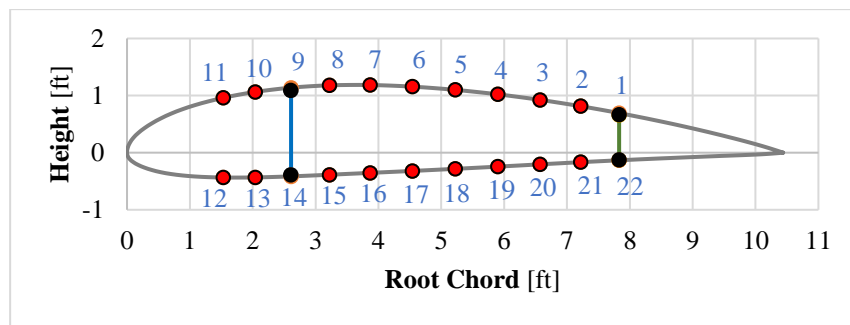


Figure 13-7 Root Chord Stringer Placement

Even though there is increasing use of composites in the aerospace industry, aluminum alloys will be used for the construction of the skin and the stringers. The lowest factor of safety was determined to be 1.75 at the max compression stringer 7, which exceeds the required factor of safety of 1.5. The stringers and skin will consist of extruded aluminum 7075-t6 that holds a yield compression allowable of 74 ksi. The use of aluminum alloys will bring the manufacturing costs down as well as ease of maintenance on the battle fields as compared to composites. Stringers and skin panels will be easier to replace with the use of fasteners and rivets without reducing the structural integrity of the part. The stringers are designed with hat cross-sectional areas to maximize the contact area with the upper and lower skin as shown below in figure 13-8. Rib placement was determined with historical data and are placed 1 foot apart from each other.

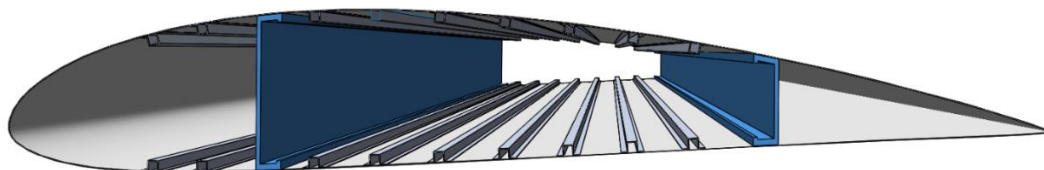


Figure 13-7 Wing Hat Stringers and C-channel Spars

The front spar and rear spar incorporate a c-channel design and are composed of carbon fiber-epoxy composites. Even though carbon-epoxy composites are more costly than aluminum alloys, they have a strength to weight ratio of about 2.9 times that of aluminum 7075-t6. This gives advantages with weight reduction therefore increasing range and endurance. Bending analysis conducted on the spars with the assumption that they will carry all the bending loads results in a factor of safety of 1.7. The C-channel spars allow for ease of inspections for damage and fractures as well make space for wing fuel tanks. The spars along and fuel tanks will be protected by the surrounding alloys during combat. High damage to spars will require dismounting of the entire wing and replacing spars. The overall preliminary structure is displayed below in figure 13-9.

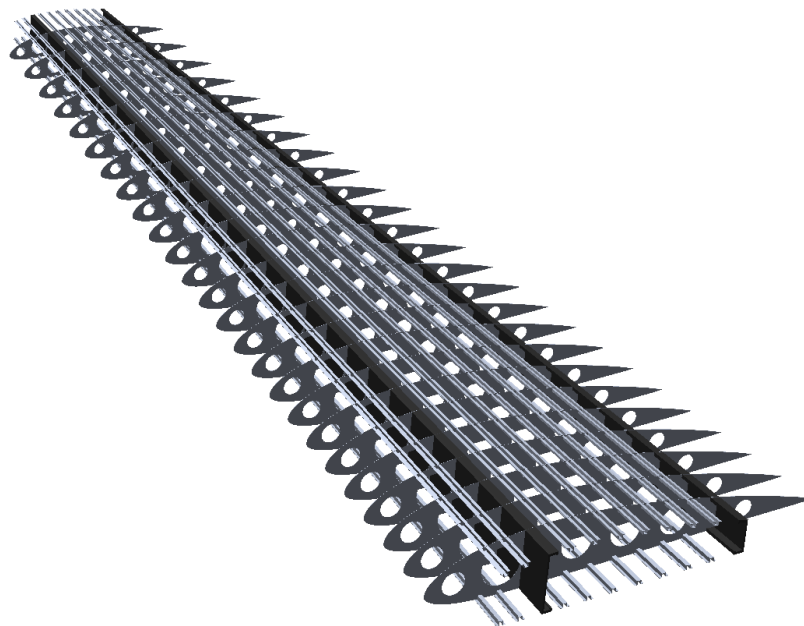


Figure 13-8 Wing Structure

13.3. Fuselage Structure

13.3.1. Fuselage Load Paths

Analysis on the fuselage was conducted in a similar fashion as the wing bending analysis. The fuselage was sectioned off into a part forward of the wing and a part aft of the wing as denoted by the dashed orange lines in figure 13-10. The arrows represent the lift load and the structural loads during a 7.5 g load. The critical section of the fuselage will be determined by analyzing and comparing the max moments between the fuselage forward of the leading edge (LE) at 14.5 ft with respect to the nose and the fuselage aft of the trailing edge (TE) at 24.9 ft with respect to the nose.

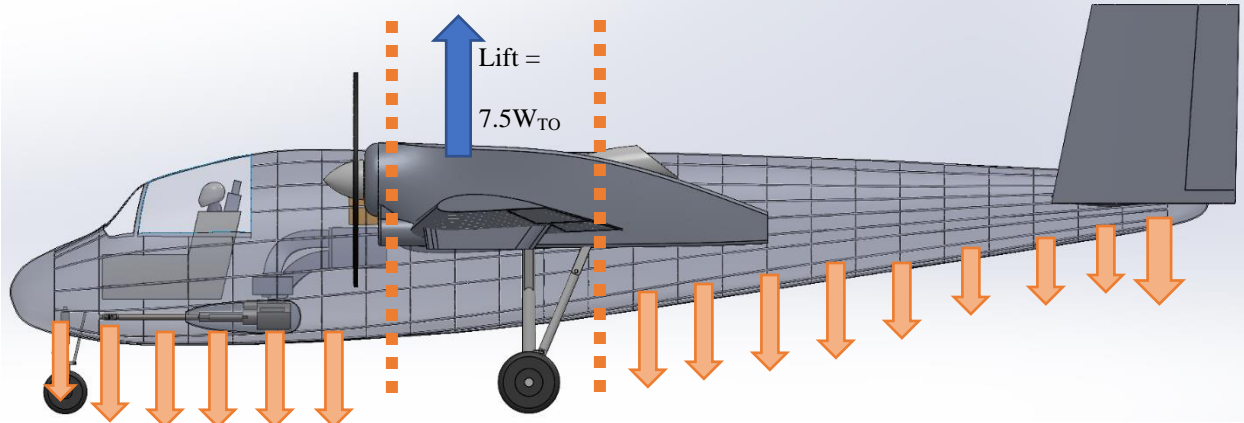


Figure 13-9 Fuselage Loading Diagram

13.3.2. Fuselage Shear Diagrams and Moment Diagrams

The shear and moment diagrams for the fuselage with respect to their sections are shown in figures 13-11 through 13-14. The shear diagrams indicate structure loads and internal loads such as guns, instruments, fuel, and so forth. The total shear load is shown by the orange line and then integrated to acquire the total moment diagrams. The critical fuselage section turned out to be forward of the leading edge with a max shear of 15.1 kips and a max moment of 140 ft-kips.

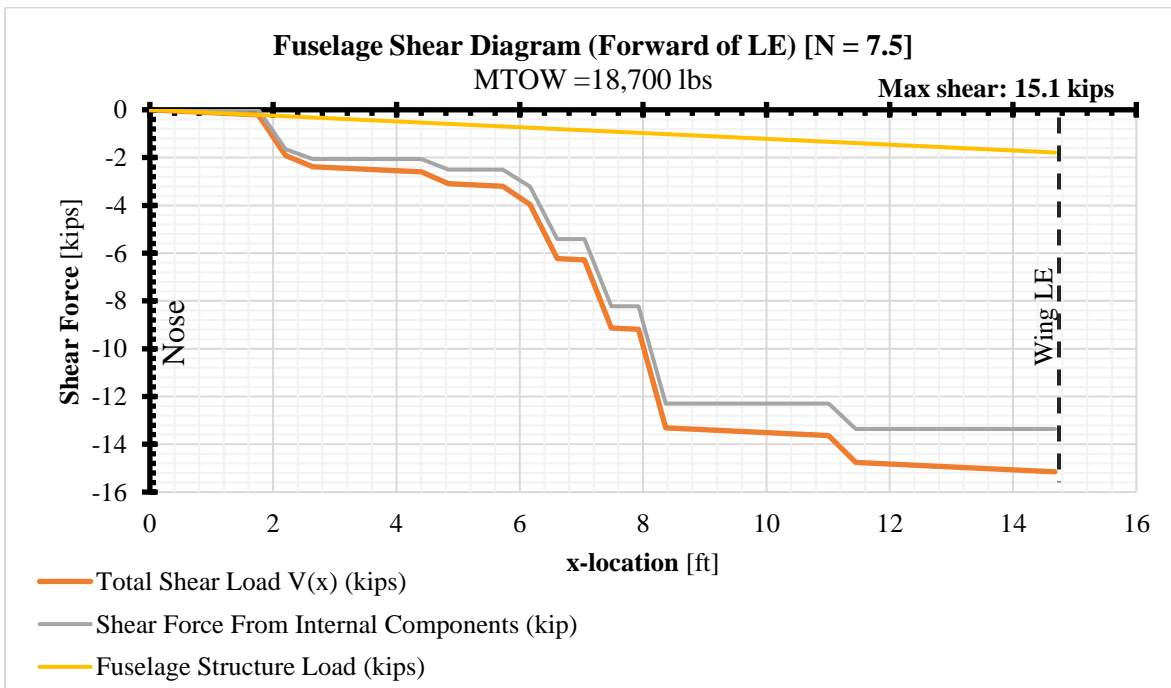


Figure 13-10 Fuselage Shear Diagram Forward of Wing Leading Edge

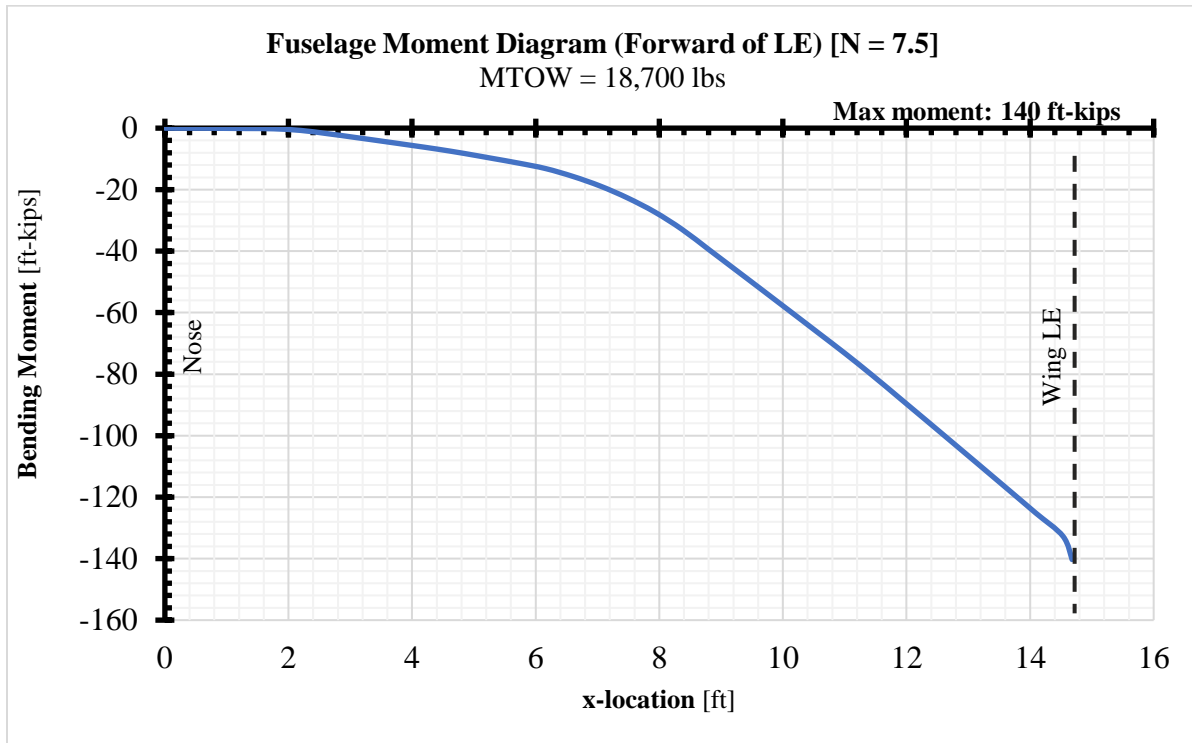


Figure 13-11 Fuselage Moment Diagram Forward of Wing Leading Edge

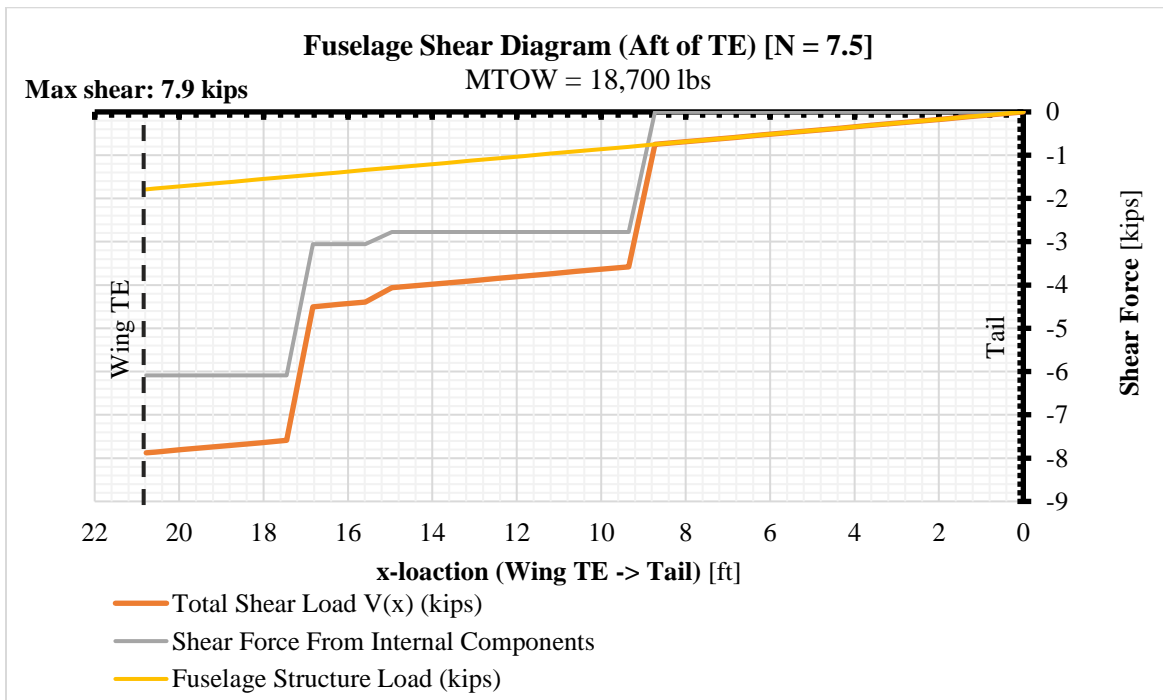


Figure 13-12 Fuselage Shear Diagram Aft of Wing Traile Edge

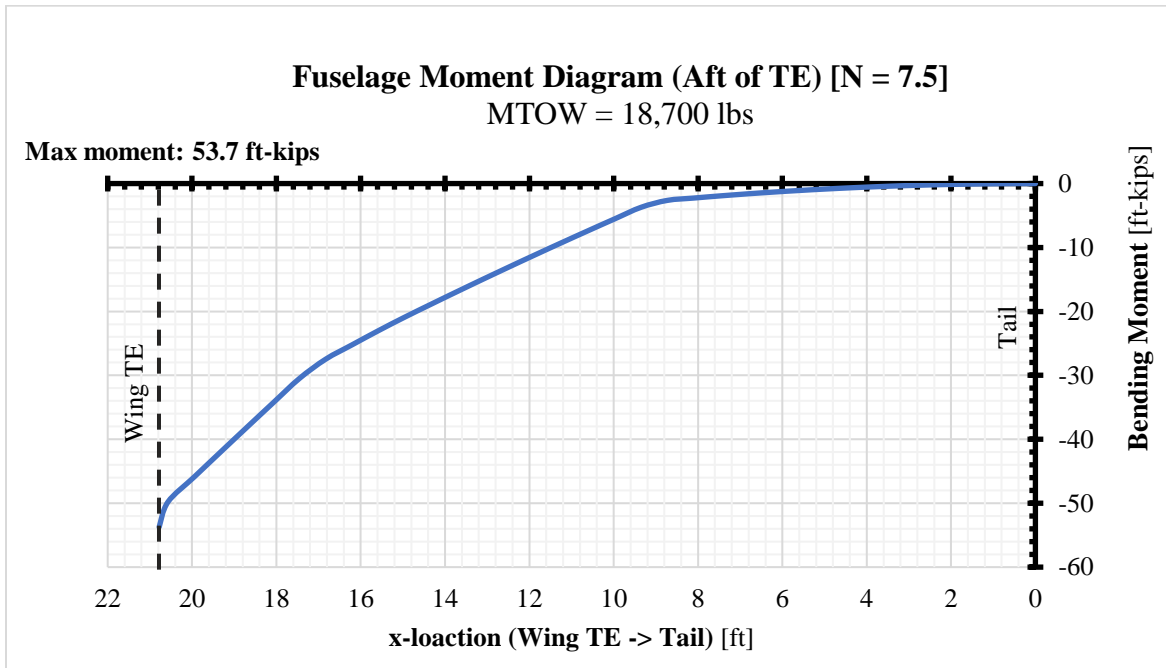


Figure 13-13 Fuselage Moment Diagram Aft of Wing Trailing Edge (TE)

13.3.3. Fuselage Bending Analysis

Preliminary fuselage bending analysis was also conducted with the use of lumped area analysis from Bruhn’s textbook [8] with the 140 ft-kip moment. The critical section in front of the leading edge was analyzed with longerons with cross section areas of 0.5 square inches. The longerons are located on the specified locations below on the left of figure 13-15. Longeron and rib spacing is based on historical data. The longeron spacing is approximately 15 inches and rib spacing is 20 inches. The fuselage longerons and skin will be made up of aluminum 7075-t6 for ease of maintenance on battle fields.

Longerons 9 and 10 will hold the max compression stress of 7.73 ksi with a factor of safety of 9.58. Longeron 19 has a max tension stress of 8.8 ksi with a factor of safety of 8.42. This is compared to the compressive yield allowable of 74 ksi and highly exceeds the 1.5 factor of safety. Ultimately, the critical factor of safety will come from detailed analysis on longeron and skin buckling. Figure 13-16 below outlines the full preliminary aircraft structure encompassing the pilots, fuel, and payload.

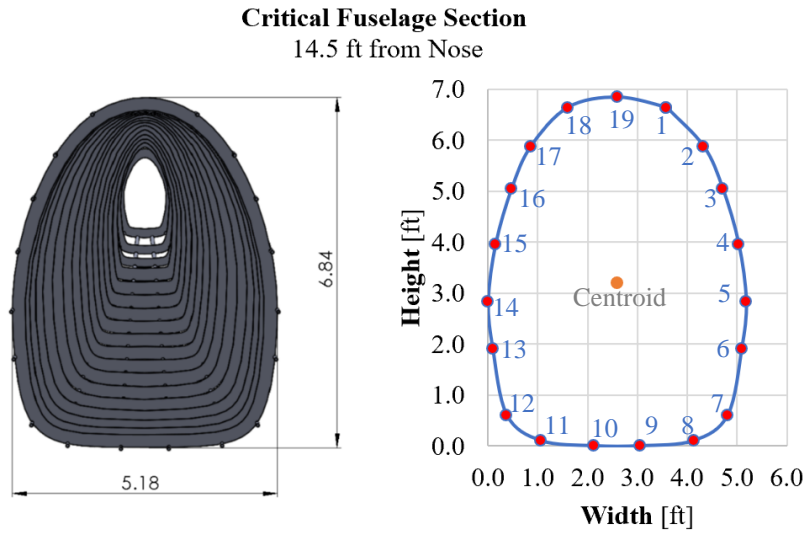


Figure 13-14 Fuselage Critical Cross Section at 14.5ft from Nose

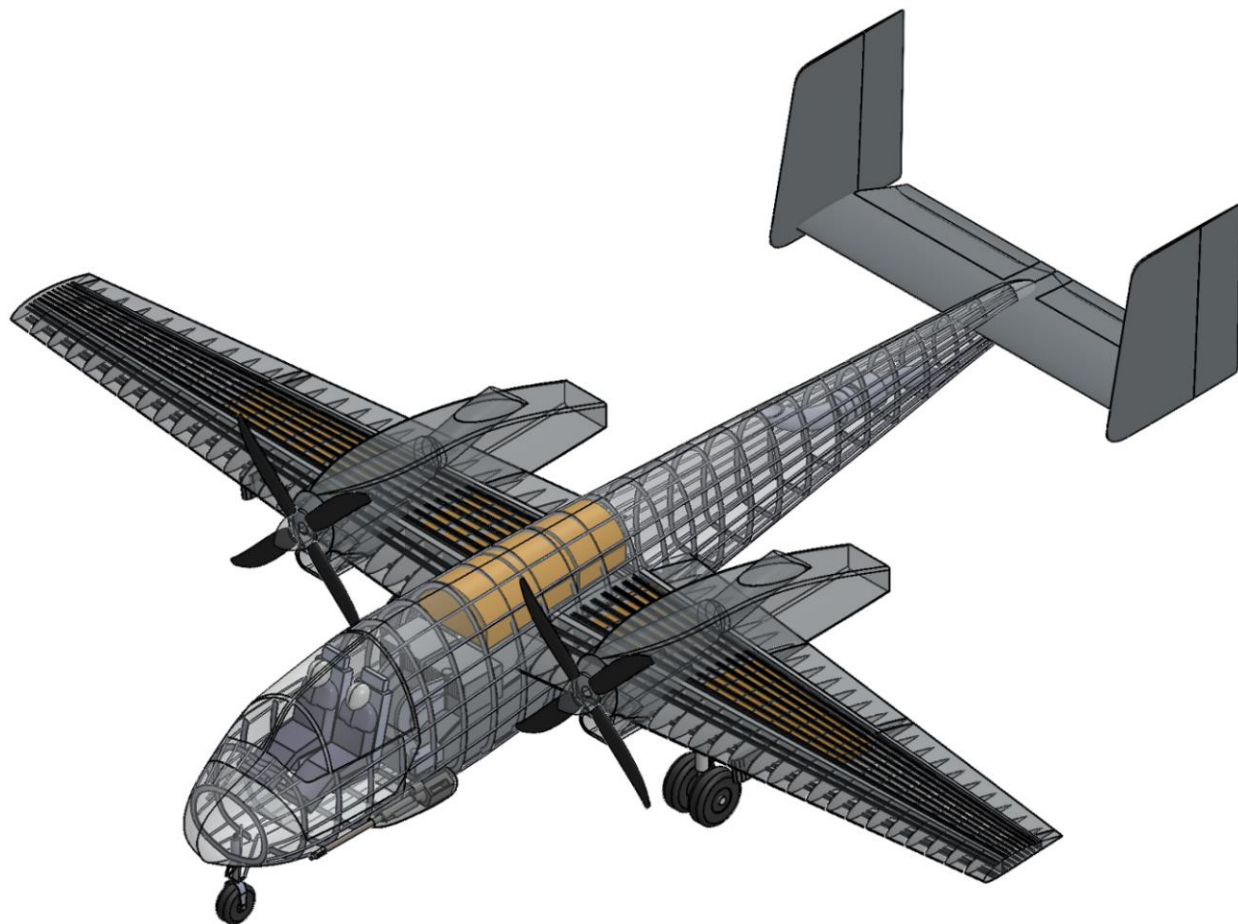


Figure 13-15 Aircraft Structure

14. Flight Systems

14.1. Fuel Systems

The analysis in section 11.6 shows that the aircraft requires 3,100 pounds. Our team opted to accommodate an additional 5% buffer to account for unusable fuel and provide a margin to ensure the final aircraft has sufficient fuel to complete its mission. The total fuel configuration is shown in table 14-1 below. A packing factor is included to account for the difference between the tank volume and the fuel volume. All tanks are self-sealing bladders.

Table 14-1 Fuel Tanks Quantity and Volume

Fuel Tanks	Fuel Weight (lbs)	Fuel Volume (gal)	Packing Factor	Tank Volume (ft ³)
L Inboard	330	50	0.75	66
R Inboard	330	50	0.75	66
L Outboard	500	75	0.75	10
R Outboard	500	75	0.75	100
Fuselage	1640	245	0.80	306
Total	3270	495	-	638

*Fuel volume is calculated at a worst-case temperature of 170°F

Figure 14-2 depicts the fuel system for the Diamondback. Most of the fuel is stored in a central fuselage tank. Each wing has two tanks, one inboard and one outboard of the engine pylon. Fuel is loaded from the starboard side of the aircraft from a central point and then distributed to the wing tanks. Cut off valves are included for every tank so if one tank is damaged, fuel from rest of the system does not drain.

Impetus Planum also explore attaching external fuel tanks to the wing pylons. Although this fuel is not necessary to complete the design or ferry mission, it expands the aircraft capability with minimal impact the design. Munitions can be loaded into the internal bomb bay and external tanks can be attached to the wing pylons for a long-range strike mission. We estimate that the additional 370 gallons would extend the aircraft range by 1000 nm. Figure 14-2 below depicts the external tanks on the aircraft and figure 14-2 the fuel block diagram.



Figure 14-1 Diamondback with External Fuel Tanks

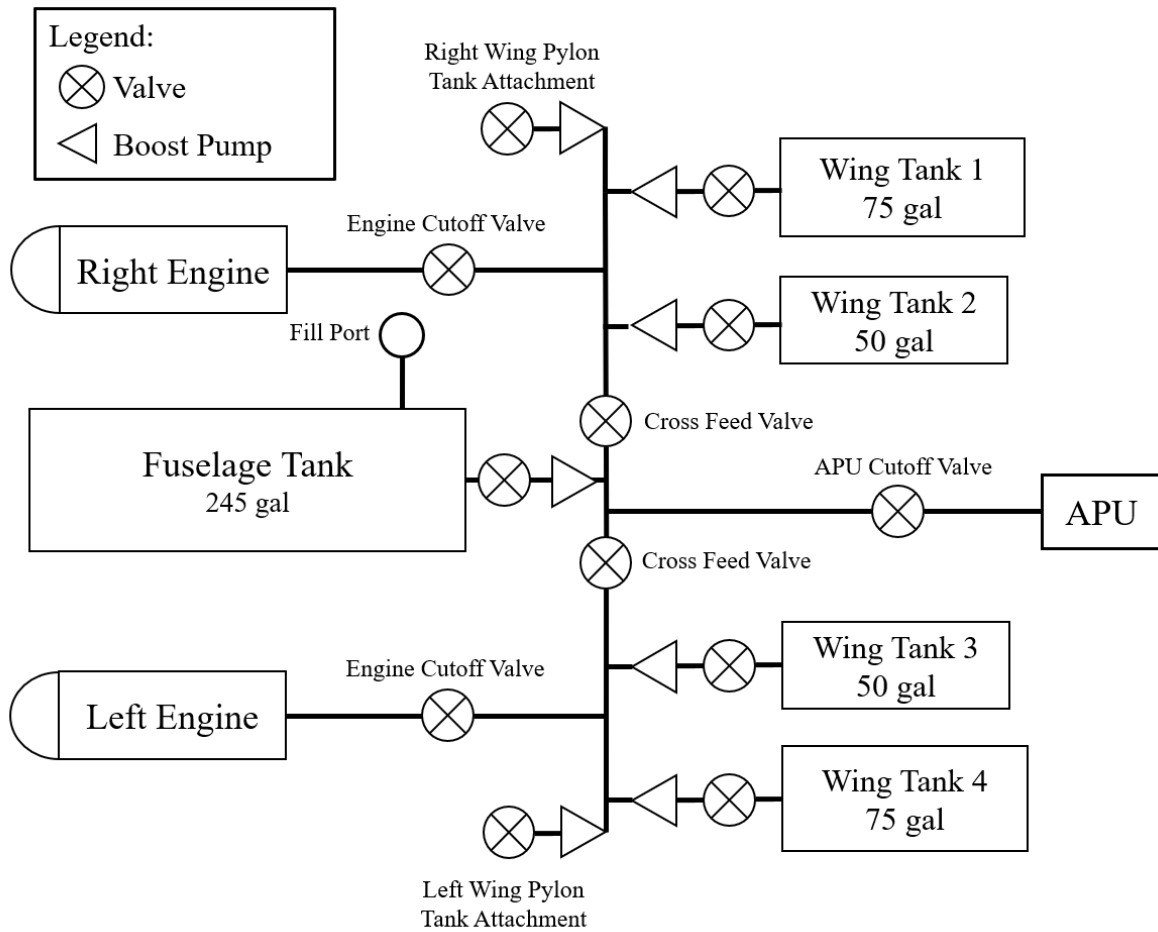


Figure 14-2 Fuel System Block Diagram

14.2. Electrical Systems

Like most other systems on the Diamondback, the electrical system consists of multiple safety-focused redundant backups. Designing for multiple electrical requirements and future expansions, the Diamondback has separate 12- and 24-volt DC circuits as well as a 120-volt AC circuit, shown in figure 14-1. The primary source of power is from two alternators mechanically coupled to each engine. These will provide the 12-volt DC power, with dual onboard converters providing the 24-volt DC and 120-volt AC power. The secondary source is the Honeywell RE-100 APU for ground power while the engines are off as well as providing both AC and DC backup power. In case of engine alternator and APU failure, the Diamondback incorporates a small ram air turbine (RAT) for emergency power generation to flight instruments and controls. Basic standby flight instruments that require power also have a backup battery in case of complete power failure.

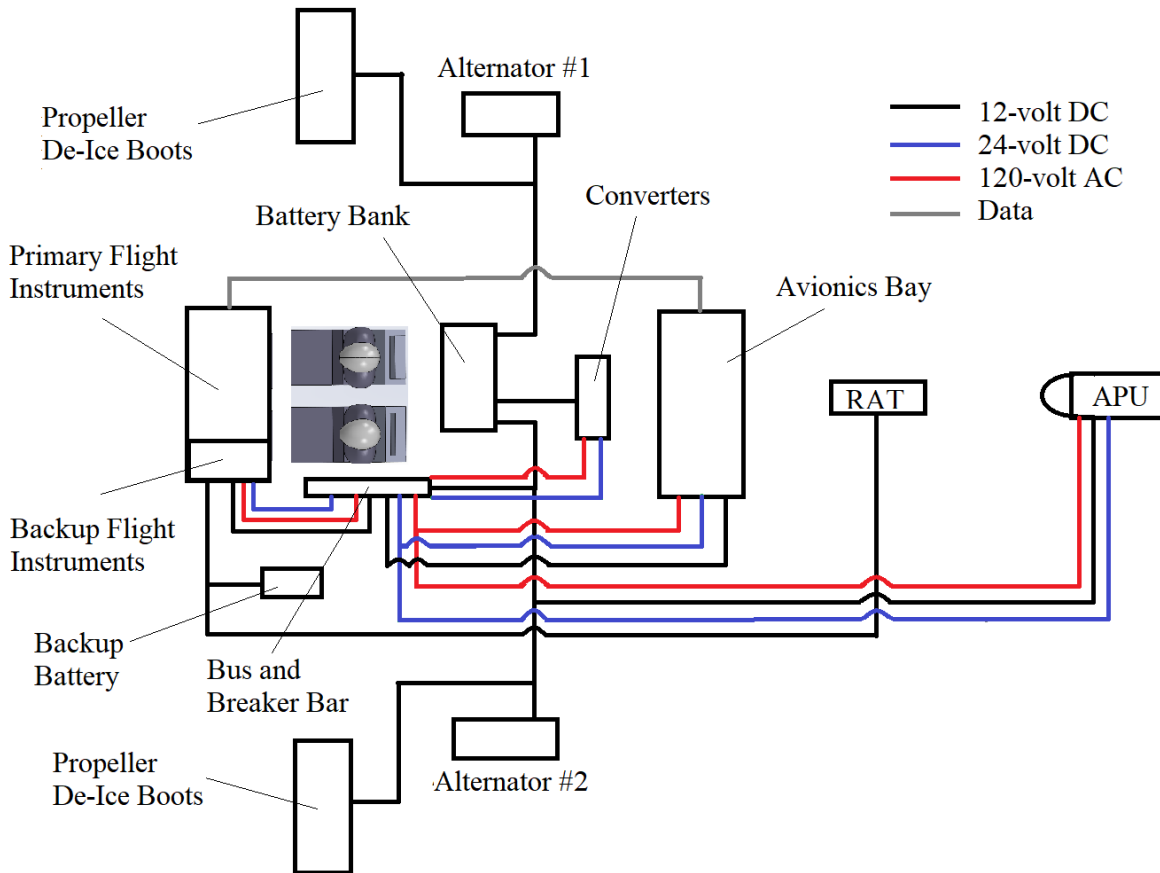


Figure 14-3 Electrical System Diagram

14.3. Pneumatic Systems

The Diamondback will incorporate a pneumatic system which is solely used to start the main engines and for emergency landing gear blow down. The selected APU on-board is the Honeywell RE-100, it weighs 83.25 pounds and operates at 70,000 RPM. This lightweight APU is used throughout the aviation industry, specifically in similarly sized aircraft such as the CJ-4. This APU will provide the necessary high pressure bleed air for primary engine start during normal operations. The wings leading edge will be heated with bleed air to provide anti ice capability. The tail will use deice boots inflated with bleed air.

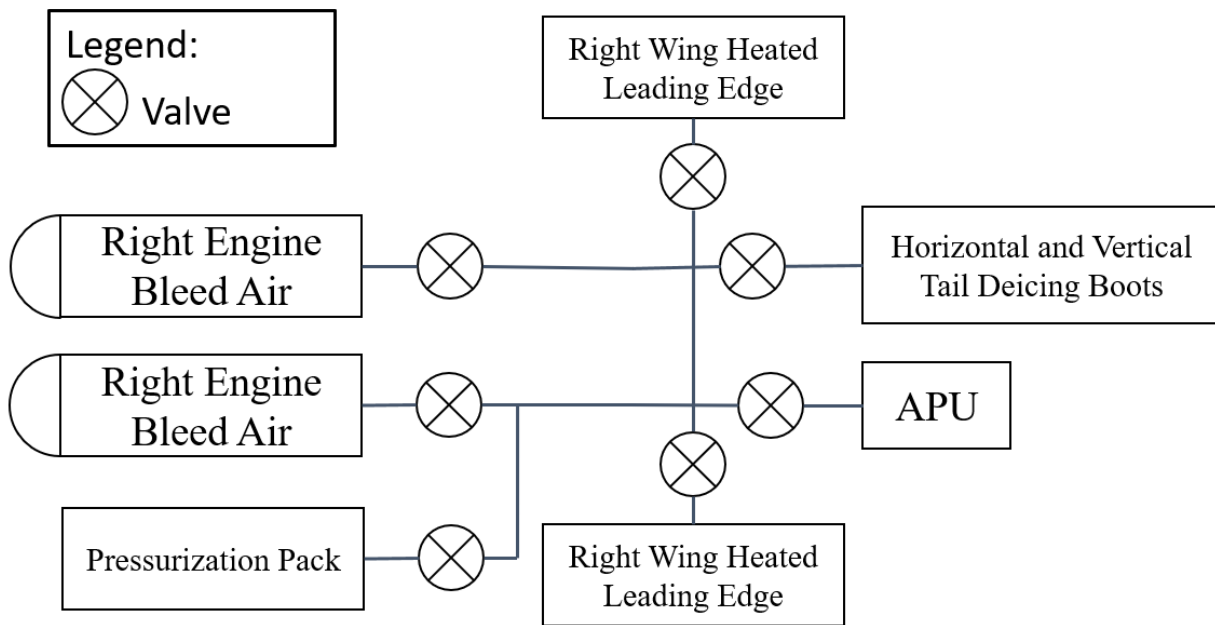


Figure 14-4 Pneumatic System Block Diagram

14.4. Hydraulics

Hydraulics will be used to control the flight control actuators, wheel brakes, flap actuators, and landing gear actuators of the aircraft, all controlled via fly-by-wire as shown in figure 14-5. A twin hydraulics system will be implemented for redundancy on the aircraft so that the hydraulics can still operate in case one of the systems fails. Additionally, a cable system will be implemented as a backup for the hydraulics, to be able to still retain control over the flight control systems in case of hydraulic failure. These systems will be primarily run off the engines' hydraulic pumps, but the APU can be used to power the backup hydraulic pump if needed.

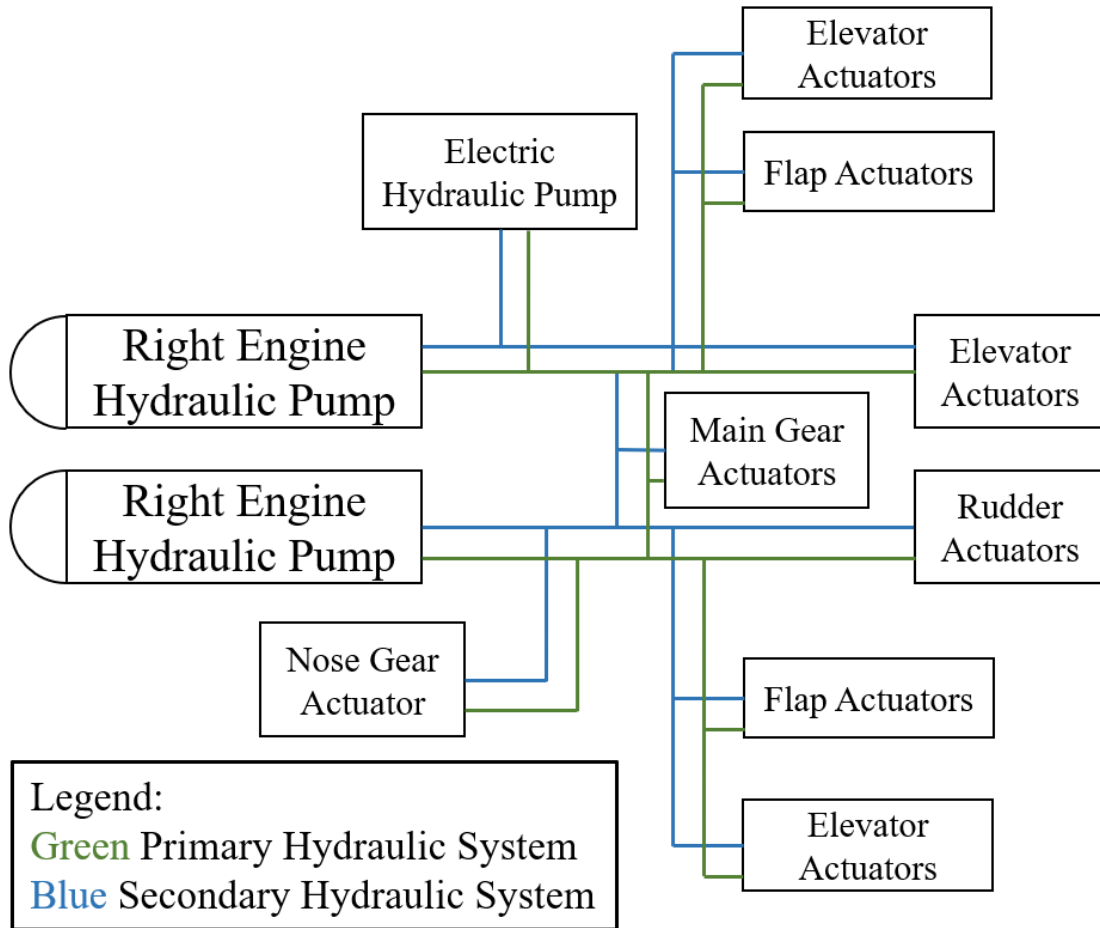


Figure 14-5 Hydraulic System Block Diagram

15. Storage and Transportation

15.1. Enclosure

The EFASS by RUBB© Building Systems will be used as a temporary mobile hanger to store and service the Diamondback. This modular 65-foot-wide hanger meets U.S. military wind and snow standards, can be assembled quickly with minimal crew, and fits within a single ISO 20 ft intermodal cargo container. Variations of this hanger also allow the use of a crane system for more advanced aircraft field maintenance such as wing or engine replacement.

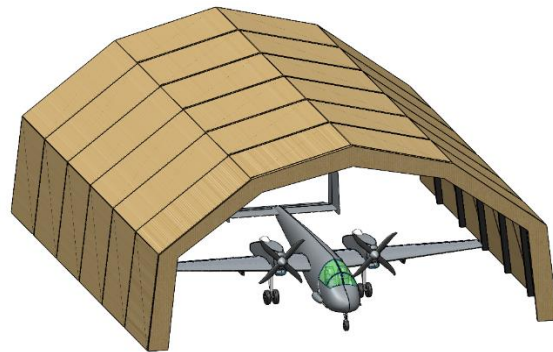


Figure 15-1 Diamondback in 20m EFASS Hangar

15.2. Aircraft Transportation

For global transportation or if the Diamondback is damaged at a forward operating base and needs to be transported to a main base for substantial repair, the aircraft can be partially disassembled and stored inside a C-17 cargo aircraft. As shown in figure 15-2 on the left, a single Diamondback plus two ISO intermodal containers with the EFASS hangar and other support equipment can fit in the aircraft. The right side shows two Diamondback aircraft inside the C-17 cargo hold.

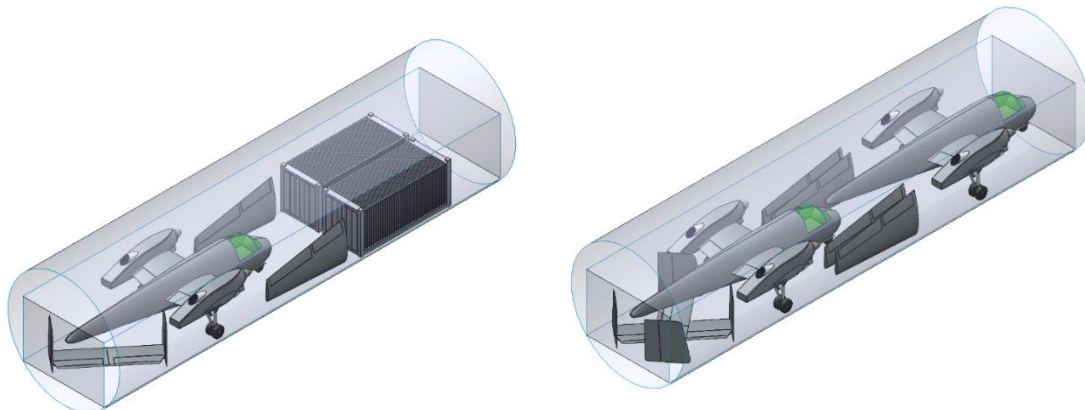


Figure 15-2 Diamondback and EFASS in the C-17 Aircraft

16. Cost

The resulting cost analysis for the Diamondback consists of two methodologies that were averaged to create a final unit flyaway cost. There are several differences between the two methods that contribute to this final unit flyaway cost of \$13.35 million.

16.1. Design Drivers and Assumptions

The effects of various design choices can create a discrepancy in cost analyses. The two approaches performed each considered similar variables, though some varying, for the design of the Diamondback.

The following design variables that are included in both cost analysis methods used are presented in table 16-1 below. Because the RFP only states the requirement for unit flyaway costs for procurement lots of 50 units, the team decided on a theoretical total number of operational units to further analyze our results and compare our costs to existing aircraft.

Table 16-1 Important Variables for Cost Analyses

Variables	Values
MTOW	18,700 lbs
Empty Weight (W_e)	11,200 lbs
Fuel Weight (including reserves)	3,300 lbs
Fuel Weight (w/o reserves)	2,900 lbs
N (number of engines)	2
Q_D (# of development units)	5
Total Number of Units	505

Further considerations were provided through the RFP as requirements such as a service life of 25 years and a minimum operating time of 1,200 flight hours per aircraft, per year. This operating time includes training, ferry, and operational flights. These considerations were used in the operations cost analyses.

The final variables needed include hourly rates for the manufacturing and production of the Diamondback, as well as a crew rate for operational cost analysis. These variables are required in both cost analysis methods and are presented in table 16-2.

Table 16-2 Hourly Rates Assumed for Analyses

Hourly Rates	Method 1: N&C (2025 US \$)	Method 2: Modified DAPCA IV (2025 US \$)
RE – Engineering Rate	\$158/h	\$159/h
RT – Tooling Rate	\$172/h	\$163/h
RM – Manufacturing Rate	\$137/h	\$135/h
RQC – Quality Control Rate	\$153/h	\$149/h
Crew Rate	\$550/h/pilot	\$550/h/pilot

It should be mentioned that the above rates are estimated using historical data and an estimated inflation rate based on historical trends. Thus, the projected unit flyaway costs are estimated at 2025 U.S. dollar values. The inflation for the above rates is considered at 2.3% from 1998-2025. Also, it should be noted that the crew rate in table 16-2 is per pilot. Since the Diamondback is a two-pilot design, the estimated crew rate would be double the rates listed above for the following analyses.

It is also worth mentioning that the hourly rates estimated for both methods can also be described as “wrap rates” as they also include direct salaries paid to employees as well as employee benefits, overhead, and administrative costs. The use of wrap rates provides a more accurate estimate of costs as it includes all the costs a company would incur.

16.2. Methodology

The first method is called the Life Cycle Cost approach, discussed by Nicolai and Carichner [2], and the second method is called the modified DAPCA IV method, which was discussed in by Raymer [3].

16.2.1. LCC Method

Nicolai and Carichner [2] discuss The Life Cycle Cost approach, or LCC, includes the following phases:

- Research, Development, Test, and Evaluation (RDT&E)
- Acquisition (production, ground equipment, initial spares, and training aids)
- Operations
- Maintenance

The RDT&E cost required is to engineer, develop, fabricate, and flight test 5 development units prior to committing to production.

Nicolai and Carichner [2] discuss the Life Cycle Cost approach, or LCC, and present equations within the textbook that were used to produce the results found below. Furthermore, historical data used for hourly rates can be found in figure 16-1, which is from Nicolai and Carichner’s [2] text. The values chosen as a basis were from the year 1998, and then converted to 2025-dollar values using an inflation rate of 2.3% as mentioned earlier.

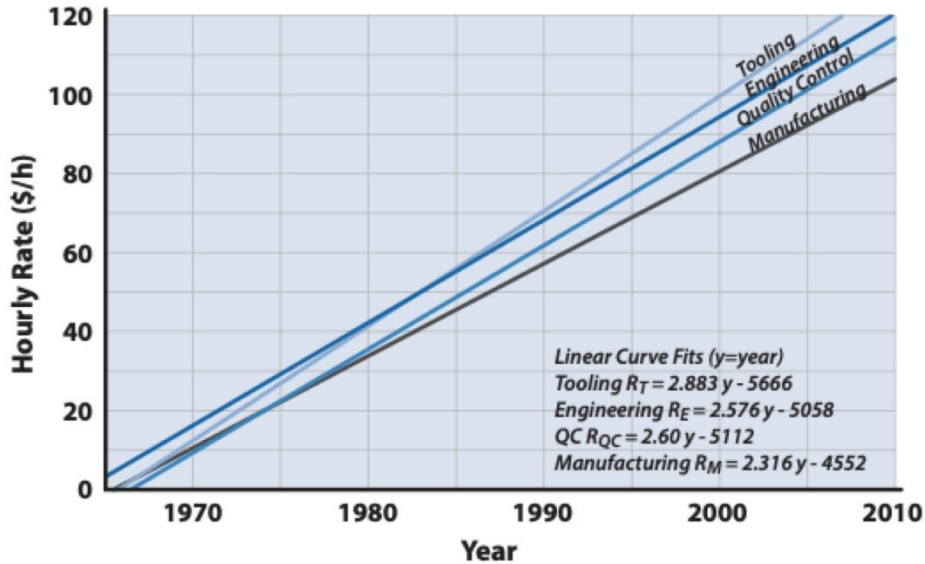


Figure 16-1 Hourly Rate Historical Data Chapter 24 Nicolai and Carichner

A significant difference between the two methods is the consideration of the number of lines of code required by the LCC method. This inclusion provides a better estimate for the avionics units onboard the aircraft, and thus was included in the unit flyaway cost predicted by this method. Thus, the team estimated a total of 8 million line of code required.

Table 16-3 shows a summary of the acquisition cost analyses conducted for 1 lot and 10 lots, and the resulting unit flyaway cost for both cases.

Table 16-3 LCC Acquisition Costs Summary

Components	Cost (50 units)	Cost (500 units)
RDT&E (5 units)	\$0.85B	\$0.85B
Production	\$1.47B	\$4.93B
Engineering	\$393M	\$563M
Tooling	\$245M	\$439M
Manufacturing	\$188M	\$1.09B
Quality Control	\$45.13M	\$185M
Unit Flyaway	\$44.04M	\$11.58M

16.2.2. Modified DAPCA IV Method

A noticeable difference between the LCC method described by Nicolai and Carichner [2] and the modified DAPCA IV method is the explicit consideration of the number of flight test aircraft. Thus, 2 out of the 5 development units were decided on for the purpose of this cost analysis. Further differences include accounting for the time of design and fabrication of the material to be used. The following table provided by Raymer's textbook [3] was used in order to estimate a weight factor to account for the chosen material for the Diamondback.

Table 16-4 Material Based Weight Factors

Material	Weight Factors
Aluminum	1
Graphite-epoxy	1.0 - 1.8
Fiberglass	1.1 - 1.2
Steel	1.5 - 2.0
Titanium	1.1 - 1.8

Parts of the Diamondbacks wing will be made of carbon fiber and aluminum while the stringers and skin are made of just aluminum, due to its lower manufacturing process time, cost, and maintenance. This material was chosen for ease of replacement. Since the Diamondback will be fabricated mainly out of Aluminum, which has a weight factor of 1 as specified in table 16-4, DAPCA IV analyses conducted already considers this material choice.

The following table summarizes the Acquisition costs for the Diamondback while applying the Modified DAPCA IV method:

Table 16-5 DAPCA IV Acquisition Costs Summary

Components	Cost (50 units)	Cost (500 units)
RDT&E (5 units)	\$0.94B	\$0.94B
Production	\$0.79B	\$7.53B
Engineering	\$389M	\$566M
Tooling	\$227M	\$417M
Manufacturing	\$439M	\$2.31B
Quality Control	\$58.43M	\$307M
Unit Flyaway	\$35.45M	\$16.05M

16.3. Unit Flyaway Costs

This section discusses the unit flyaway costs found using each analysis method and taking an average of the two. This was one for one lot as well as 10 lots, which will be discussed later in this section for cost comparison purposes. The following table 16-6 presents the unit flyaway costs estimated:

Table 16-6 Unit Flyaway Costs

Method	Unit Flyaway Cost (\$M)	Unit Flyaway Cost (\$M)
	1 lot = 50 units	10 lots = 500 units
Nicolai & Carichner LCC	\$44.04M	\$11.58M
Modified DAPCA IV	\$35.45M	\$15.13M
Average	\$39.74M	\$13.35M

It should be noted that these costs do not include the non-recurring RDT&E cost for 5 development units of the Diamondback. The following table presents these additional costs:

Table 16-7 RDT&E Costs

Method	Q _D (# of units)	Cost (\$)
Nicolai & Carichner LCC	5	\$0.85B
Modified DAPCA IV	5	\$0.94B
Average	-	\$0.89B

16.3.1. Cost Comparison

First, to compare the unit flyaway costs estimated by both methods, we must keep in mind the varying assumptions of each method. The unit flyaway cost for one lot applying the LCC method is much higher; However, when the number of lots increase, the LCC unit flyaway cost decreases much more significantly than the DAPCA IV unit flyaway cost. The variance in the resulting costs as well as the considerations of each method prompted the team to take the average of the two estimates, as a reasonable final cost.

Next, in order to conduct a sanity check of estimated costs found during the conducted analyses overall and compare these costs with existing aircraft, the team decided a total number of operational units to be produced in order to more accurately compare the unit flyaway cost for the Diamondback with other pre-existing aircraft presented in the following table below:

Table 16-8 Unit Flyaway Cost Comparison

Aircraft	Unit Flyaway Cost (\$M)	# Units Produced
Diamondback	13.8	500
AH-64E Apache	27.5	690
A-10 Thunderbolt II	20.9	700
A-29 Super Tucano	31	200

Based on previous trends in the number of production aircraft, the team decided a total of 500 operational units for comparison purposes was ideal. Based on the data presented, the average unit flyaway cost for 10 lots of the Diamondback is still much cheaper in comparison to existing aircraft with slightly larger numbers of produced units. It is also important to note that the unit flyaway costs of all the aircraft in table 16-8 are in estimated 2025 US dollar values.

16.4. Breakeven Data

The breakeven charts below are presented for 1 lot and 10 lots using each method for a total of 4 graphs. The breakeven analyses include the total number of operational units in the calculations conducted. Thus, the following 4 graphs provide the breakeven points out of 50 units and 500 units. The analyses also assume a selling price based on an assumed profit of approximately 12% in each case. Additionally, the star in each graph represents the breakeven point.

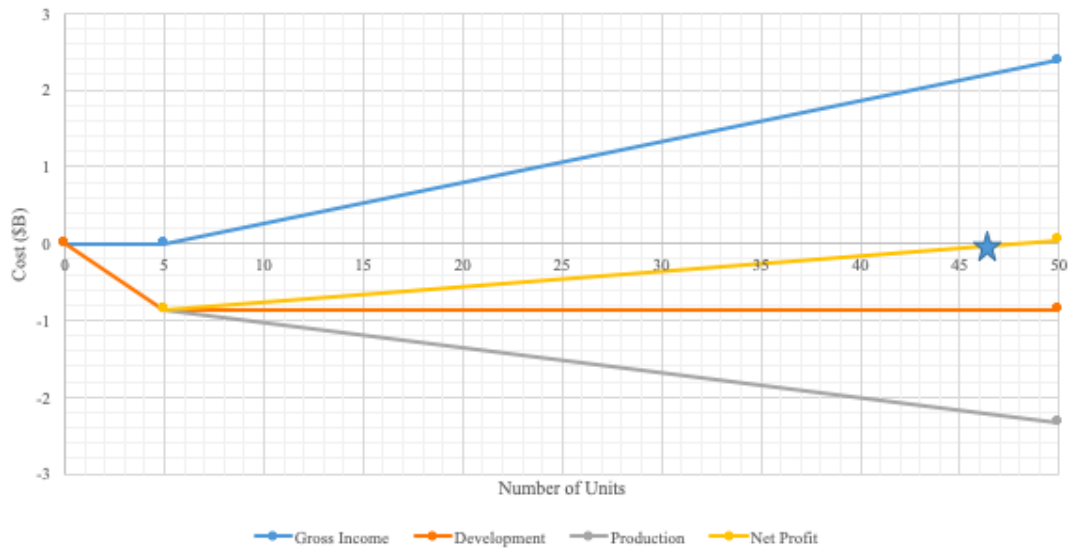


Figure 16-2 LCC Breakeven Point (1 Lot)

The above figure displays a breakeven point at 47 units, under a selling price of \$49.35M/unit.

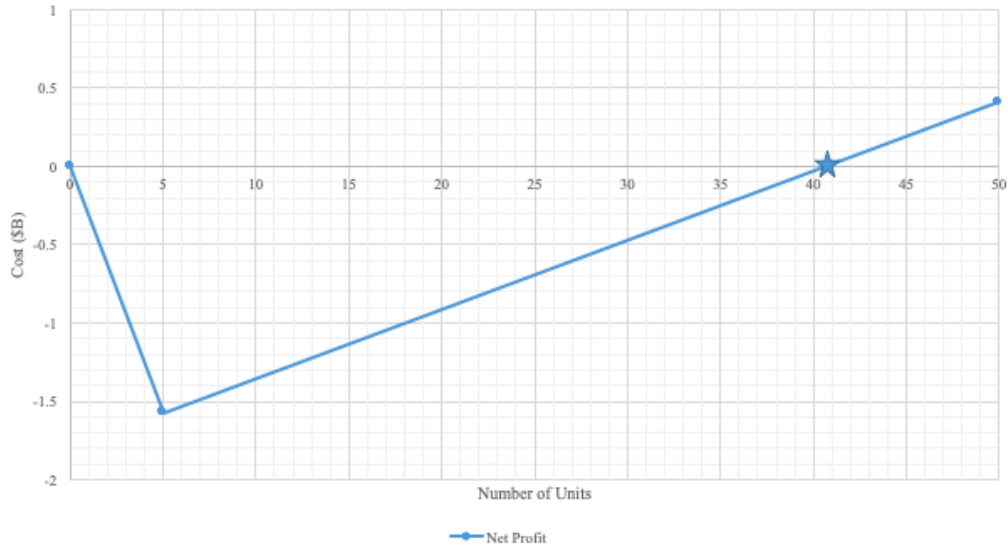


Figure 16-3 DAPCA IV Breakeven Point (1 Lot)

The above figure displays a breakeven point at 41 units, under a selling price of \$39.74M/unit.

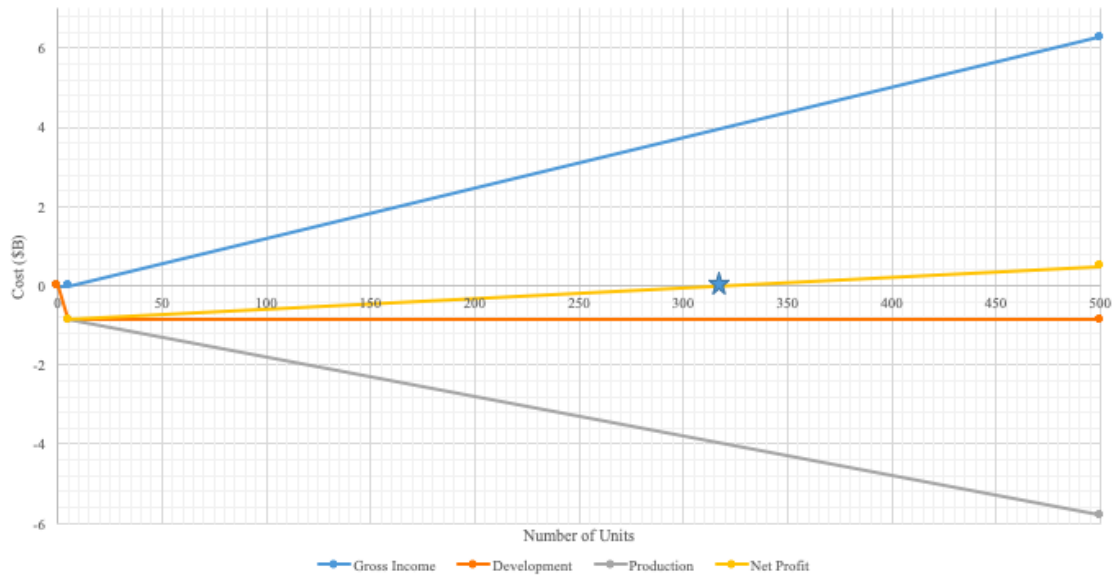


Figure 16-4 LCC Breakeven Point (10 Lots)

The above figure displays a breakeven point at 320 units, under a selling price of \$12.97M/unit.

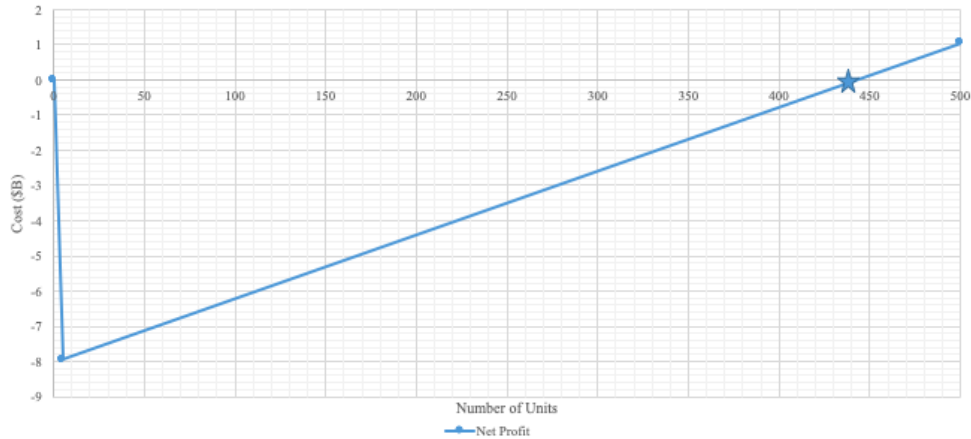


Figure 16-5 DAPCA IV Breakeven Point (10 Lots)

The above figure displays a breakeven point at 440 units, under a selling price of \$16.96M/unit.

16.5. Operations & Maintenance Costs

The operating cost was based mainly on the 1,200 minimum flight hours per year’s requirement. Thus, the cost analysis was conducted for one lot per year and 10 lots per year. Each method considered different components required for operation and maintenance, thus the cost analysis was conducted for both methods, and then averaged to accommodate for the “missing” components in each method.

16.6. Service Life Requirement

The RFP requires the design of the Diamondback to meet the performance requirements it has specified with the consideration of both acquisition and operational costs over an expected 25- year service period. The following subsections will discuss the operational costs in detail considering this requirement as well as the required minimum flight hours per year. Meanwhile, the next section will discuss the acquisition costs in greater detail, as well as provide a summary of the operational costs discussed, and an overall program life cost under this service life assumption.

16.6.1. LCC Method

The operations costs comprise of petroleum, oil, and lubricants (POL), salaries of operating and support personnel, spares, and other indirect costs. The costs of these components are estimated using the LCC method and presented in the following table for 50 units or one lot:

Table 16-9 Operations and Maintenance Costs for 25 Years of Service

Components	Cost
Spare Tires	\$125M
Engine Maintenance	\$317M
Airframe Maintenance	\$257M
Fuel, Oil, Lubricants	\$2.73B
Crew Operations (Pilot Salary)	\$33.59M

The above components also consider a 2.3% inflation rate as specified earlier. The costs for spare tires, fuel, oils, and lubricants were estimated based on current data found for these specified components and contribute to the overall operations cost for the required minimum 25 years of service. The tires chosen are Goodyear tires, specified in table 10-3. The fuel cost considered was for Jet A-1 fuel at \$4.5/gal and was used in the engine maintenance cost analysis.

16.6.2. Modified DAPCA IV Method

The operations costs under the modified DAPCA IV method is comprise of very few components. Their costs are listed in table 16-10 below for 25 years of service for one lot:

Table 16-10 Operations and Maintenance Costs for 25 Years of Service

Components	Cost
Spare Tires	\$2.5B
Fuel, Oil, Lubricants	\$3.17B
Crew Operations (Pilot Salary)	\$1.65B
Total Maintenance	\$1.81B

16.6.3. Final Operations Cost

Since the operations cost for each method considers varying components, though some similar such as the crew cost, the final operations cost applying both methods account for these different variables and is presented in the simplified table below for 25 years of service.

Table 16-11 Final Operations Costs for 25 Years

# of Lots	Cost Per # of Lots	
	1 Lot	10 Lots
Operating	\$5.83B	\$58.36B
Maintenance	\$1.19B	\$11.94B
Total	\$7.02B	\$70.3B

16.7. Program Life Cost and Disposal

The program life cost comprises of acquisition and operations cost for the 25 years of service required. The acquisition cost is comprised of many components which are presented in table 16-12 below. The operations cost comprises of mainly maintenance and operating costs for the required service time.

Below is a summary of the final program life cost of the Diamondback assuming 1,200 flight hours per aircraft, per year, for 25 years of service, for a total of 500 operational units, or 10 lots of 50:

Table 16-12 Diamondback Program Life Cost Breakdown

Program Cost	
Acquisition	Cost (for 500 units)
RDT&E (5 units)	\$0.89B
Production	\$6.23B
Engineering	\$564M
Tooling	\$428M
Manufacturing	\$1.7B
Quality Control	\$246M
Unit Flyaway	\$6.90B
Profit	\$739M
Operation	Cost (for 500 units)
Operating	\$58.36B
Maintenance	\$11.94B
Total Program Cost	\$88.00B

Once the Diamondback has reached the end of its useful life or is damaged beyond repair, it will be transported back to the U.S. for disposal. Any military technology or hazardous materials will be removed from the aircraft and disposed of properly. The option to either scrap the Diamondback for raw materials or place it into an aircraft boneyard for storage is available.

17. Entry into Service Schedule

The following figure 17-1 represents not only the schedule followed by the team throughout this year up until the point of this submittal, but it also includes a hypothetical service schedule (in red text) to continue to develop the Diamondback and operate for 25 years under the numerous assumptions the team made throughout our design, as discussed throughout this report. The key elements of this schedule include the yearly timeline in the top row, the numerous stages of our design and theoretical service process in the third row, and the upside-down triangle symbols that represent key presentations completed, this submittal, and hypothetical future presentations to be completed (using red text).

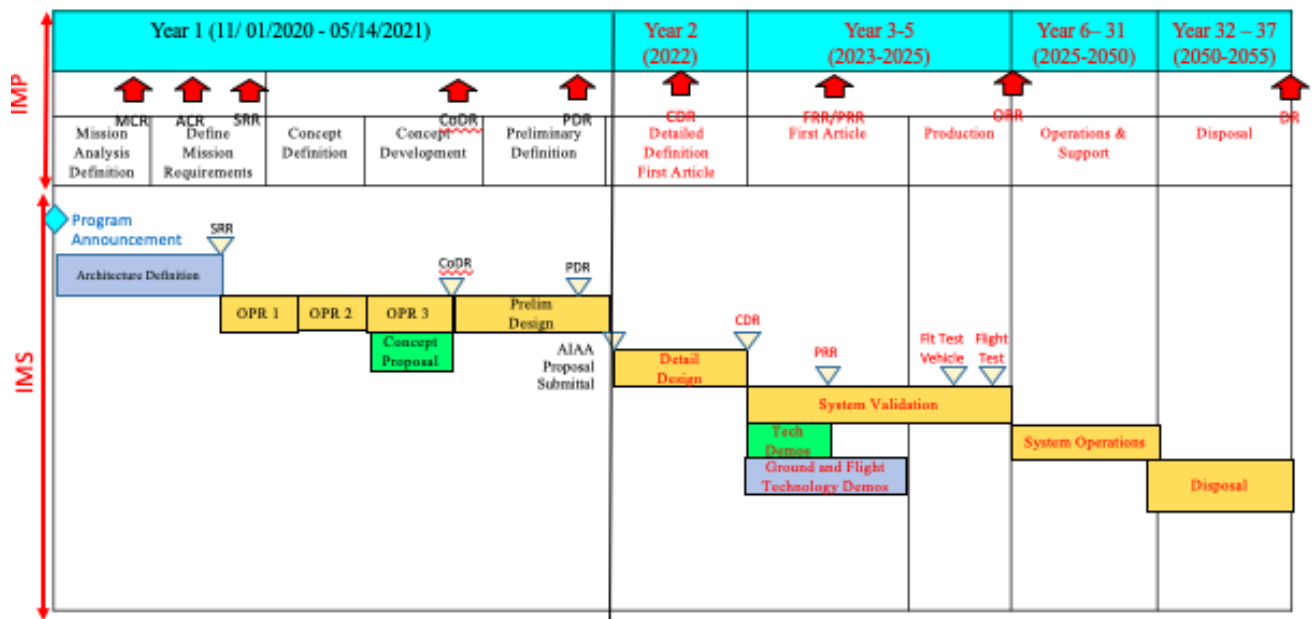


Figure 17-1 Entry Into Service Schedule

18. TRL Tracking

Table 18-1 below summarizes the major components used on the Diamondback and their respective TRL values. The requirement T12 that all technologies should be TRL 8 or above which our aircraft complies with.

Table 18-1 Component TRL Tracking

Component	TRL
PW-126A	9
Rubb 20.1m EFASS	9
Mk16-US16LA Ejection Seat	9
AN/ALE-47 Counter Measure Dispenser	9
RR170 Mk3 Chaff	9
MJU-50/B Flares	9
M230 Chain Gun	9
Goodyear 892C61B1 Main Tire	9
GUA 806C81-2 Nose Tire	9
Honeywell RE-100 APU	9

References

- [1] “Request for Proposal Austere Field Light Attack Aircraft.” *Https://Www.aiaa.org/*, AIAA, www.aiaa.org/docs/default-source/uploadedfiles/education-and-careers/university-students/design-competitions/undergraduate-team-aircraft-design-competition/aiaa-2021-undergraduate-team-aircraft-design-rfp---light-attack-aircraft-2-.pdf?sfvrsn=b54e3cac_2.
- [2] Nicolai, Leland M., and Grant E. Carichner. *Fundamentals of Aircraft and Airship Design: Aircraft Design*. Vol. 1, American Institute of Aeronautics and Astronautics, 2010.
- [3] Raymer, Daniel P. *Aircraft Design: A Conceptual Approach*. 6th ed., American Institute of Aeronautics and Astronautics, Inc., 2018.
- [4] McCormick, Barnes W. *Aerodynamics, Aeronautics and Flight Mechanics*. 2nd ed., John Wiley & Sons, 1995.
- [5] “Aircraft Brakes.” *Aeronautics Guide*, www.aircraftsystemstech.com/p/aircraft-brakes_9081.html.
- [6] Abbott, Ira H., and Doenhoff Albert E Von. *Theory of Wing Sections: Incl. a Summary of Airfoil Data*. Dover Publ., 1959.
- [7] Schaufele, Roger D. *The Elements of Aircraft Preliminary Design*. Aries Publications, 2007.
- [8] Bruhn, E. F., and Bollard R J H. *Analysis and Design of Flight Vehicle Structures*. Jacobs, 1973.
- [9] “Repairability of Sheet Metal Structures (Part Three).” *Flight Mechanic*, www.flight-mechanic.com/repairability-of-sheet-metal-structures-part-three/.
- [10] Coburn, Todd D. *Aerospace Strength Handbook*. Vol I and II, Copyright © 12 Jan 2020, Todd D. Coburn.
- [11] Nelson, Robert C. *Flight Stability and Automatic Control*. 2nd ed, WCB/McGraw-Hill, 1998.
- [12] “Embraer EMB 314 Super Tucano.” Wikipedia, Wikimedia Foundation, 7 May 2021, en.wikipedia.org/wiki/Embraer_EMB_314_Super_Tucano.

- [13] “Fairchild Republic A-10 Thunderbolt II.” Wikipedia, Wikimedia Foundation, 14 May 2021, en.wikipedia.org/wiki/Fairchild_Republic_A-10_Thunderbolt_II.
- [14] “North American Rockwell OV-10 Bronco.” Wikipedia, Wikimedia Foundation, 13 May 2021, en.wikipedia.org/wiki/North_American_Rockwell_OV-10_Bronco.
- [15] “25mm Bushmaster.” *Weaponsystems.net*, weaponsystems.net/system/524-25mm+Bushmaster.
- [16] “Conferences by Year.” *NDIA Proceedings*, ndia.dtic.mil/.
- [17] “GAU-22/A 25mm Gatling Gun.” *General Dynamics Ordnance and Tactical Systems*, 23 July 2018, www.gd-ots.com/armaments/aircraft-guns-gun-systems/gau22a/.
- [18] “M299/M310 Hellfire Longbow Missile Launcher for Rotary Wing Aircraft.” *Marvin Engineering Co*, marvineng.com/product/m299m310-longbow-missile-launcher/.
- [19] “Ordnance, Explosives, and Related Items.” *Home*, bulletpicker.com/.
- [20] *Wikipedia*, Wikimedia Foundation, 3 Feb. 2021, www.wikipedia.org/.
- [20] “PT6A.” School of Aeronautics and Astronautics - Purdue University, engineering.purdue.edu/AAE/research/propulsion/Info/jets/tprops/pt6a.
- [21] “Pratt & Whitney Canada PW100.” Wikipedia, Wikimedia Foundation, 12 May 2021, en.wikipedia.org/wiki/Pratt_%26_Whitney_Canada_PW100.
- [22] “Rolls-Royce AE 2100.” Wikipedia, Wikimedia Foundation, 7 May 2021, en.wikipedia.org/wiki/Rolls-Royce_AE_2100.
- [23] “Baker.” Martin, 12 Apr. 2021, martin-baker.com/.
- [24] “Aces 5 Next Generation Ejection Seat.” Collins Aerospace: Redefining Aerospace, www.collinsaerospace.com/what-we-do/Military-And-Defense/Interiors/Aces-5-Next-Generation-Ejection-Seat.